AIRBORNE PSEUDOLITES IN A GLOBAL POSITIONING SYSTEM DEGRADED ENVIRONMENT

THESIS

Halit Oktay, First Lieutenant, TURAF

AFIT/GSS/ENY/11-M03

DEPARTMENT OF THE AIR FORCE
AIR UNIVERSITY

AIR FORCE INSTITUTE OF TECHNOLOGY

Wright-Patterson Air Force Base, Ohio

AFIT/GSS/ENY/11-M03

AIRBORNE PSEUDOLITES IN A GLOBAL POSITIONING SYSTEM DEGRADED ENVIRONMENT

THESIS

Presented to the Faculty

Department of Aeronautics and Astronautics

Graduate School of Engineering and Management

Air Force Institute of Technology

Air University

Air Education and Training Command

In Partial Fulfillment of the Requirements for the

Degree of Master of Science

Halit Oktay, B.S.E.E.

First Lieutenant, TURAF

March 2011

AFIT/GSS/ENY/11-M03

AIRBORNE PSEUDOLITES IN A GLOBAL POSITIONING SYSTEM DEGRADED ENVIRONMENT

Halit Oktay, B.S.E.E.
First Lieutenant, TURAF

Approved:

Lt Col M. Stepaniak, PhD (Chairman)	14 Mar 2011 Date
Maj K. Fisher, PhD (Member)	14 Mar 2011 Date
Dr. M. Pachter (Member)	March 14, 2011 Date

Abstract

The high accuracy of the Global Positioning System allows for precision navigation in support of current and future military operations. However, generating a three-dimensional position using GPS requires a clear line-of-sight between the user and at least four GPS satellites, and so the GPS service can be denied in scenarios such as a street surrounded by tall buildings. Therefore, there is a need for augmentation in these environments. Pseudolites, which transmit GPS-like ranging signals, can be deployed in order to improve the geometry and provide additional ranging signals. Users can then receive and process both GPS and pseudolite signals simultaneously with slight software modifications.

In this thesis, in order to provide precise positioning in an urban environment, a conceptual design of the airborne pseudolite augmentation system is introduced. The impact of the restricted satellite availability due to obstructions is examined for various urban terrain zones. Then, the ability of the pseudolite to improve both availability and accuracy is investigated. A comparison of the system performance when relying on GPS only and when using an airborne pseudolite augmentation is presented for various positioning scenarios. Simulations show that required accuracy and availability can be obtained by using an appropriately equipped airborne pseudolite. Finally, the improvement gained by the addition of second pseudolite to the most challenging urban environments is examined.

This research provides a simulation tool for showing the effectiveness of airborne pseudolites on enhancing a military GPS receiver's positioning accuracy in challenging GPS environments. Possible applications range from urban areas to canyons or harsh geographical conditions for tactical operations by the armed forces.

Acknowledgements

First and foremost, I would like to thank to my lovely wife and my daughter for their countless hours of patience and support. They were my inspiration throughout this endeavor.

I would also like to express my sincere appreciation to my committee for their time and energy to review this thesis. The largest source of thanks goes out to my advisor, Lieutenant Colonel Michael Stepaniak, because without him, this thesis would not have been possible. I certainly appreciate his insight and his experience.

I would also like to express my gratitude to the faculty members for teaching me all the precious classes.

Finally, I would like to thank to the Republic of Turkey and the great Turkish Nation for providing me the opportunity to attend this program. I hope I can pay them back everything they provided me by serving during rest of my life.

Halit Oktay

Table of Contents

Page

List of Figures

List of Tables

List of Abbreviations

Abbreviation		Page
US	United States	1
GPS	Global Positioning System	1
LOS	Line Of Sight	1
GLONASS	Global Navigation Satellite System	2
GNSS	Global Navigation Satellite System	2
GPS	Global Positioning System	4
GNSS	Global Navigation Satellite System	4
CDMA	Code Division Multiple Access	4
PRN	Pseudo-Random Noise	4
DoD	Department of Defense	5
C/A	Coarse-Acquisition	5
P	Precise	5
MCS	Master Control Station	6
DGPS	Differential GPS	8
MEO	Medium Earth Orbit	12
FDMA	Frequency Division Multiple Access	15
TDMA	Time Division Multiple Access	15
TCXO	Temperature Compensated Crystal Oscillator	17
SPS	Standard Positioning Service	18
GDOP	Geometric Dilution of Precision	20
INS	Inertial Navigation System	20
UGV	Unmanned Ground Vehicle	20
SLAM	Simultaneous Localization And Mapping	20
SCPA	Self-Calibrating Pseudolite Array	21
US	United States	24
DOP	Dilution of Precision	25

Abbreviation		Page
DOP	Dilution of Precision	61
LOS	Line Of Sight	63
AGL	Above Ground Level	64
SPS	Standard Positioning Service	75
LADGPS	Local Area Differential GPS	75
CPDGPS	Carrier Phase Differential GPS	75
GPS	Global Positioning System	83
LOS	Line Of Sight	83
PPS	Precise Positioning Service	84
UAV	Unmanned Air Vehicle	85
DOP	Dilution of Precision	86
PDOP	Position Dilution Of Precision	86

AIRBORNE PSEUDOLITES IN A GLOBAL POSITIONING SYSTEM DEGRADED ENVIRONMENT

I. Introduction

1.1 Motivation

Today, one can easily define navigation as the science of monitoring and controlling the motion of a vehicle from one location to another. In contrast to this short definition, navigation has a long and challenging history. For centuries, people have been trying to give reliable answers to the questions of where they are and how to get to their destination. Early mariners had followed coast lines closely in order to avoid getting lost until they learned to how to chart their courses by following stars. Afterwards, they were brave enough to try crossing vast oceans, despite the fact that stars are only visible on clear nights. After the major inventions in navigation, such as the compass, sextant and chronometer, they acquired the ability of generating more precise latitude and longitude information. The combinations of these tools were used as a primary navigation aid until the beginning of 20th century. Radio based navigation aids, which transmit electronic signals, were developed and widely used in World War II. However, these more complex systems were neither accurate enough to navigate precisely nor capable of operating over a wide area. In order to solve these problems and to provide accurate coverage to entire world, scientists decided to place artificial stars in the sky. This is one of the main ideas behind the development of the United States (US) Global Positioning System (GPS) [1].

Even though GPS was initially developed to satisfy military requirements, today it is widely used in many fields of civilian life. If there is an unobstructed line of sight (LOS) to four or more GPS satellites, it provides reliable position, velocity and time information in all-weather globally. There are also other radio based satellite

navigation systems, but as the Russian global navigation satellite system (GLONASS) is in the process of restoration, the European Union's Galileo positioning system is not scheduled to be operational until 2013 and the Chinese Beidou navigation system is still regional, GPS is the only fully operational, space-based global navigation satellite system (GNSS) in the year 2011.

As the dependency on GPS increases considerably day by day, research efforts on augmentations for GPS become more important in order to overcome deficiencies in availability and accuracy. There are already various types of augmentations available to enhance GPS performance. Pseudolites, which transmit GPS-like ranging signals, can be presented as one of these augmentation systems, particularly in those areas where the LOS to the satellites is restricted. In order to improve the geometry and provide additional ranging signals, pseudolites can be deployed on the ground, in the air or on a ship. Users can then receive and process both GPS and pseudolite signals simultaneously with slight software modifications.

1.2 Problem statement

The high accuracy of the GPS allows for precision navigation in support of current and future military operations. For example, GPS-aided smart weapon systems deliver an unprecedented all-weather strike capability, GPS-based autopilots guide unmanned platforms for near continuous surveillance, and hand held receivers allow coordination among ground forces. However, generating a three-dimensional position using GPS requires a clear LOS between the user and at least four GPS satellites, and so the GPS service can be denied in scenarios such as street surrounded by tall buildings. Due to fact that future wars will take place in urban areas with buildings, there is a need for augmentation in these environments. Compared to ground-based pseudolites, airborne pseudolites can more readily provide and maintain direct LOS to the user. Even though there are several technological challenges in developing airborne pseudolites such as accurately determining and broadcasting the position of pseudolite in a timely manner or adjusting power level of the pseudolite signal to

reduce the effects of interference with the operation of GPS receiver situated closer to the pseudolite, none of them are insurmountable.

The primary goal of this research was to present a conceptual design of the airborne pseudolite augmentation system in order to provide precise positioning in an urban environment. The airborne pseudolite system was then evaluated in terms of accuracy and availability to determine its effectiveness compared to GPS-only configuration. To improve the geometry between the transmitters and receiver, an analysis of the airborne pseudolite location has been carried out. Furthermore, the impact of applying differential corrections to the airborne pseudolite was examined. Finally, the improvement obtained by the addition of second airborne pseudolite to the most challenging environments was investigated.

1.3 Thesis overview

Chapter II presents not only the background for GPS and pseudolites in greater detail, but also related research about pseudolite augmentation systems. In Chapter III, scenario description, assumptions and the structure of the simulation are described. Moreover, a background of position estimation, dilution of precision and availability of GPS are detailed. Chapter III finishes with the discussion about the algorithm and calculations that used to combine GPS satellites and pseudolites. Chapter IV presents the analysis of the data generated by the simulations. Chapter V summarizes the results and provides recommendations for future research on an airborne pseudolite augmentation system.

II. Background

2.1 Overview

This chapter presents the background information for this research and begins with a discussion on the Global Positioning System (GPS) signal structure and measurements, which are similar to pseudolite measurements. The next section introduces the pseudolite definition and describes the differences between GPS and pseudolites. This is followed by the issues and the error sources that emerge with pseudolite applications. The last section of this chapter gives the related research efforts for this study.

2.2 Global Positioning System

GPS is a fully operational space-based global navigation satellite system (GNSS). The system provides reliable, continuous, three-dimensional position and time information to users with the proper receiving equipment in all weather. The satellite constellation is nominally made up of 24 satellites, orbiting in nearly circular orbits and inclined to the equatorial plane at an angle of 55° (±3°). Six orbital planes are used, each having four non-uniformly distributed satellites. The altitude of the satellites is approximately 20,200km and so that each satellites orbital period is 11 hours and 58 minutes, which corresponds to one half of a sidereal day [20]. The satellites broadcast their time and position information on two frequencies using a technique called code division multiple access (CDMA). Though the satellites transmit on the same frequency, each satellite generates a different code than those employed by other satellites. These codes were selected because they have low cross-correlation properties compared to each other and so that the messages from multiple satellites do not interfere with one another. An excellent and detailed overview of the GPS is provided by any number of sources [14, 19, 24].

2.2.1 GPS Signal. Currently, each GPS satellite transmits continuously two types of encoded pseudo-random noise (PRN) signals via using two center frequencies

in the L-band, namely L1 (1575.42 MHz) and L2 (1227.60 MHz) respectively. The L1 channel transmits two signals, one for civil users, and the other for U.S. Department of Defense (DoD) authorized users. Furthermore, three messages are transmitted on L1, the coarse-acquisition (C/A) code, the precise (P) code and the navigation message. On the other hand, the lone signal on L2 is designed for DoD-authorized users only and contains the P code and the navigation message for eliminating the civilian users from full accuracy of the system. It is worthwhile to note that a new military signal called M-code and a new civilian signal called L5 will be available after the GPS modernization project.

Very precise atomic clocks are mounted on the GPS satellites to guarantee the synchronization of the transmitted signal. The three components of signal (called carrier, code and navigation data) are also derived coherently from these atomic clock standards [19]. The satellite's location, which is given through ephemeris data in the navigation message, can be used to determine position of the receiver at the time of signal reception. In order to measure the difference in time between the satellite transmission and the reception of the signal, receivers generate internally a replica of PRN-code and compare it to the incoming PRN-code transmitted by the satellites. However, this measurement does determine the true range to the satellite due to the effects of the clock error. The true range can be found by modifying the original pseudorange measurement for clock and environmental errors. Another measurement to calculate the true position of the receiver is the carrier phase measurement. It is found by tracking of the carrier signal phase component and offer a more precise solution (on the order of centimeters) than the pseudorange measurements. With this type of measurement, the integer number of complete signal cycles that occurred before reception must be determined [9].

2.2.2 Pseudorange Measurements. Pseudorange, commonly called code phase measurement, is the true range between the GPS satellite and the receiver. The pseudorange is calculated by multiplication of the speed of light and the time

difference between the transmission and reception time (to present the range solution in meters) pluses the errors from number of sources. It can be expressed as the following equation [19]:

$$\rho = r + c(\delta t_r - \delta t_{sv}) + T + I + m_\rho + v_\rho \tag{2.1}$$

where

ρ = GPS pseudorange measurement (meters)
r = true range from the user to satellite (meters)
c = speed of light (meters / seconds)
δt_r = receiver (user) clock error (seconds)
δt_{sv} = transmitter (satellite vehicle) clock error (seconds)
T = errors due to tropospheric delay (meters)
I = errors due to ionospheric delay (meters)
m_ρ = errors due to pseudorange multipath (meters)
v_ρ = errors in pseudorange due to receiver noise (meters)

The time errors have a significant impact on the measurement and stem directly from the clocks in the transmitter and the receiver. Since GPS satellites use atomic clocks and estimated corrections uploaded by the Master Control Station (MCS) regularly, the transmitter clock error is very small. However, most receivers have inexpensive and relatively imprecise clocks leading to large clock errors. In order to get an accurate position solution, this receiver clock error must be estimated or rejected by differencing techniques [3].

2.2.3 Carrier-Phase Measurements. The carrier phase measurement for GPS can also be used for positioning, especially when high accuracy is desired. It is much more accurate than the code phase measurement since the phase of a signal can be determined precisely. However, it can be difficult to apply due to the unknown

integer ambiguity. This measurement can be modeled as:

$$\phi = \lambda^{-1}(r + c(\delta t_r - \delta t_{sv}) + T - I + m_\phi + v_\phi) + N \tag{2.2}$$

where

$$\begin{aligned}
\phi &= \text{carrier-phase measurement (meters)} \\
\lambda &= \text{carrier wavelength (meters / cycles)} \\
r &= \text{true range from the user to satellite (meters)} \\
c &= \text{speed of light (meters / seconds)} \\
\delta t_r &= \text{receiver (user) clock error (seconds)} \\
\delta t_{sv} &= \text{transmitter (satellite vehicle) clock error (seconds)} \\
T &= \text{errors due to tropospheric delay (meters)} \\
I &= \text{errors due to ionospheric delay (meters)} \\
m_\phi &= \text{errors due to carrier-phase measurement multipath (meters)} \\
v_\phi &= \text{errors in carrier-phase measurement due to receiver noise (meters)} \\
N &= \text{carrier-phase integer ambiguity (cycles)}
\end{aligned}$$

In terms of their error sources, both the carrier phase equation and the pseudorange equation are very similar to each other. However, some sources of errors have different impacts on them. For instance, errors due to measurement multipath and receiver noise are remarkably less for carrier phase than the pseudorange measurement. Furthermore, the sign of the ionospheric error is reversed from the pseudorange measurement equation. This happens, because the ionosphere advances a carrier phase measurement, but delays a pseudorange measurement and referred to as code-carrier divergence phenomenon [19]. It is important to note that ionospheric delay term is neglected, when using the same measurement for most of the pseudolite applications [3].

The carrier wavelength is a new term and inserted to convert the units of the right hand side of the equation from meters to cycles. Another new term, the carrier-

phase integer ambiguity, stands for the unknown number of carrier cycles that have passed in the signal by the time of reception and must be determined for the high level of accuracy [5].

2.2.4 Carrier-Phase Ambiguity Resolution. Typically, solving for the ambiguities requires enough angular motion between the transmitter and the receiver so as to make the correct ambiguities visible. Because of the fact that the angular motion between the GPS satellites and the user on the earth surface is relatively slow, solution can take up to tens of minutes in GPS applications. In pseudolite applications, contrarily, the angular motion can be significantly faster and the required time period of resolution of the ambiguity may be much shorter [3].

The process of the choosing the correct integer value for the phase ambiguity is called by carrier-phase ambiguity resolution and not always feasible to accomplish. Selection of the wrong integer can cause erroneous results [5]. There are several techniques used to find the integer ambiguities in carrier-phase measurements. The simplest and widely applied technique is to use the pseudorange measurement to restrict the search matrix and to model the ambiguity as a constant [7].

2.2.5 Differential GPS. Differential GPS (DGPS) is used to improve performance via reducing the effect of common errors in GPS measurements. Many error sources in GPS measurements are identical or significantly similar for two nearby receivers and DGPS exploits the correlation of errors between receivers. If GPS error corrections are calculated for a receiver located at a known point, these corrections can be applied to other receivers. DGPS is a general term. There are several different approaches and their possible combinations can be applied. Depending on the approach used, DGPS accuracy can range from 1 meter down to 1 millimeter. Two types of differencing methods are commonly used, the first is single differencing and the second is double differencing.

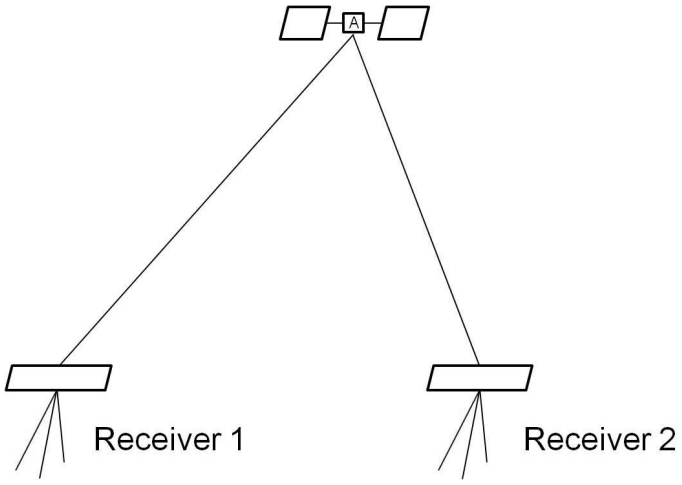

Figure 2.1: Single Difference GPS Measurement Scenario.

2.2.5.1 Single Differencing. Single differencing can be simply defined as the difference of the measurements between one GPS satellite and two receivers, with one receiver placed at a known location as a reference receiver. Figure 2.1 depicts an example of single difference GPS measurement scenario between two receivers.

The notation (Δ) will used for single differencing between two receivers and it can be described as the following equation:

$$\Delta\rho^A_{1,2} = \rho^A_1 - \rho^A_2 \tag{2.3}$$

where ρ^A_1 is the pseudorange measurement between receiver 1 and satellite A, and ρ^A_2 is the pseudorange measurement between receiver 2 and satellite A.

Single differencing eliminates the satellite clock error. Moreover, it also reduces the effects of the error associated with the ephemeris, ionosphere and troposphere. On the other hand, the amount of the error that is cut down by single differencing depends on the baseline distance between the two receivers [7]. Expanding Equation 2.3 with respect to Equation 2.1 yields

$$\begin{aligned}\Delta\rho^A_{1,2} = {} & r^A_1 + c(\delta t^A_{r1} - \delta t^A_{sv1}) + T^A_1 + I^A_1 + m^A_{\rho 1} + v^A_{\rho 1} \\ & -r^A_2 - c(\delta t^A_{r2} - \delta t^A_{sv2}) - T^A_2 - I^A_2 - m^A_{\rho 2} - v^A_{\rho 2}\end{aligned} \tag{2.4}$$

Combining like terms gives

$$\begin{aligned}\Delta\rho^A_{1,2} = (r^A_1 - r^A_2) + c(\delta t^A_{r1} - \delta t^A_{r2}) - c(\delta t^A_{sv1} - \delta t^A_{sv2}) \\ +(T^A_1 - T^A_2) + (I^A_1 - I^A_2) + (m^A_{\rho 1} - m^A_{\rho 2}) + (v^A_{\rho 1} - v^A_{\rho 2})\end{aligned} \tag{2.5}$$

Since the measurements are synchronous and the satellite clock error is the same for both receivers, it is canceled. The remaining differences will be represented as (Δ) and the above single difference pseudorange measurement equation can now be rewritten as

$$\Delta\rho^A_{1,2} = \Delta r^A_{1,2} + c\Delta t^A_{r1,2} + \Delta T^A_{1,2} + \Delta I^A_{1,2} + \Delta m^A_{\rho 1,2} + \Delta v^A_{\rho 1,2} \tag{2.6}$$

The similar technique can be used for single difference carrier-phase measurement and it can be shown in the Equation 2.7.

$$\Delta\phi^A_{1,2} = \phi^A_1 - \phi^A_2 \tag{2.7}$$

$$= \lambda^{-1}(\Delta r^A_{1,2} + c\Delta t^A_{r1,2} + \Delta T^A_{1,2} - \Delta I^A_{1,2} + \Delta m^A_{\phi 1,2} + \Delta v^A_{\phi 1,2}) + \Delta N^A_{1,2} \tag{2.8}$$

Note that, like the single differencing with pseudorange measurement, the satellite clock error is eliminated again. However, the carrier-phase integer ambiguity term is also emerged.

Single differencing will amplify multipath and measurement noise by factor of $\sqrt{2}$ in the GPS case [3, 9].

2.2.5.2 Double Differencing. Double differencing is the difference between two single difference measurements and used to eliminate both satellite and receiver clock error terms. Double difference GPS measurement concept between satellites A and B with receivers 1 and 2 is depicted in Figure 2.2.

Equation 2.6 of single difference pseudorange measurement is used to calculate double difference pseudorange measurement and the resulting equation is presented

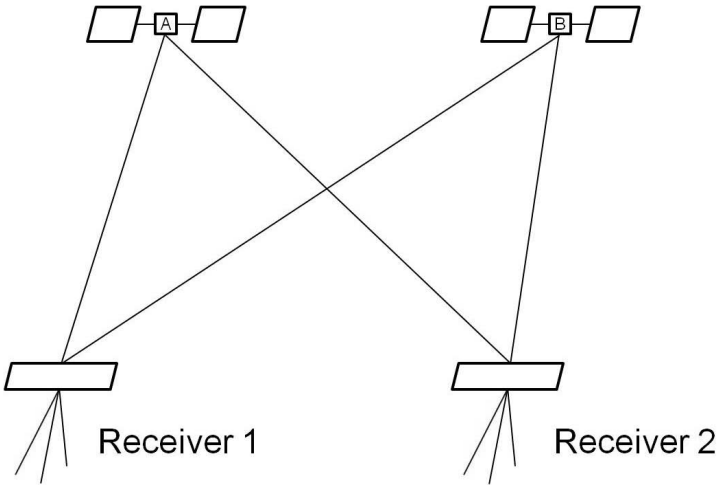

Figure 2.2: Double Difference GPS Measurement Scenario.

as

$$\nabla\Delta\rho_{1,2}^{AB} = \Delta\rho_{1,2}^{A} - \Delta\rho_{1,2}^{B} \tag{2.9}$$

$$= \rho_1^A - \rho_2^A - (\rho_1^B - \rho_2^B) \tag{2.10}$$

$$= \nabla\Delta r_{1,2}^{AB} + \nabla\Delta T_{1,2}^{AB} + \nabla\Delta I_{1,2}^{AB} + \nabla\Delta m_{\rho 1,2}^{AB} + \nabla\Delta v_{\rho 1,2}^{AB} \tag{2.11}$$

The double difference carrier-phase measurement can be adapted from Equation 2.9, which is shown below in Equation 2.12:

$$\nabla\Delta\phi_{1,2}^{A} = \Delta\phi_1^A - \Delta\phi_2^A \tag{2.12}$$

$$= \lambda^{-1}(\nabla\Delta r_{1,2}^{A} + \nabla\Delta T_{1,2}^{A} - \nabla\Delta I_{1,2}^{A} + \nabla\Delta m_{\phi 1,2}^{A} + \Delta v_{\phi 1,2}^{A}) + \nabla\Delta N_{1,2}^{A} \tag{2.13}$$

While double differencing offers additional reduction of the tropospheric and ionospheric errors, it is also magnifying the multipath and measurement noise by factor of 2 [5, 7].

2.3 Pseudolites

The term pseudolite (short for "pseudo-satellite") has been used to describe ground-based transmitters that propagate GPS-like signals. In the late of 1970s, the time when GPS was first developed, researchers proved that ground-based transmitters could serve as an efficient augmentation to the existing satellite based navigation system [12]. Pseudolites were used to verify the operation and the accuracy of the system during the concept demonstration phase of GPS before any satellites were launched [14]. Since then, pseudolites have been used for improving geometry for precise positioning, especially in the vertical component [11].

Pseudolites offer the flexibility to adjust the location, frequency and power of the transmitter. Pseudolites can be placed in a location to augment coverage to adverse environments such as urban canyons, deep open-cut mines and GPS jammed environments where the number of visible satellites may not be enough to determine precise position. Because of the fact that the pseudolite is not a GPS satellite which use atomic clocks and has an altitude of approximately 20,200km, many assumptions made with GPS navigation cannot be applied to it [25]. On the other hand, many of the error sources in the pseudolite measurements are similar to the error sources in GPS measurements. The following sections describe the discussion of differences between pseudolite and GPS navigation, pseudolite equations, pseudolite errors and mobile pseudolites related previous research.

2.3.1 GPS versus Pseudolites. Location of the transmitter is the biggest difference between GPS and pseudolites. GPS transmitters are located on Medium Earth Orbit (MEO) satellites. Pseudolites are positioned much closer to the user and they can be located not only on the ground as a static location, but also on the ship vessels or stratospheric airships as a kinematic location. Other differences between them are listed below.

- Due to the short distances from receivers to pseudolite transmitters compared with GPS operation, the measurement model becomes more non-linear and

may lead to divergence of the computation process. Prior to generate a three-dimensional position using a pseudolite-only system, it is crucial to use knowledge of the initial location of the receiver [7]. Therefore, the effects of non-linearity should be carefully analyzed for the pseudolite-only systems. In this research, initialization is assumed to be sufficient to guarantee convergence.

- In lieu of orbital errors in GPS operation, pseudolite systems are sensitive to offsets in the physical location of the pseudolite and the phase center of the transmitter antenna. Because the airborne pseudolite is navigating itself using GPS in this research, the impact of applying different GPS service types and differential corrections were investigated.
- Multipath can be a challenging problem due to the low elevation angles of the pseudolite transmitters especially in ground-based pseudolite applications. Thus, well designed multipath mitigation techniques may be needed.
- Due to the fact that pseudolite signals do not travel through the ionosphere, the usual ionospheric error is not present.
- Standard tropospheric models are designed for signals from GPS satellites, which are coming from more than 20000km away. Consequently, they cannot be used to compensate for pseudolite operation. Alternative tropospheric delay estimation methods should be needed.
- With regard to the relatively short distance between the user and the pseudolite, the strong signal at the GPS receiver may overwhelm the weak signal from GPS satellite. This dynamic range problem can create major difficulties in receiver design.
- Pseudolites can operate either at GPS L1, L2 and L5, or any other available frequency band. Similarly, other parameters to operate such as chipping rates or code sequences can be different from GPS operation. It is assumed in this research that airborne pseudolite is able to generate complete GPS signal structure for PRN numbers 33 and 34.

2.3.2 Pseudolite equations. The equations for the GPS and pseudolite reference systems are very similar to each other except from the ionospheric error term. Because pseudolites are usually ground based or located close to the earth surface, they do not travel through the ionosphere. Hence, the ionospheric error term can be removed from the pseudorange measurement model when applied to pseudolites. On the other hand, pseudolites typically do not have atomic based clocks and thus the transmitter clock error may be larger than GPS satellites [9]. The equations associated with the pseudolite pseudorange and carrier-phase measurements are represented as

$$\rho = r + c(\delta t_r - \delta t_{pl}) + T + m_\rho + v_\rho \tag{2.14}$$

$$\phi = \lambda^{-1}(r + c(\delta t_r - \delta t_{pl}) + T + m_\phi + v_\phi) + N \tag{2.15}$$

2.3.3 Pseudolite error sources. Although pseudolites offer better GPS signal availability and tremendous geometric flexibility, the short distances between the receivers and pseudolites may cause different error sources, such as near-far problem. The following sections present additional discussion about errors that come along with pseudolite applications and mitigation approaches of these errors.

2.3.3.1 Near-Far Problem. GPS satellites have near-circular orbits around the Earth with an altitude of approximately 20200km. Changes in this relatively large distance between GPS satellite and the typical user due to their motion are negligible. The user receiver usually expects to see the strength of the signal around -130 dBm from all visible GPS satellites. On the other hand, the distance between pseudolites and the user receivers is much shorter, thus, movements of the user may cause significant differences in this distance. Because of the fact that the received power is inversely proportional to the square of the distance between the transmitter and the user, a GPS receiver can see vastly different strengths of the pseudolite signal [13]. With respect to this dynamic range problem, pseudolites deployed to the theater of operation can potentially jam GPS receivers at close distances and limit

the operating range. This problem is schematically depicted in Figure 2.3. The pseudolite signal is too weak to be tracked by receiver at the range of the "far boundary". In contrast, the strong pseudolite signal starts to jam the GPS satellite signals at the "near boundary". Therefore, the receiver must stay between these boundaries in order to navigate with signals from both pseudolite and GPS satellites [8].

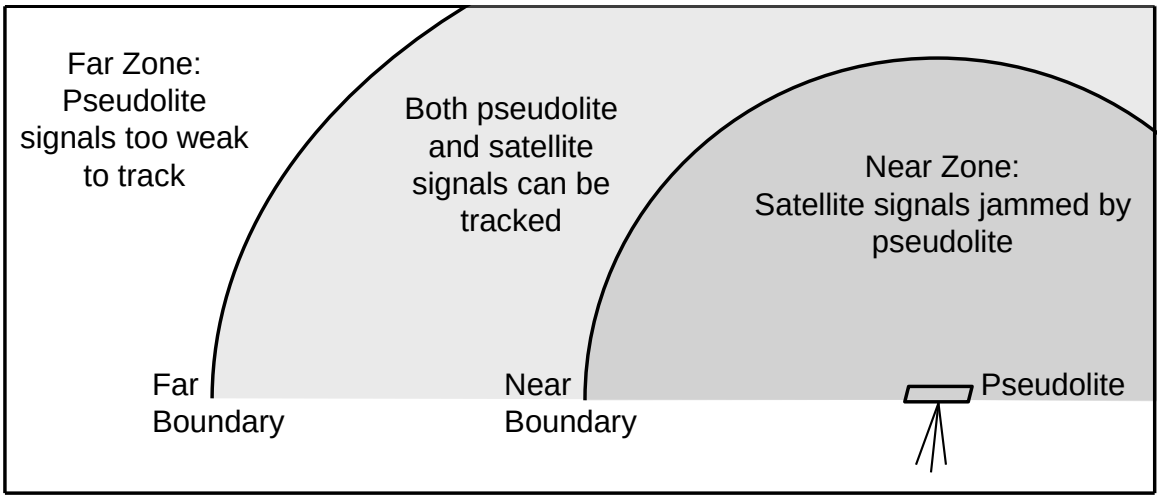

Figure 2.3: Illustration of the Near/Far Problem [8].

Pseudolite signals can be more than 60 dB stronger than GPS signals while the distance between pseudolite and the receiver varies from 50 kilometers to 50 meters. If we assume that pseudolite transmits the signal on C/A code, this is the worst case code separation (21.6 dB). Therefore, approximately 38 dB (60 - 21.6) stronger pseudolite signal can dominate the receiver at 50 meters [12].

Mitigation techniques to the near-far problem are to reduce the interference by sending the pseudolite signals at a different frequencies from GPS as a variation of Frequency Division Multiple Access (FDMA), using a longer code sequence than existing GPS code in CDMA or pulse the signal with random or fixed cycle rates using Time Division Multiple Access (TDMA). The most promising method among these three techniques is to use a pulsing scheme. This reduces the interference approximately 10 dB [13] and allows the GPS receiver to track other signals while in close

distance to a transmitting pseudolite [3]. Instead of applying the preceding mitigation techniques which require additional hardware, using a sophisticated transmit antenna on the pseudolite platform, a directional antenna that shapes its beam to reduce the signal power level over the operating area, can be take into consideration. Additional information about this problem and solution techniques can be found in [8].

2.3.3.2 Multipath Error. Pseudolite-based applications multipath error has similar characteristics with GPS systems. Signals should travel along a direct path from its transmitter antenna to a receiver's antenna. However, the signals at the receiver antenna can be consist of both direct signals and reflected (multipath) signals because of the reflective surrounding objects [3, 9]. These multipath signals, which are delayed comparatively to the direct signal, have variety of power level, phase and polarization with respect to its reflecting surface [13]. In pseudolite applications, conversely to the near-far problem, multipath is an issue for not only GPS users, but also system designers. The amplitude of the multipath error differs with the environment of the application. For ground-based applications, due to the low elevation angles of the transmitters, multipath error is significantly amplified. In a static environment, when both pseudolite and receiver are stationary, the multipath bias is constant and can be accommodated. In kinematic mode, however, the potential multipath biases are not uniform and thus very hard to correct [34].

Though multipath error can be difficult to mitigate, there are several methods to eliminate it. First, appropriately selection of used transmitting and receiving antennas can effectively attenuate multipath signals. Another type of mitigation method is modeling multipath error in software, which can be efficient for static environment but inconvenient for dynamic environments. Lastly, multipath error can also be minimized by receiver correlation techniques [13]. For this research, this issue was addressed by using appropriate transmitting and receiving antennas.

2.3.3.3 Synchronization. Each GPS satellite has three or four onboard cesium or rubidium atomic clocks. Block II and IIA satellites have carried

two of each. Block IIR satellites carry three rubidium standards. MCS monitors the performance of the each clock onboard and uploads estimated corrections to the satellites as a part of the navigation message at least once a day [19]. These corrections are used by the GPS receivers to correct for the clock drifts. In contrast, most pseudolites have typically inexpensive, less precise temperature compensated crystal oscillators (TCXO). With respect to insufficient precision of these oscillators, asynchronously operating pseudolite-only systems cannot provide accurate positioning. The most commonly used technique is to eliminate pseudolite and receiver clock biases is double-differencing with a reference receiver. However, this brings about operational constraints due to the requirement of the data link between the user and reference receivers. Moreover, all pseudolites used in the system must have to visibility with the reference receiver for precise positioning. A good discussion about the pseudolite synchronization can be found in [13]. In this research, the pseudolite was approximately synchronized to GPS time through a GPS receiver installed on airborne platform for the navigation of the airborne platform itself. The detailed resulting synchronization error will be investigated in Section 3.8.

2.3.3.4 Tropospheric Error. A large error source of the pseudolite applications stems from the tropospheric delay, incurred while the signal propagates through the portion of the atmosphere between 0km and 10km. Because of the spatial variations in atmospheric pressure, humidity and temperature, modeling of lower troposphere is very difficult [33]. Severity of the signal's delay depend upon the refractivity index of the air mass, which is function of the density of the wet and dry components of the air in troposphere [19]. As the dry portion of the air density contributes roughly 90% of the delay, wet air density, which is much difficult to predict, accounts for only 10% [3].

Typically, the tropospheric error is compensated by applying a model such as Saastamoinen, Hopfield or Biberger models. The transmitter elevation angle is one of the critical elements for these models. Although the delay is calculated at zenith

angle, mapping functions are used to transform the result for the desired elevation angles. However, all these methods, which are designed for signals from GPS satellites, can be insufficient for ground-based pseudolite operations, because the mapping functions gives inaccurate solutions at lower elevation angles. Pseudolite applications require more applicable models for further reduction of tropospheric error. Due to fact that mitigation models do not significantly remove tropospheric delay, its error contribution has been assumed as equal as the Standard Positioning Service (SPS)-GPS service for the simulations in this study. More detailed information can be found in [5].

2.3.3.5 Location Errors and Geometry. Even though near-far, multipath, synchronization and tropospheric errors are accepted as the main challenges in pseudolite applications, there are other issues that stem from the design of the specific application. Pseudolite transmitter antenna location is one of these issues. A detailed discussion about the impact of pseudolite location errors in positioning was demonstrated by Wang and Lee [35]. Slight error of pseudolite location may cause large error in the measurements models and so effects the final positioning solution. Furthermore, the experienced impacts differ with the geometry between the pseudolite and the receiver. This error adds a bias into the pseudolite measurements in static mode. In kinematic applications, however, single-differenced measurement errors can be much worse than the pseudolite location error with respect to the geometry. In order to acquire precise navigation and positioning solution, the pseudolite antenna has to be mounted accurately on a stable platform [13]. In this research, the airborne pseudolite location is determined by the airborne platform reference GPS receiver and this location is transmitted on the pseudolite signal to the ground user through the ephemeris algorithm. Consequently, ephemeris error will be maximum during the airborne pseudolite's intended maneuvers and unintended motion caused by high wind buffeting.

Another challenging issue that needs to be addressed for precise navigation solutions is obtaining proper transmitter-receiver geometry. Solely poor geometry may cause the largest error source of the system. In the GPS case, transmitters are located on satellites at a distance of more than 20000km with desirable elevation angles between 10° and 90° in all directions. However, when a GPS satellite is setting or rising, it appears to be on the horizon relative to the receiver with low elevation angle. Even though the position error is usually not affected by a single low elevation angle satellite since there are always other visible satellites with higher elevation angles, poor positioning solution can be yielded when all measurements are at low elevation angles. Augmentation of GPS with pseudolites is one of the main reasons of this problem and pseudolites can efficiently improve the geometry. On the other hand, the pseudolite-only systems, especially ground-based ones, have large errors due to their geometric deployment in vertical direction. Proper deployment of pseudolites in a specific geographic area is critical to obtaining precise navigation and positioning solution [9].

2.4 Related Research

The general idea of a pseudolite is older than the GPS system itself. Pseudolites were originally invented to test the GPS concept at a desert test range, even before the first satellite, Navstar 1, launched in 1978 [8]. New concepts related with pseudolites have been introduced for a diversity of navigation and positioning applications during the past decades. The research efforts of the ground-based pseudolites have been conducted over a long period of time. In 1985, pseudolites have been introduced to improve GPS signal geometry for mobile receivers [10]. In the next decade, 1995, the application of airborne pseudolites was suggested by Raquet at al. [22]. H. Stewart Cobb built a basic ground-based pseudolite and accomplished a fruitful experiment in 1997 [8]. Chris Rizos showed that pseudolites could augment the GPS positioning accuracy and was a beneficial supplement tool to the satellite based positioning systems [23]. On the other hand, the research of mobile pseudolite had started and

progressed more recently. This section presents an overview of the previous research in mobile pseudolite concepts and recent improvements in mobile pseudolite positioning applications.

A team at Holloman Air Force Base, New Mexico, invented a concept of an inverted GPS system, which used fixed receivers at known points and a mobile pseudolite [22]. The main intention of this system was to provide a realistic reference trajectory for aircrafts in order to precisely test other navigation systems. By positioning the receivers on the ground, they not only gained flexibility and reduced the cost, but also took the advantage of increased resistance to GPS jamming. These receivers tracked signals from the mobile pseudolite and the GPS satellites simultaneously. A central computer processed the received signals and generated trajectory of the pseudolite mounted test vehicle. Their results showed that it is feasible to provide instantaneous position of a mobile pseudolite precisely by ground-based inverted GPS systems.

Jason B. McKay and Meir Pachter determined that the accuracy of the generated trajectory by the inverted GPS systems is limited by the geometry of ground-based receiver array. Their research aimed to optimize the receiver array configuration to minimize the overall system's sensitivity and increase the accuracy of the trajectory produced [17,18]. Instead of using Geometric Dilution of Precision (GDOP), they focused on the condition number of the visibility matrix H to find good receiver array configurations. The results of their research demonstrated that geometric sensitivity to measurement error in the ground-based inverted GPS systems can be reduced via an appropriate array configuration.

More recently, a group from The Swedish Defence Research Agency investigated collaborative GPS/inertial navigation system (INS) navigation techniques in an urban environment, which are based on communication between the two unmanned ground vehicles (UGV) [4]. They worked principally two different navigation techniques, simultaneous localization and mapping (SLAM)/INS and GPS/INS. SLAM/INS was

based on measurements of the environment, which use a range measuring device such as laser range finder. Hence, it's performance good in an environment where the user stands among objects with desirable geometrical features such as buildings. On the other hand, GPS/INS offers the best performance on clear visibility of GPS satellites, e.g. outside of the urban environments.

Edward LeMaster worked with Stephen Rock at Stanford University to develop a local-area GPS pseudolite-based navigation system for a Mars rover [16]. They invented a new navigation system which was named as self-calibrating pseudolite array (SCPA). Even though SCPA navigation applies differential GPS technique, it does not use traditional GPS satellites or pseudolites. Instead of using separate receivers and pseudolites, the main elements of SCPA are GPS transceivers. They placed at least three stationary transceivers over a local area and other mobile transceivers determined their 2-dimensional positions inside of that area with respect to them. Their process also takes place in the class of applications which is known as SLAM and is applied to variety of robotic applications.

Zheng Wang and his team at the Chinese Academy of Sciences researched a new simultaneous locating and calibrating algorithm for the pseudolite based mobile navigation system [36]. Their system was composed of a pseudolite-array with stationary transceivers and a mobile transceiver which is attached to a robot. The major problem with their system was determining simultaneously the accurate position of the stationary transceivers and accurate trajectory of the mobile robot. They applied the Unscented Kalman Filter algorithm to deal with this problem.

Jeffrey Tuohino and his team carried out military pseudolite field-tests [29]. Even though the military pseudolites provide accurate GPS navigation in hostile territories, there are still a number of issues that must be mitigated such as line-of-sight visibility and pseudolite geometry. These problems can be solved by military pseudolites which are deployed on airborne platforms. However, this brings about the problem of precisely transmitting the pseudolite position to the receivers. Not only

intended maneuvers, but also unintended movements due to air turbulence make the ephemeris algorithms highly dynamic for airborne platforms.

An airborne pseudolite ephemeris algorithm, which meets this requirement, was built by the joint design effort between Rockwell Collins and Massachusetts Institute of Technology Lincoln laboratory. They successfully performed two flight test demonstrations with two different airborne platforms, a Saberliner-50 aircraft at Cedar Rapids, IA and a Hunter UAV at the EPG Test Range in Ft. Huachuca, AZ. Besides a single airborne pseudolite operated from an airborne platform, three additional ground pseudolites were used to augment the GPS positioning of the receivers. While first flight demonstration in November focused on characterizing the receiver's navigation accuracy using pseudolites, a main impact point of the second UAV flight test was to concentrate on pseudolite working performance in the jamming environment. The results of these flight tests indicated that airborne pseudolite based navigation performance is compatible with satellite based navigation [29].

Jay Sklar offered a military pseudolite system as an alternative approach to the adaptive antenna systems for more robust performance of GPS operation [26]. It is pointed out in his paper that a set of four pseudolite mounted airborne platforms serve many users than any of each adaptive antenna system. Moreover, the result of the overall system not only cut down the total cost, but also reduce the GPS signal interference better than widely deployed adaptive antenna systems. Issues which must be taken into consideration for pseudolite operation such as near-far problem were also summarized by Jay Sklar. Since the signal transmitted by the pseudolites is stronger than the GPS satellite signals, users in the theater, who are not modified for receiving pseudolite signal, will interfere with pseudolite-ready receivers operation. He stressed that the impacts of these problems will depend on the transmitted power of the pseudolite.

Toshiaki Tsujii and his team from University of New South Wales worked with Masatoshi Harigae to propose a concept of a new GPS navigation and positioning

system augmented by pseudolites installed on high altitude platform systems, such as the stratospheric airship and the high altitude unmanned aerial vehicle [28]. The advantages of pseudolites mounted on stratospheric airships rather than the ground-based pseudolite systems were presented. Since the distance between the receiver and the pseudolite is from 20km to 100km in their concept, the dynamic range is much less, thus the "near-far" problem is not severe as with ground-based pseudolite applications. Furthermore, the elevation angle is higher than the ground-based pseudolites, so the multipath problem is not a serious problem. However, they determined that the most challenging issue for this concept is the accurate positioning of the pseudolite antenna. In this paper, three different methodologies were offered for this problem. They introduced the term of GPS *transceiver*, which combines the function of a GPS receiver and pseudolite. In order to estimate relative positions among them, such GPS transceivers can communicate and synchronize each other. Even though the GPS transceiver method seems the best approach to the problem, they conducted an experimental test for the inverted-GPS approach as a preliminary feasibility study. Their research showed that the static mode provided excellent positioning stability while the kinematic mode suggested the need of further investigations.

Later, Toshiaki Tsujii and his team at Japan Aerospace Exploration Agency carried out flight tests to augment the GPS positioning, which were the first flight tests using a helicopter mounted pseudolite as a signal transmitting source [27]. The inverted-GPS method was applied to prove the results. Pseudolite ephemeris data was successfully generated and it was verified that the pseudolite signal was considerably similar with GPS signal. Their results revealed that a pseudolite installed on station-keeping flying vehicle such as the stratospheric airship or the high altitude unmanned aerial vehicle can be used like an orbiting GPS satellite.

Most recently, Burri Chandu and his team at Indian Institute of Technology, Bombay, investigated the modeling and simulation of a precise navigation system based on pseudolites installed on stratospheric airship platforms [6]. Their concept consisted of four pseudolites mounted on stratospheric airships, six ground stations,

and a control station in order to determine the position of a moving aerial vehicle within a specific coverage area without depending on GPS signals. With respect to the results of this paper, it is clear that the errors in determination of pseudolite antenna position amplify the errors in user position.

In this thesis, in contrast with the previous research efforts which mostly used several pseudolites and various layouts of several ground stations, only one airborne pseudolite's impact on a military GPS receiver's positioning accuracy in challenging GPS environments will be investigated with a preference toward not using any reference stations or data links.

2.5 Summary

This chapter has provided a basic overview of the United States (US) GPS including the signal structure and measurements. Afterwards, the pseudolite definition has been introduced in depth. Challenges and issues of pseudolite applications have also been described. Lastly, relevant literature review has been covered to accomplish this research. The next chapter will discuss the design of the simulation used in this research along with the methodology.

III. Methodology and Algorithm Development

3.1 Overview

This chapter begins by laying out the initial set up and design of the simulation, including the scenario, assumptions and simulation steps. Immediately following the initial set up, it develops the estimation of position based on measurements of pseudoranges along with the weighted least squares method. Next, dilution of precision (DOP) and availability terms are introduced. After covering the determination of system error budgets in Section 3.8, this chapter ends with a description of the algorithm that was used to combine Global Positioning System (GPS) satellites and pseudolite.

3.2 Scenario

The world's urban population growing at a rate four times that of its rural population, and by 2050, two-thirds of the earth's population, over 6 billion people, will be living in towns and cities [2]. Anna Tibaijuka, former executive director of the United Nations human settlements programme stated in the World Urban Forum 2010 that the world will be 70 percent urban by 2050, based on the average daily rural and urban population increases.

While populations are shifting from rural to urban areas, centers of gravity of many conflicts such as tribal, ethnic or ideological is shifting to urban areas too. With respect to a variety of recent urban operations in different places around the world such as Panama City, Grozny and Sarajevo, it is obvious that future military operations will have an urban component.

Due to their physical and social sophistication, urban areas are not only tremendously difficult to operate in, but also mostly avoided by armed forces. Where these kinds of operations are inevitable, aerospace forces can make crucial contributions to the ground forces by detecting hostile forces and providing navigation and communication relays for improving their situational awareness [32].

In this scenario, it is assumed that a military Precise Positioning Service (PPS) GPS user is executing operations in an urban environment while a military pseudolite deployed on an airborne platform is augmenting the GPS system to provide accurate navigation to the user. In the preceding paragraphs, urban military operations have described in a broader meaning. In the next subsections, operational and tactical challenges of urban physical environment will be characterized.

3.2.1 Urban Terrain Zones. Buildings, streets and other man-made constructions dominate urban terrain. Even though these structures have certain basic similarities, they differ considerably in height, size, type of construction, etc. One of the most striking characteristics of the urban terrain, the dimensions of buildings and other man-made structures, significantly limits line of sight (LOS). A GPS user standing in the middle of a wide-straight street bordered on both sides by one story buildings can see sufficient GPS satellites to determine a precise position. On the other hand, a GPS user who is in the center of a deep urban canyon and bordered on both sides by high buildings cannot see adequate amount of GPS satellites to provide accurate navigation [32].

The number of GPS satellites visible to the user over the buildings will depend on the height of the buildings and the distance between the buildings. The taller the surrounding buildings, the lower amount of GPS satellites that will be visible to the user. Similarly, reducing the spacing between the buildings will reduce coverage by GPS satellites [32]. These relationships are illustrated in Figure 3.1.

Figure 3.2 gives a basic example of how to determine the elevation mask angle for a user standing at the middle of two buildings. Line AB is one-half of the average street width and line BC is the average building height. Elevation mask angle can be defined as angle θ and can be calculated by the arctangent function of the height of triangle ABC divided by its base ($\theta = atan(\frac{BC}{AB})$). The satellites that have equal or higher elevation angles than the computed elevation mask angle will be considered visible. Similarly, azimuth angle can be defined and calculated with respect to the

length and the width of the buildings. In this research, due to the great potential for the multipath problems and atmospheric delay at lower elevations, a minimum elevation mask angle is set at 5°. Hence if the satellite's azimuth angle is inside of the computed azimuth angle restrictions and it has an equal or higher elevation angle than 5°, it will be accepted as visible and tracked by the user.

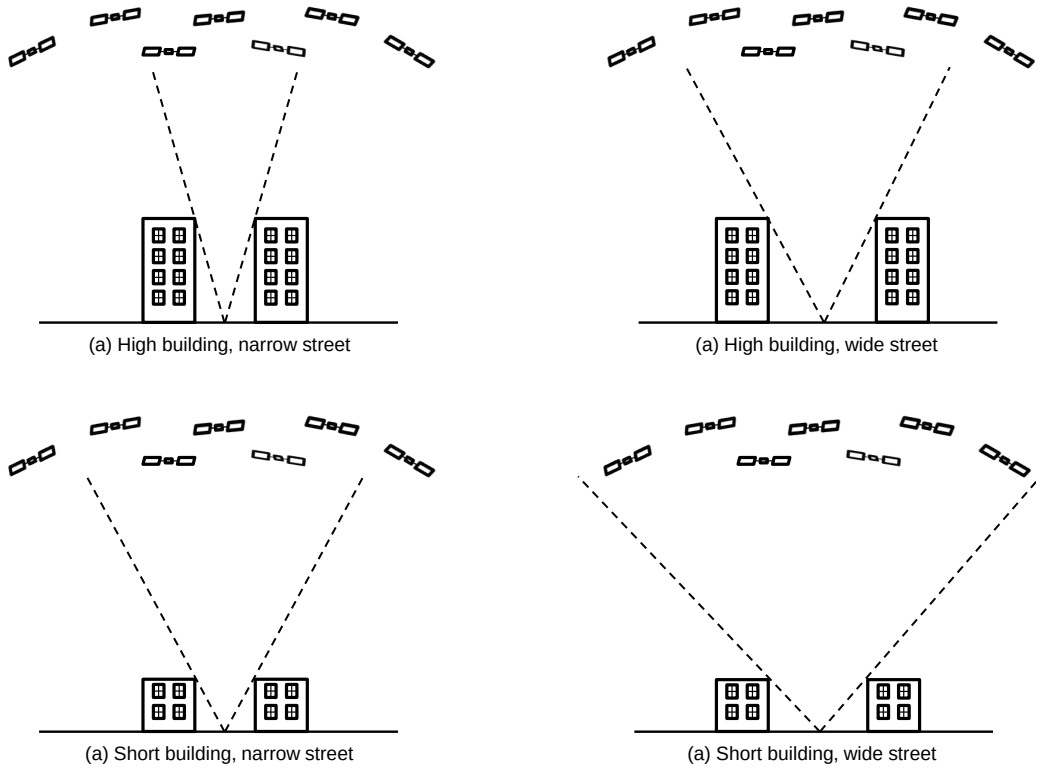

Figure 3.1: Building Height and Street Width Affect Visible Satellites.

Dr. Richard Ellefsen, a geography professor at San Jose State University, tried to develop a militarily useful urban terrain classification system in the late 1970s and early 1980s. He looked through the physical characteristics and patterns found in different parts of sample cities around the world and defined his Urban Terrain Zones (UTZ) based on vast data on the size, height, separation, etc. of the buildings. In his latest study, he used 14 different cities throughout the world for samples and defined seven new UTZ classifications [32]. The new UTZ classifications and their typical location within a city are listed in Table 3.1.

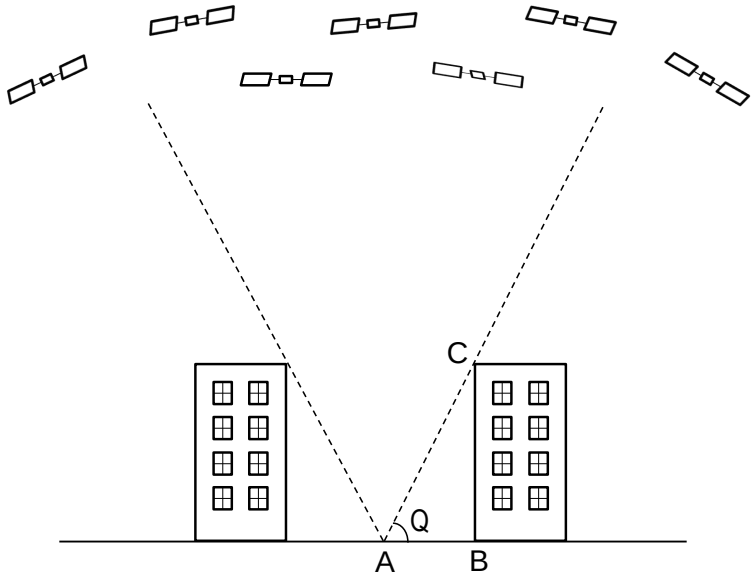

Figure 3.2: Determining Elevation Mask Angle.

Table 3.1: Urban Terrain Zone Classification System [32]

	Urban Terrain Zone (UTZ)	Typical Location Within City
I	Attached and Closely Spaced Inner-City Buildings	City Core
II	Widely Spaced High-Rise Office Buildings	City Core and Edge of Built-Up City (e.g.,near airports)
III	Attached Houses	Near City Core
IV	Closely Spaced Industrial/Storage Buildings	Along Railroads Near Core and on Docks
V	Widely Spaced Apartment Buildings	Edge of City
VI	Detached Houses	Near Core and in Suburbs
VII	Widely Spaced Industrial/Storage Buildings	At City Edge Near Highways

Figure 3.3 illustrates that the studied cities are build up mostly of detached houses and widely spaced apartment buildings. Although the word city is more likely to be associated with attached and closely spaced buildings (UTZ I) or widely spaced high-rise office buildings (UTZ II), these zones cover only 4 percent of the total area of the cities studied. On the flip side of the coin, the most valuable, important and cultural structures are located in these small UTZs. Consequently, they are not only attractive, but also focus of adversary actions during urban operations. Besides, due to their enormously limited LOS characteristics, an adversary can take advantage of these city cores to challange allied forces operations [32]. For this reason, widely spaced high-rise office buildings (UTZ II) is selected for as the primary urban terrain in this scenario. A military PPS-GPS user will try to execute operations with GPS-aided equipments at different locations on streets between tall buildings. Second, detached houses (UTZ VI), where the user can see much more GPS satellites, is chosen in order to give a different perspective to the readers.

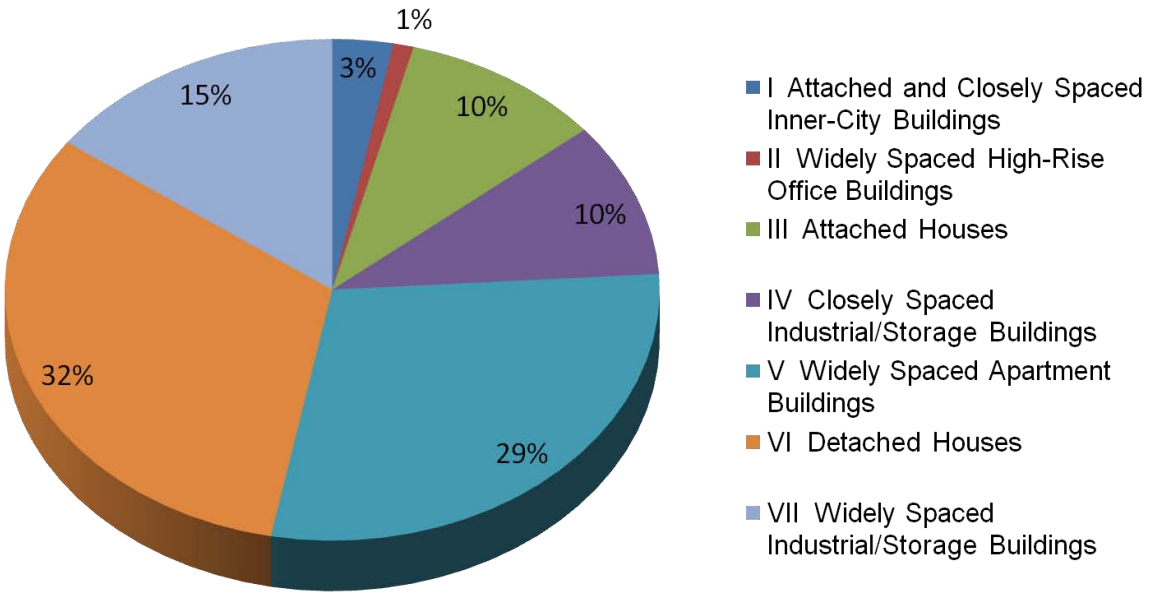

Figure 3.3: Proportion of Surveyed Cities in Each UTZ [32].

As well as determining the fraction of city area that split into each UTZ, Dr. Ellefsen quantified several building features such as average building height, footprint, pitch or flat roof, and separation between buildings. His values for these building features are demonstrated in Table 3.2.

Table 3.2: Building Features by Urban Terrain Zone [32]

UTZ Type	Footprint (m^2)	Avg. Height (m)	Roof Type	Avg. Seperation (m)
I	2000	30	Flat	5
II	4000	45	Flat	30
III	500	6	Both	20
IV	4000	9	Both	25
V	1000	20	Flat	50
VI	100	6	Both	15
VII	10000	9	Pitch	70

With the goal of enhancing GPS availability for the user in urban terrain by a military pseudolite, which is mounted on an airborne platform, and after the preceding discussion about urban form as background, it is worthwhile to take a look at what kind of ground-based threats should we expect and how it effects the operational altitude and range of the pseudolite mounted airborne platform. Because this research will define operating conditions for this scenario, the next subsection discusses different aspects of urban air defenses.

3.2.2 Air Defenses on Urban Terrain. The most common threats to aerospace operations over urban environments are man portable air defense systems (MANPADS), small arms and smaller mobile surface-to-air-missiles (SAM) such as SA-8 or Stinger.

Even though some small radar-guided SAM systems can be deployed to urban areas, the presence of tall buildings creates intense clutter on their radar's field, thus their normal capabilities are restricted dramatically. Similarly, unless deployed on top of buildings, large anti-aircraft artilleries, which require several personnel and must be towed or vehicle-mounted, could not take advantage of their effective range. Hence,

shoulder-launched SAMs, small arms and other light infantry weapons are likely to be the primary threats against air assets operating over urban environment [32].

The best way to survive over well air-defended urban terrain is to keep out of the effective altitudes and ranges of these threats. Whereas most of the small arms can be lethal below 3,000 feet (ft), the shoulder-launched MANPADS introduce the biggest threat with effective altitudes up to 20,000 ft and ranges between 3 and 4 nautical miles. These small missile systems, typically equipped with infrared guidance, can be carried, targeted and launched by single operator. On the other hand, due to the fact that MANPADS rely on visual target detection, it may be difficult to detect a target even if it is within effective engagement range and/or attack prior to launch. Missed target engagement chances may be particularly problematic when engaging small unmanned air vehicles (UAV) with minimal heat signatures.

Imagine armed forces are executing a joint military operation with other fixed-wing aircrafts, helicopters, and ground troops in urban environment. Pseudolite-mounted unmanned air platforms may also required to enhance GPS availability for ground troops operating in a joint military operation with other fixed-wing aircrafts, helicopters. In this mission, altitude deconfliction constrains the unmanned air platforms to maintain altitudes below the manned aircrafts. Comparatively large unmanned air platforms operating from ground level to altitudes of 10,000 ft, such as Predator or Global Hawk would be extremely vulnerable to a MANPADS. Not only are these air platforms clearly visible, but also even the oldest MANPADS are significantly accurate and effective at these altitudes. While they may be suitable for some low-threat environments, as the threat level increases, a different type of UAVs are required. Because of these reasons, in this scenario, smaller, quieter, inexpensive unmanned air platforms with very low visibility and infrared signature, such as low-altitude mini-UAVs are chosen to mount pseudolite on it and deployed to operate at 1,000 ft above ground level (AGL) over urban terrain.

3.3 Assumptions

The following assumptions are made in this thesis:

- All 32 GPS satellites in constellation are operational and active.
- The ground user is using a PPS-GPS receiver in order to determine an accurate position in an urban environment.
- The airborne pseudolite is also equipped with a GPS receiver which it uses to determine its own position and to synchronize its clock with GPS time.
- The airborne pseudolite is flying at 1,000 ft AGL, hence all GPS satellites are clearly visible to it.
- The pseudolite is using the same carrier frequency, PRN codes 33 to 36 and navigation message protocol as those of GPS satellites. Thus user can receive and process both GPS and pseudolite signals simultaneously with slight software modifications.
- The power level of pseudolite transmitter is adjusted to not interfere with satellite signals in the working area.

3.4 Simulation Steps

Because of the fact that GPS is currently fully operational, real ephemeris data throughout the United States, its territories, and a few foreign countries can be provided by the National Geodetic Survey (NGS), which manages a network of Continuously Operating Reference Stations (CORS). In this research, 24 hours of real GPS ephemeris data with intervals of 30 seconds, which was collected by Dayton, OH site of CORS at 14th of October 2010, is downloaded from the website of NGS and used in simulation steps. The GPS satellite's Earth-Centered-Earth-Fixed (ECEF) coordinates, that are obtained from real ephemeris data, are converted to geodetic coordinates (longitude, latitude and altitude) by the built in Matlab® function called *ecef2lla*. After acquiring geodetic coordinates for both user and GPS satellites, the

elevation angle, slant range, and azimuth angle of GPS satellites as viewed from user are computed by the *elevation* function in Matlab®.

Three dimensional models of different urban environments with variety of building heights, footprints and street widths are designed in Solidworks® environment and according to these dimensions, azimuth and elevation mask angles are determined for several user positions between buildings. A Matlab® script is written to determine line of sights from satellite vehicles to various user positions. If the GPS satellite's elevation angle is larger than the computed elevation mask angle and the azimuth angle is within computed azimuth mask angle restrictions, than it is considered as visible to user for that time period. An array of possible pseudolite mounted air platform locations at a specific altitude are defined over the user and same method is used to detect visible ones.

Position dilution of precision (PDOP) values are calculated in Matlab® environment with respect to the location of both visible GPS satellites and airborne pseudolites. A comparison between the performances of GPS only system and an airborne pseudolite augmented system was presented for various positioning scenarios. Geometric analysis of the optimal airborne pseudolite location was examined. Moreover, the impact of the applied different service types and differential corrections to the reference GPS receiver of the airborne platform was investigated. Ultimately, addition of the second airborne pseudolite to the most challenging urban environments was analyzed

3.5 Position Determination with Pseudoranges

Prior to solving for three dimensional user position, satellite-to-receiver range determination with non-synchronized clocks must be resolved. In Chapter II, a number of different error sources that affect range measurements accuracy such as multipath and tropospheric delays were examined. On the other hand, all these error sources can be considered negligible in pseudorange measurement equations, when

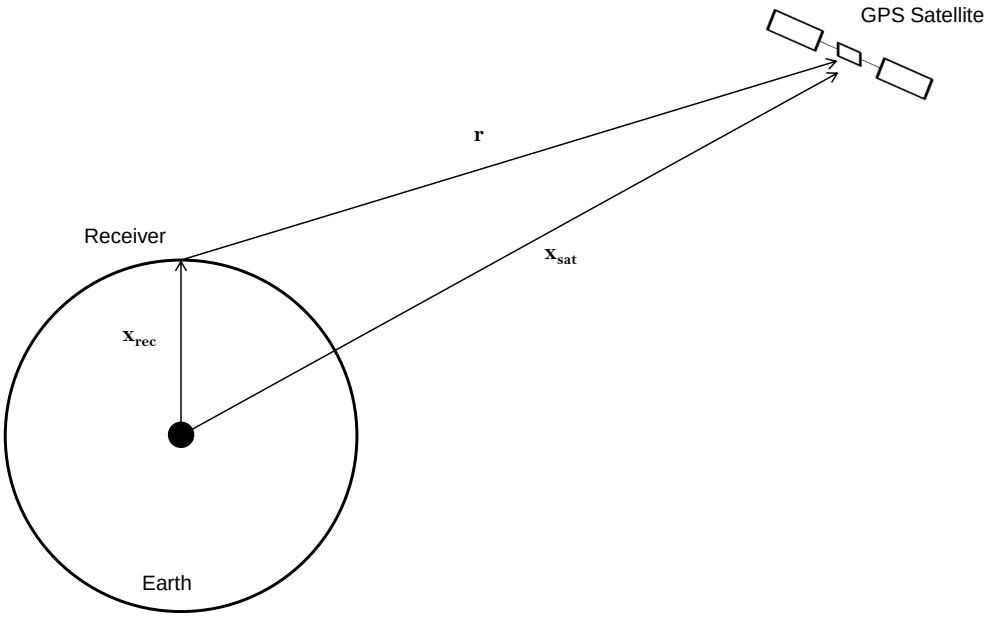

Figure 3.4: Vector Demonstration of Receiver Position.

compared to the errors stem from clock offset between GPS satellite's very precise atomic clocks and receiver's less stable quartz clocks. In this research, all error sources other than clock offset are taken into consideration in system error budget calculations.

It is desired to determine vector $\mathbf{x_{rec}}$, which indicates a receiver's position according to the ECEF Cartesian coordinate system origin in Figure 3.4. Therefore, the receiver's position coordinates x_r, y_r, z_r within the ECEF Cartesian coordinate system are considered unknown. The satellite is located at coordinates x_s, y_s, z_s and vector $\mathbf{x_{sat}}$, which is computed using ephemeris data broadcast by the satellite, shows the position of the satellite with respect to the ECEF Cartesian coordinate system origin. The satellite to receiver vector $\mathbf{r}$ is

$$\mathbf{r} = \mathbf{x_{sat}} - \mathbf{x_{rec}} \tag{3.1}$$

If r indicates the magnitude of $\mathbf{r}$, it can be written as:

$$r = \| \mathbf{x_{sat}} - \mathbf{x_{rec}} \| \tag{3.2}$$

If we assume that the receiver clock error t_r is the only remaining error, the pseudorange ρ can be computed by the true range r plus the multiplication of receiver clock error and the signal propagation velocity (assumed to be the speed of light).

$$\rho = \| \mathbf{x_{sat}} - \mathbf{x_{rec}} \| + \ ct_r \tag{3.3}$$

In view of the pseudorange measurement equation which includes four unknowns: three components of x_{sat} and t_r, at least four equations are required to solve for four unknowns. In other words, a minimum four satellites are required to determine the receiver's instantaneous position in three dimensions (x_r, y_r, z_r) and the receiver clock error t_r. Thus, Equation 3.3 can be expanded as:

$$\begin{aligned} \rho_k &= \sqrt{(x_k - x_r)^2 + (y_k - y_r)^2 + (z_k - z_r)^2} + ct_r \\ &= f(x_r, y_r, z_r, t_r) \end{aligned} \tag{3.4}$$

where x_r, y_r, z_r, and t_r are unknowns and k ranges from 1 to K for referencing the GPS satellites in view. In order to solve these K nonlinear equations, a simple approach of iterative technique based on linearization can be useful. The idea is to start with approximate estimates of receiver position $(\hat{x}_r, \hat{y}_r, \hat{z}_r)$ and receiver clock error $\hat{t}_r$, and refine them iteratively until the estimates fit the measurements sufficiently. Knowing roughly where the receiver is, the true position (x_r, y_r, z_r) can be computed from the approximate position of receiver by a displacement $(\Delta x_r, \Delta y_r, \Delta z_r)$. With respect to the approximate estimates of receiver position $(\hat{x}_r, \hat{y}_r, \hat{z}_r)$ and receiver clock error $\hat{t}_r$,

an approximate pseudorange can be represented by

$$\begin{aligned} \hat{\rho}_k &= \sqrt{(x_k - \hat{x}_r)^2 + (y_k - \hat{y}_r)^2 + (z_k - \hat{z}_r)^2} + c\hat{t}_r \\ &= f(\hat{x}_r, \hat{y}_r, \hat{z}_r, \hat{t}_r) \end{aligned} \tag{3.5}$$

where the true position of receiver and the receiver clock error are:

$$\begin{aligned} x_r &= \hat{x}_r + \Delta x_r \\ y_r &= \hat{y}_r + \Delta y_r \\ z_r &= \hat{z}_r + \Delta z_r \\ t_r &= \hat{t}_r + \Delta t_r \end{aligned} \tag{3.6}$$

and the vector form is

$$\mathbf{x_r} = \hat{\mathbf{x}}_\mathbf{r} + \mathbf{\Delta x_r} \tag{3.7}$$

Thus, it can be written that:

$$f(x_r, y_r, z_r, t_r) = f(\hat{x}_r + \Delta x_r, \hat{y}_r + \Delta y_r, \hat{z}_r + \Delta z_r, \hat{t}_r + \Delta t_r) \tag{3.8}$$

If right-hand side of Equation 3.8 is linearized by using a first order Taylor series expansion:

$$\begin{aligned} f(\hat{x}_r + \Delta x_r, \hat{y}_r + \Delta y_r, \hat{z}_r + \Delta z_r, \hat{t}_r + \Delta t_r) = f(\hat{x}_r, \hat{y}_r, \hat{z}_r, \hat{t}_r) \\ + \frac{\partial f(\hat{x}_r, \hat{y}_r, \hat{z}_r, \hat{t}_r)}{\partial \hat{x}_r} \Delta x_r + \frac{\partial f(\hat{x}_r, \hat{y}_r, \hat{z}_r, \hat{t}_r)}{\partial \hat{y}_r} \Delta y_r \\ + \frac{\partial f(\hat{x}_r, \hat{y}_r, \hat{z}_r, \hat{t}_r)}{\partial \hat{z}_r} \Delta z_r + \frac{\partial f(\hat{x}_r, \hat{y}_r, \hat{z}_r, \hat{t}_r)}{\partial \hat{t}_r} \Delta t_r \\ + Higher\ Order\ Terms \end{aligned} \tag{3.9}$$

The higher order partial derivatives can be neglected to eliminate nonlinear terms. The partial derivatives evaluate as follows:

$$\begin{aligned}
\frac{\partial f(\hat{x}_r, \hat{y}_r, \hat{z}_r, \hat{t}_r)}{\partial \hat{x}_r} &= -\frac{x_k - \hat{x}_r}{\hat{r}_k} \\
\frac{\partial f(\hat{x}_r, \hat{y}_r, \hat{z}_r, \hat{t}_r)}{\partial \hat{y}_r} &= -\frac{y_k - \hat{y}_r}{\hat{r}_k} \\
\frac{\partial f(\hat{x}_r, \hat{y}_r, \hat{z}_r, \hat{t}_r)}{\partial \hat{z}_r} &= -\frac{z_k - \hat{z}_r}{\hat{r}_k} \\
\frac{\partial f(\hat{x}_r, \hat{y}_r, \hat{z}_r, \hat{t}_r)}{\partial \hat{t}_r} &= c
\end{aligned} \tag{3.10}$$

where

$$\hat{r}_k = \sqrt{(x_k - \hat{x}_r)^2 + (y_k - \hat{y}_r)^2 + (z_k - \hat{z}_r)^2} \tag{3.11}$$

Using Equation 3.5 and Equation 3.10 into Equation 3.9, yields linearization of pseudorange equation with respect to the unknowns $\Delta x_r, \Delta y_r, \Delta z_r$ and Δt_r as:

$$\rho_k = \hat{\rho_k} - \frac{x_k - \hat{x}_r}{\hat{r}_k}\Delta x_r - \frac{y_k - \hat{y}_r}{\hat{r}_k}\Delta y_r - \frac{z_k - \hat{z}_r}{\hat{r}_k}\Delta z_r + c\Delta t_r \tag{3.12}$$

If Equation 3.12 is rearranged with the known quantities on the left and unknowns on the right side, we get:

$$\hat{\rho_k} - \rho_k = \frac{x_k - \hat{x}_r}{\hat{r}_k}\Delta x_r + \frac{y_k - \hat{y}_r}{\hat{r}_k}\Delta y_r + \frac{z_k - \hat{z}_r}{\hat{r}_k}\Delta z_r - c\Delta t_r \tag{3.13}$$

This expression can be simplified by introducing new variables where:

$$\begin{aligned}
\Delta\rho &= \hat{\rho_k} - \rho_k \\
a_{xk} &= \frac{x_k - \hat{x}_r}{\hat{r}_k} \\
a_{yk} &= \frac{y_k - \hat{y}_r}{\hat{r}_k} \\
a_{zk} &= \frac{z_k - \hat{z}_r}{\hat{r}_k}
\end{aligned} \tag{3.14}$$

The direction cosines of the unit vector pointing from the approximate receiver position to the k^{th} GPS satellite are symbolized by the a_{xk}, a_{yk}, and a_{zk} terms in Equation 3.14. With respect to these new variables, Equation 3.13 can be rewritten as:

$$\Delta\rho_k = a_{xk}\Delta x_r + a_{yk}\Delta y_r + a_{zk}\Delta z_r - c\Delta t_r \tag{3.15}$$

The unknown quantities: $\Delta x_r, \Delta y_r, \Delta z_r$ and Δt_r, can be determined by solving the set of linearized equations for the same K measurements:

$$\begin{aligned}
\Delta\rho_1 &= a_{x1}\Delta x_r + a_{y1}\Delta y_r + a_{z1}\Delta z_r - c\Delta t_r \\
\Delta\rho_2 &= a_{x2}\Delta x_r + a_{y2}\Delta y_r + a_{z2}\Delta z_r - c\Delta t_r \\
\Delta\rho_3 &= a_{x3}\Delta x_r + a_{y3}\Delta y_r + a_{z3}\Delta z_r - c\Delta t_r \\
\vdots &= \vdots \\
\Delta\rho_K &= a_{xK}\Delta x_r + a_{yK}\Delta y_r + a_{zK}\Delta z_r - c\Delta t_r
\end{aligned} \tag{3.16}$$

The set of K linear equations can be expressed in matrix notation by introducing the new definitions where

$$\mathbf{\Delta}\rho = \begin{bmatrix} \Delta\rho_1 \\ \Delta\rho_2 \\ \Delta\rho_3 \\ \vdots \\ \Delta\rho_K \end{bmatrix}, \mathbf{H} = \begin{bmatrix} a_{x1} & a_{y1} & a_{z1} & 1 \\ a_{x2} & a_{y2} & a_{z2} & 1 \\ a_{x3} & a_{y3} & a_{z3} & 1 \\ \vdots & \vdots & \vdots & \vdots \\ a_{xK} & a_{yK} & a_{zK} & 1 \end{bmatrix}, \text{ and } \mathbf{\Delta x} = \begin{bmatrix} \Delta x_r \\ \Delta y_r \\ \Delta z_r \\ -c\Delta t_r \end{bmatrix}$$

Finally, we can get the compact equation as

$$\mathbf{\Delta}\rho = \mathbf{H}\mathbf{\Delta x} \tag{3.17}$$

which has the solution, for $K = 4$:

$$\mathbf{\Delta x} = \mathbf{H^{-1}}\mathbf{\Delta}\rho \tag{3.18}$$

In this equation, $\mathbf{\Delta x}$ is user position displacement vector, $\mathbf{H}$ is measurement matrix and $\mathbf{\Delta}\rho$ is pseudorange difference vector.

If $K = 4$, four equations for four unknowns can be solved directly and the user's coordinate's x_r, y_r, z_r and the receiver clock error t_r can be computed by using Equation 3.6.

If K is lower than four or the equations are linearly dependant, then the $\mathbf{H}$ will be rank-deficient and Equation 3.18 cannot be solved for $\mathbf{\Delta x}$. On the other hand, with the GPS constellation of 24 or more satellites, such situations are seldomly seen and receiver has an over-determined system of equations.

If the sky is unobstructed for the receiver, more than four GPS satellites are visible and improved estimation of the unknowns can be obtained by using least-squares estimation techniques. The least-squares solution can be written as

$$\mathbf{\Delta x} = (\mathbf{H^T H})^{-1}\mathbf{H^T \Delta}\rho \tag{3.19}$$

The new estimates of the receiver position is

$$\mathbf{\hat{x}_{r_{new}}} = \mathbf{\hat{x}_{r_{old}}} + \mathbf{\Delta x} \tag{3.20}$$

The solution may be iterated until receiver's estimated position is sufficiently close to true position and the change in the estimates is small. Each iteration lead a new estimation based upon the old value and the corrections. Typically, the estimates converge quickly. The acceptable displacements are determined by the receiver's accuracy requirements.

It is important to stress that least-squares solution assumes all independent measurements are of equal quality and share the same variance. However, this assumption practically never true. For those situations where the measurements do not identically distributed or independent of each other, weighted least squares can be

applied. The weighted least square of Equation 3.19 is

$$\mathbf{\Delta x} = (\mathbf{H^T W H})^{-1}\mathbf{H^T W \Delta}\rho \tag{3.21}$$

where $\mathbf{W}$ is a weight matrix with diagonal elements. Because of the applied weight affects not only the measurement, but also the final navigation solution slightly, different weight values should be assigned to all measurements for different systems in order to obtain realistic solutions. For the purpose of this research, it is assumed that the measurements from different satellites and the pseudolite do not contain a bias and are independent from each other. In this way, it can be written that

$$\mathbf{W} = \mathbf{R^{-1}} \tag{3.22}$$

where $\mathbf{R^{-1}}$ is the inverse of the covariance matrix [14, 19, 31].

It is worthwhile to note that if we have equal confidence in all measurements, then $\mathbf{R}$ is simply the identity matrix and weighted least squares problem is transformed into a least squares problem.

3.6 Dilution of Precision in GPS

Even though the concept of DOP originated from the Loran-C navigation system users, the term DOP has been widely used with the GPS system. In the case of GPS, the concept of DOP is the idea that GPS satellites-user relative geometry affects the position error that results from measurement errors. The more convenient geometry provides lower DOP value. Furthermore, the lower DOP and the lower measurement error together improve the quality of the position solution. [14, 15, 19].

GPS receivers provide position solution by the process of determining where several spheres intersect. Each GPS satellite is located at the center of the sphere and the distance from the GPS satellite to the receiver is calculated as the radius of the sphere. If these spheres intersect exactly at one point, only one possible solution

is computed for current position. On the other hand, this assumption never true in reality, and the intersection of these spheres take an odd shape. Figure 3.5 demonstrates an area created by the intersection of three GPS satellites and the receiver's real position can be located at any point within the gray-colored area.

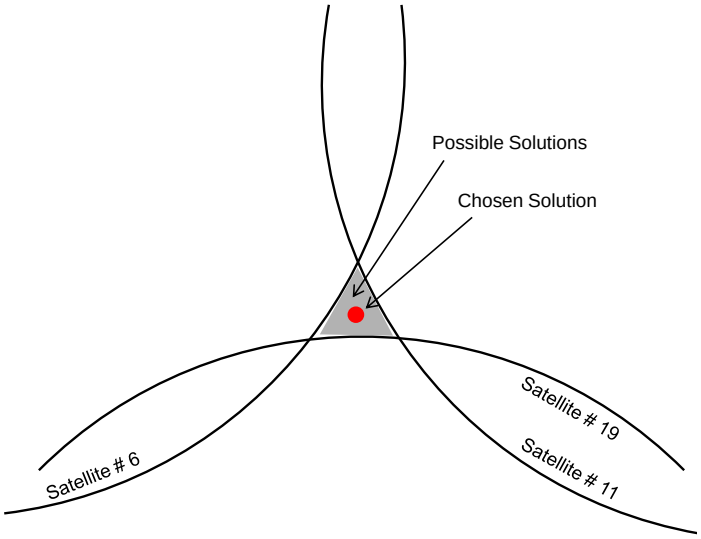

Figure 3.5: One of Several Possible Position Solution must be chosen by GPS Receiver.

If the area expands larger, precision of the receiver's current location becomes diluted. We can prevent from this situation by either adding more visible GPS satellites to the system or placing GPS satellites evenly distributed throughout the sky. Figure 3.6 illustrates that in order to build a high precision environment with low DOP value, three more evenly distributed GPS satellites added to the system [21].

Derivation of DOP relations in GPS stem from the linearization of the pseudorange equations given in previous section. If the pseudorange errors are considered to be random variables, Equation 3.19 states $\mathbf{\Delta x}$ as a random variable functionally dependant on $\mathbf{\Delta}\rho$. It is generally assumed that the elements of error vector $\mathbf{\Delta}\rho$ are zero mean and jointly Gaussian. If the geometry is assumed fixed, then the $\mathbf{\Delta x}$ is also zero mean and Gaussian [14]. Substituting from Equation 3.19, while assuming

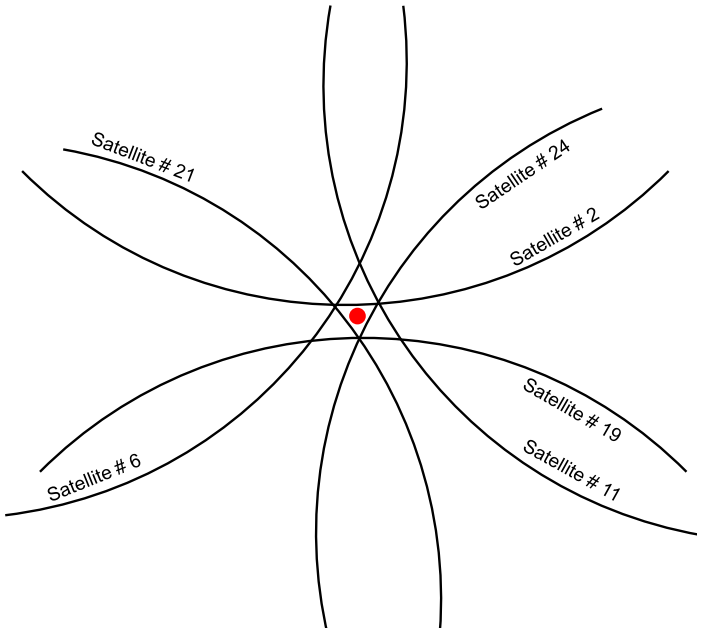

Figure 3.6: High Precision Environment with Low DOP Created by Addition of Three Evenly-Distributed Satellite.

the geometry as fixed

$$\mathrm{Cov}\{\mathbf{\Delta x}\} = \mathrm{Cov}\{(\mathbf{H^T H})^{-1}\mathbf{H^T}\mathbf{\Delta}\rho\} \tag{3.23}$$

Due to $\mathrm{Cov}\{\mathbf{A\Delta}\rho\} = \mathbf{A}\,\mathrm{Cov}\{\mathbf{\Delta}\rho\}\mathbf{A^T}$, one obtains

$$\mathrm{Cov}\{\mathbf{\Delta x}\} = (\mathbf{H^T H})^{-1}\mathbf{H^T}\,\mathrm{Cov}\{\mathbf{\Delta}\rho\}\mathbf{H}(\mathbf{H^T H})^{-1} \tag{3.24}$$

Once more, the general assumption that the measurement errors are identically distributed, independent and have a variance equal to the square of the satellite user equivalent range error (UERE), then the covariance of $\mathbf{\Delta}\rho$ takes the form of

$$\mathrm{Cov}\{\mathbf{\Delta}\rho\} = \mathbf{I}\sigma^{\mathbf{2}}_{\mathbf{UERE}} \tag{3.25}$$

Thus, Equation 3.24 can be rewritten as

$$\mathrm{Cov}\{\mathbf{\Delta x}\} = (\mathbf{H^T H})^{-1}\sigma^2_{\mathbf{UERE}} \tag{3.26}$$

Similarly, substituting from Equation 3.21 for the weighted least squares problem, the covariance of weighted measurements can be expanded as

$$\begin{aligned} \mathrm{Cov}\{\mathbf{\Delta x}\} &= \mathrm{Cov}\{(\mathbf{H^T W H})^{-1}\mathbf{H^T W}\mathbf{\Delta}\rho\} \\ &= \mathrm{Cov}\{(\mathbf{H^T R^{-1} H})^{-1}\mathbf{H^T R^{-1}}\mathbf{\Delta}\rho\} \end{aligned} \tag{3.27}$$

With regard to the fact that $\mathrm{Cov}\{\mathbf{A\Delta}\rho\} = \mathbf{A}\,\mathrm{Cov}\{\mathbf{\Delta}\rho\}\mathbf{A^T}$, the Equation 3.27 becomes

$$\begin{aligned} \mathrm{Cov}\{\mathbf{\Delta x}\} &= (\mathbf{H^T R^{-1} H})^{-1}\mathbf{H^T R^{-1}}\,\mathrm{Cov}\{\mathbf{\Delta}\rho\}\mathbf{R^{-T} H}(\mathbf{H^T R^{-1} H})^{-\mathbf{T}} \\ &= (\mathbf{H^T R^{-1} H})^{-1}\mathbf{H^T R^{-1}}\sigma^2_{\mathbf{UERE}}\mathbf{R R^{-1} H}(\mathbf{H^T R^{-1} H})^{-1} \\ &= (\mathbf{H^T R^{-1} H})^{-1}\mathbf{H^T R^{-1} H}(\mathbf{H^T R^{-1} H})^{-1}\sigma^2_{\mathbf{UERE}} \\ &= (\mathbf{H^T R^{-1} H})^{-1}\sigma^2_{\mathbf{UERE}} \end{aligned} \tag{3.28}$$

As stated earlier, the vector $\mathbf{\Delta x}$ has four components, x_r, y_r, z_r and ct_r. The covariance of $\mathbf{\Delta x}$ is a 4x4 matrix and can be defined as

$$\mathrm{Cov}\{\mathbf{\Delta x}\} = \begin{bmatrix} \sigma^2_{x_r} & \sigma_{x_r y_r} & \sigma_{x_r z_r} & \sigma_{x_r ct_r} \\ \sigma_{x_r y_r} & \sigma^2_{y_r} & \sigma_{y_r z_r} & \sigma_{y_r ct_r} \\ \sigma_{x_r z_r} & \sigma_{y_r z_r} & \sigma^2_{z_r} & \sigma_{z_r ct_r} \\ \sigma_{x_r ct_r} & \sigma_{y_r ct_r} & \sigma_{z_r ct_r} & \sigma^2_{ct_r} \end{bmatrix} \tag{3.29}$$

The user position has been estimated in the ECEF Cartesian coordinate frame till now. However, the ECEF coordinates are not easy for user to assess position error. Instead of working with ECEF coordinate frame, the user position usually converted to geodetic coordinates: latitude, longitude and height. This approach is generally more meaningful to a user for understanding position error [19]. Therefore, the $\mathbf{H}$ matrix should be modified in order to define errors relative to the local east-north-up (ENU) coordinate frame.

A position vector can be transformed from ECEF to ENU by direction cosine matrix (DCM) and it can be represented as

$$\mathbf{C_E^G} = \begin{bmatrix} -sin\lambda_0 & cos\lambda_0 & 0 \\ -sin\phi_0 cos\lambda_0 & -sin\phi_0 sin\lambda_0 & cos\phi_0 \\ cos\phi_0 cos\lambda_0 & cos\phi_0 sin\lambda_0 & sin\phi_0 \end{bmatrix} \tag{3.30}$$

where λ is the longitude and ϕ is the latitude in ENU coordinate frame.

New $\mathbf{H^G}$ matrix for DOP calculations can be obtained by transforming "a" vectors, unit line-of-sight vectors between receiver and satellite, from ECEF frame to ENU frame using DCM

$$\mathbf{a^G} = \mathbf{C_E^G a^E} \tag{3.31}$$

After obtaining $\mathbf{H^G}$ matrix, the covariance matrix of $\mathbf{\Delta x}$ becomes

$$\mathrm{Cov}\{\mathbf{\Delta x}\} = \begin{bmatrix} \sigma_E^2 & \sigma_{NE} & \sigma_{EU} & \sigma_{Ect_r} \\ \sigma_{EN} & \sigma_N^2 & \sigma_{NU} & \sigma_{Nct_r} \\ \sigma_{EU} & \sigma_{NU} & \sigma_U^2 & \sigma_{Uct_r} \\ \sigma_{Ect_r} & \sigma_{Nct_r} & \sigma_{Uct_r} & \sigma_{ct_r}^2 \end{bmatrix} \tag{3.32}$$

The Geometric Dilution of Precision (GDOP) is the most common parameter and represented by the equation

$$\sqrt{\sigma_E^2 + \sigma_N^2 + \sigma_U^2 + \sigma_{ct_r}^2} = GDOP \times \sigma_{UERE} \tag{3.33}$$

which has the form of general formula that estimates error in GPS solution

$$(error\ \ in\ \ GPS\ \ solution) = (geometry\ \ factor) \times (pseudorange\ \ error\ \ factor) \tag{3.34}$$

The matrix $(\mathbf{H^T H})^{-1}$ is called the DOP matrix and the components of it not only quantify measurement errors to position errors, but also provide a relationship for GDOP. The DOP matrix provides a simple characterization of the GPS satellite-user geometry and has an expanded representation of

$$(\mathbf{H^T H})^{-1} = \begin{bmatrix} D_{11} & D_{12} & D_{13} & D_{14} \\ D_{21} & D_{22} & D_{23} & D_{24} \\ D_{31} & D_{32} & D_{33} & D_{34} \\ D_{41} & D_{42} & D_{43} & D_{44} \end{bmatrix} \tag{3.35}$$

GDOP can be computed from the DOP matrix

$$GDOP = \sqrt{D_{11} + D_{22} + D_{33} + D_{44}} \tag{3.36}$$

It is clear from Equation 3.36 that GDOP is merely a function of satellite-user geometry. It stands for the amplification factor of the measurement errors onto the solution [19].

There are several other DOP parameters commonly used for different applications. These are defined by PDOP, horizontal dilution of precision (HDOP), vertical dilution of precision (VDOP) and time dilution of precision (TDOP). These DOP parameters can be defined with satellite UERE and components of the covariance matrix of $\mathbf{\Delta x}$ in ENU coordinate frame as

$$\begin{aligned} \sqrt{\sigma_E^2 + \sigma_N^2 + \sigma_U^2} &= PDOP \times \sigma_{UERE} \\ \sqrt{\sigma_E^2 + \sigma_N^2} &= HDOP \times \sigma_{UERE} \\ \sigma_U &= VDOP \times \sigma_{UERE} \\ \sigma_{ct_r} &= TDOP \times \sigma_{UERE} \end{aligned} \tag{3.37}$$

These DOP values can also be represented in terms of the elements of DOP matrix as

$$\begin{aligned} PDOP &= \sqrt{D_{11} + D_{22} + D_{33}} \\ HDOP &= \sqrt{D_{11} + D_{22}} \\ VDOP &= \sqrt{D_{33}} \\ TDOP &= \sqrt{D_{44}} \end{aligned} \tag{3.38}$$

Because the PDOP is best amongst the other DOP parameters to characterize the 3 dimensional positioning errors, it was chosen as the comparison criteria in this research.

3.7 Availability of GPS

Availability of a navigation system can be defined as the ability to provide accaptable navigation service to the users within a particular area. Both the physical characteristics of the terrain and the system capabilities have strong impacts on the

availability. In order to describe a navigation system as an available, its accuracy would meet the required threshold criteria.

With respect to Equation 3.34, GPS accuracy is generally expressed as the product of a geometry factor and pseudorange error factor. Thus, the number of visible satellites for a particular area and time of the day, geometry between these visible satellites and the user must be determined at the beginning. Additionally, the azimuth and elevation angle of the terrain that may block the satellite signal must be described accurately in order to ensure a precise determination of the number of visible satellites [14].

Desired accuracy level designates the threshold criteria for the availability of a navigation system. For this research, the threshold of the maximum acceptable PDOP value is assigned to 6, which is generally approved as an availability threshold for GPS service [30].

3.8 System Error Budget

There are several sources of error that affect pseudorange and carrier-phase measurements. This section will not provide an examination of these error sources, but instead summarize developing the pseudorange error budgets to aid our understanding of pseudolite augmented GPS accuracy. As represented earlier in Equation 3.34, error in the GPS solution is a function of both the geometry factor and the pseudorange error factor. The geometry factor (DOP) is discussed in the previous section.

In order to analyze the impacts of errors on position accuracy, the errors are generally expressed in terms of their impact on individual satellites pseudoranges. The combined effect of these error sources on pseudorange measurements is termed as the user range error (URE), also known as the UERE, and it can be defined as the root-sum-square of each error sources related with a given satellite [14].

Table 3.3 shows estimates of typical UERE budgets for different GPS services. Acronyms used in the Table 3.3 stand for the type of GPS service that they be-

long to such as standard positioning service (SPS), PPS, local area differential GPS (LADGPS) and carrier phase differential GPS (CPDGPS). It is important to stress that the error budgets presented in Table 3.3 are approximate numbers and the actual values vary for different measurement scenarios. For example, a user placed near reflectors may double the size of the error due to multipath. Similarly, residual ionospheric error may expand extremely for a single-frequency receiver during high solar activity [14].

Table 3.3: Typical UERE Budgets for different GPS services

	$1\sigma Error(length)$			
Error Source	SPS	PPS	LADGPS	CPDGS
Broadcast clock	1.1 m	1.1 m	0.0 m	0.0 m
L1 P(Y) L1 C/A group delay	0.3 m	0.0 m	0.0 m	0.0 m
Broadcast ephemeris	0.8 m	0.8 m	0.1-0.6 mm	0.1-0.6 m
Residual ionospheric error	7.0 m	0.1 m	0.2-4 cm	0.2-4 cm
Residual tropospheric error	0.2 m	0.2 m	1-4 cm	1-4 cm
Receiver noise and resolution error	0.1 m	0.1 m	0.1 m	0.2-0.4 cm
Multipath	0.2 m	0.2 m	0.2 m	0.3-0.6 cm
System UERE	7.1372 m	1.3964 m	0.2306 m	0.0578 m

The UERE is generally assumed to be identically distributed from satellite to satellite and so independent. However, this assumption is not appropriate for every situation. For instance, in case of the addition of airborne pseudolite to the GPS constellation, the UERE associated with the pseudolite should be modified with a different variance than the standard GPS satellites.

Care must be taken in precise positioning by a pseudolite-augmented GPS system. Effects of error sources on pseudolite measurements should be investigated cautiously for determining the UERE budget.

Because the pseudolite mounted air platform is located well below than the ionospheric region of the atmosphere, where is between approximately 70 km and 1000 km above the Earth's surface, the signal from it does not suffer from the ionospheric

delay. This characteristic can offer a great advantage for the cases where the solar activity is significantly high.

The tropospheric error for the pseudolite mounted air platform signal is similar to the GPS signal since the tropospheric region of the atmosphere is located under the ionosphere. On the other hand, the standard tropospheric delay models cannot be applied to compensate for pseudolite tropospheric delay. The model parameters are designated for signals from the GPS satellites. Therefore, pseudolite applications require alternative tropospheric delay estimation methods [28]. It is assumed in this research that the tropospheric error of pseudolite system error budget has the same value as the SPS-GPS service.

Receiver noise and multipath error also exist on the pseudolite measurements and present similar characteristics with GPS system. Hence, it is assumed that these error sources have the same magnitude with the PPS-GPS service in pseudolite system error budget. Unique signal structures and pulsing schemes can be applied to reduce the effects of energy jamming. Similarly, good hardware design, including the receiver and pseudolite transmitter antennas, and software-based mitigation techniques help to mitigate multipath efficiently.

The accuracy of the pseudolite's position depends on the movement of pseudolite's airborne platform and is a limiting factor. Due to the lower altitude of airborne pseudolite, broadcast ephemeris error is more serious than for GPS satellites. In case of the ground-based, stationary pseudolite augmentation systems, this error is not significant since the actual location of the pseudolite transmitter antenna can be determined accurately by conventional positioning techniques. However, because the airborne pseudolite is always moving, continuously positioning and precisely broadcasting it's coordinates to the receiver is crucially necessary. Thus, the broadcast ephemeris error dominates the resulting error budget [28].

Another key element of the pseudolite system UERE budget is pseudolite time synchronization error. This term can be defined as the ability of the pseudolite to

align its transmitted signal to GPS time. Due to the lower stability of pseudolite clock compared to the GPS atomic clocks, the drift error of pseudolite clock plays an important role in the error budget calculations [29].

The quality of estimated user position error and clock bias error that obtained from an instantaneous measurement can be expressed as

$$3-D\ \ Position\ \ estimation\ \ error\ \ =\ \ \sigma_{UERE} \times PDOP \tag{3.39}$$

$$Clock\ \ bias\ \ estimation\ \ error\ \ =\ \ \sigma_{UERE} \times TDOP \tag{3.40}$$

where σ_{UERE} values vary between different GPS systems such as SPS, PPS, LADGPS or CDGPS [19]. In other words, the type of GPS receiver system mounted on the air platform determines the σ_{UERE} value used in calculations of pseudolite system's UERE budget. In order to determine PDOP and TDOP parameters for the pseudolite system, first, an airborne pseudolite was defined at 1000 ft AGL altitude over working area. Second, LOS from GPS satellite vehicles to the airborne pseudolite were determined and visible GPS satellites were detected for 24 hours of real GPS ephemeris data with intervals of 30 seconds. After achieving DOP matrices for each time interval, desired PDOP and TDOP parameters computed by Equation 3.37 and then one final value of each DOP parameter were obtained based on the average of all computed values for 24 hours. The resulting error budgets are listed in Table 3.4.

Table 3.4: Pseudolite system UERE Budgets for different receivers

	$1\sigma Error(length)$			
Error Source	SPS	PPS	LADGPS	CPDGS
Broadcast clock	5.6935 m	1.1139 m	0.1839 m	0.0461 m
L1 P(Y) L1 C/A group delay	0.3 m	0.0 m	0.0 m	0.0 m
Broadcast ephemeris	11.2507 m	2.2012 m	0.3635 m	0.0911 m
Residual ionospheric error	0.0 m	0.0 m	0.0 m	0.0 m
Residual tropospheric error	0.2 m	0.2 m	0.2 m	0.2 m
Receiver noise and resolution error	0.1 m	0.1 m	0.1 m	0.1 m
Multipath	0.2 m	0.2 m	0.2 m	0.2 m
System UERE	12.6164 m	2.4852 m	0.5059 m	0.3169 m

3.9 Combining GPS Satellites and Pseudolites

With respect to Equation 3.15, pseudorange equations for "k" GPS and "n" pseudolite can be expressed as follows:

$$\begin{aligned}
\Delta\rho_{1GPS} &= a_{x1GPS}\Delta x_r + a_{y1GPS}\Delta y_r + a_{z1GPS}\Delta z_r - c\Delta t_{rGPS} \\
\Delta\rho_{2GPS} &= a_{x2GPS}\Delta x_r + a_{y2GPS}\Delta y_r + a_{z2GPS}\Delta z_r - c\Delta t_{rGPS} \\
\vdots &= \vdots \\
\Delta\rho_{kGPS} &= a_{xkGPS}\Delta x_r + a_{ykGPS}\Delta y_r + a_{zkGPS}\Delta z_r - c\Delta t_{rGPS}
\end{aligned} \tag{3.41}$$

$$\begin{aligned}
\Delta\rho_{1Pseudo} &= a_{x1Pseudo}\Delta x_r + a_{y1Pseudo}\Delta y_r + a_{z1Pseudo}\Delta z_r - c\Delta t_{rPseudo} \\
\Delta\rho_{2Pseudo} &= a_{x2Pseudo}\Delta x_r + a_{y2Pseudo}\Delta y_r + a_{z2Pseudo}\Delta z_r - c\Delta t_{rPseudo} \\
\vdots &= \vdots \\
\Delta\rho_{nPseudo} &= a_{xnPseudo}\Delta x_r + a_{ynPseudo}\Delta y_r + a_{znPseudo}\Delta z_r - c\Delta t_{rPseudo}
\end{aligned}$$

In this research, it was stated earlier that the pseudolite-mounted air platform is self-surveying its own location via GPS operation. Thus, it is assumed that there is no time-offset between ephemeris data broadcasted by GPS satellites and pseudolites.

The new $\mathbf{H_{SYST}}$ matrix can be defined by

$$\mathbf{H_{SYST}} = \begin{bmatrix} a_{x1Pseudo} & a_{y1Pseudo} & a_{z1Pseudo} & 1 \\ \cdots & \cdots & \cdots & \vdots \\ a_{xnPseudo} & a_{ynPseudo} & a_{znPseudo} & 1 \\ a_{x1GPS} & a_{y1GPS} & a_{z1GPS} & 1 \\ \cdots & \cdots & \cdots & \vdots \\ a_{xkGPS} & a_{ykGPS} & a_{zkGPS} & 1 \end{bmatrix} \tag{3.42}$$

where a_i represent the direction cosines of unit vectors pointing from the receiver to the GPS satellites and pseudolites.

The DOP matrix also need to be redefined with respect to new $\mathbf{H_{SYST}}$ matrix as

$$DOP = (\mathbf{H_{SYST}}^{\mathbf{T}}\mathbf{H_{SYST}})^{-\mathbf{1}} \tag{3.43}$$

Nevertheless, different measurements from GPS satellites and pseudolites are not independent from each other or identically distributed. Hence, different weights must be assigned to all measurements. Equation 3.22 dictates that the weight matrix $\mathbf{W}$ is equal to inverse of the covariance matrix $\mathbf{R}$. On the other hand, this covariance matrix $\mathbf{R}$ also needs to be modified in order to combine pseudolite with the GPS satellites [31]. The variance of the k^{th} GPS measurement error is symbolized by σ^2_{kGPS} and similarly, the variance of the n^{th} pseudolite measurement error is symbolized by $\sigma^2_{nPseudo}$. Then, the covariance matrix of the measurements can be expanded as

$$\mathbf{R} = \begin{bmatrix} \sigma^2_{1Pseudo} & 0 & \cdots & 0 & \cdots & 0 \\ 0 & \ddots & 0 & \cdots & & \vdots \\ \vdots & 0 & \sigma^2_{nPseudo} & 0 & & 0 \\ 0 & & 0 & \sigma^2_{1GPS} & 0 & \\ \vdots & & \cdots & 0 & \ddots & 0 \\ 0 & \cdots & 0 & \cdots & 0 & \sigma^2_{kGPS} \end{bmatrix} \tag{3.44}$$

The new DOP matrix influenced by $\mathbf{H_{SYST}}$ and the covariance matrix of the measurements becomes

$$DOP = (\mathbf{H_{SYST}}^{\mathbf{T}}\mathbf{R}^{-\mathbf{1}}\mathbf{H_{SYST}})^{-\mathbf{1}} \tag{3.45}$$

After obtaining the DOP matrix, desired DOP parameters can be calculated by the equations given at previous section.

3.10 Summary

In this chapter, big picture of the scenario, assumptions and the structure of the simulation have been introduced. The details of the algorithms and calculation process have been discussed. In the next chapter, the results obtained from the simulation and analysis will also be presented.

IV. Results and Discussion

4.1 Overview

This chapter presents simulation results and an analysis of the effectiveness of airborne pseudolites. The first section provides the scenario descriptions and visibility analysis of Global Positioning System (GPS) satellites with respect to the test cases. The second section investigates the results that can be obtained by using only GPS satellites. Immediately following it, results for both GPS only data and pseudolite augmented data are provided in order to evaluate algorithm performance. The forth section discusses the impacts of the pseudolite location on the geometric strength of positioning solutions. The effects of applying differential GPS services to the airborne pseudolite are covered by the next section. This chapter ends with the analysis of the second pseudolites addition to the most challenging urban environments.

4.2 Visibility Analysis of GPS Satellites

The pseudolite-aided GPS navigation is investigated by simulating a ground user located at different points in a simplified urban environment consisting of 12 buildings. Figure 4.1 and Figure 4.2 illustrate different views of the primary selected urban terrain, widely spaced high-rise office buildings (UTZ II). Dayton, OH was selected as a representative city for this research. In order to make the simulated city environment more similar to Dayton's downtown area, as shown in Figure 4.3, it is assumed that the city environment has a 20° rotation from north to the west direction.

As inferred from Table 3.2, each building is 45 m high, and has a 4000 square-m footprint area which represented by product of 80 m length by 50 m width. The streets are 30 m wide.

In the simulation, the ground user is equipped with a Precise Positioning Service (PPS)-GPS receiver and stands at three different locations between the buildings, labeled as points A, B and C in Figure 4.2. Therefore, all three points have different sets of visible satellites. In Figure 4.2, the locations are shown where point A has

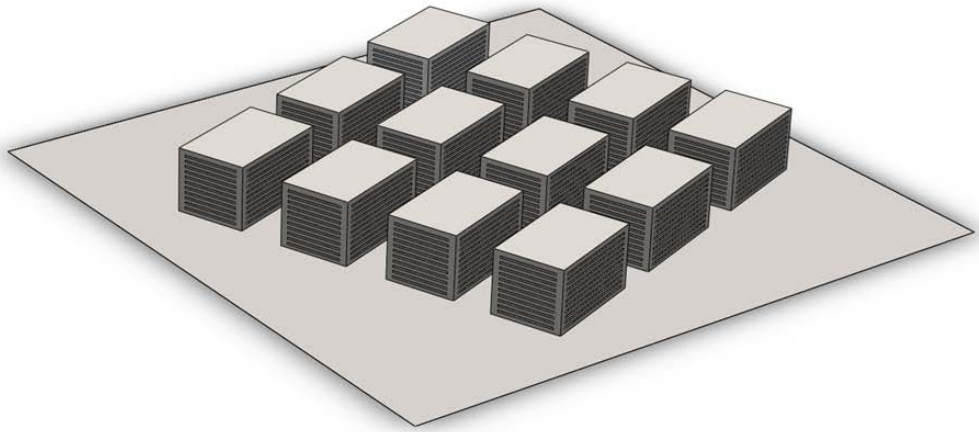

Figure 4.1: Side view of the UTZ type II.

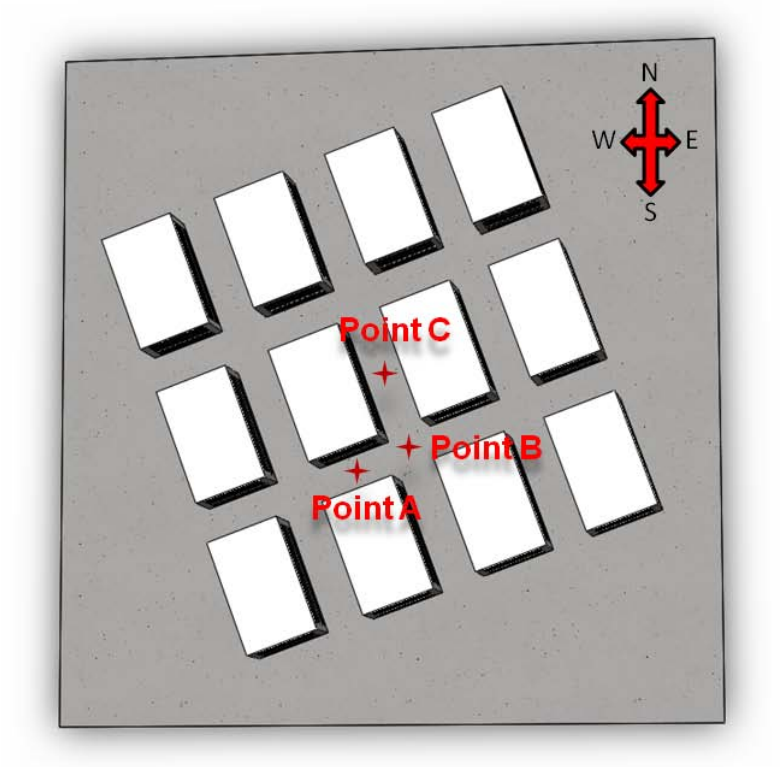

Figure 4.2: Top view of the UTZ type II.

Figure 4.3: Dayton Downtown Aerial Photo.

a line of sight in east-west direction and point C has a line of sight in south-north direction. As point B is in the center of the streets crossing, it has a line of sight in both directions.

In Figure 4.4, orbital ground tracks of the visible satellites for a 5° mask angle over Dayton, OH are demonstrated in dark colored lines. In order to highlight the difference, all 32 GPS satellites orbital ground tracks are shown with light colored lines in the same figure. A theoretical ground user, who stands in Dayton with a clear line of sight in all directions, would see this set of GPS satellites tracks for every 24 hours. Due to fact that the earth's spin period in space is not exactly 24 hours, these successive ground tracks appear to repeat from day to day and shift to the west from ground user's viewpoint. This worldwide grid is sampled every 30 seconds in time for 24 hours of real GPS ephemeris data.

The visible satellite's orbital ground tracks for a ground user located on point A, B and C are portrayed with different colors in Figure 4.5, 4.6 and 4.7. Similar to the Figure 4.4, the visible satellite's orbital ground tracks for a ground user, who has a clear line of sight in all directions, are depicted with light colored lines in the same figures. One can infer easily from these figures that the geometry of the buildings significantly limits the visibility of the GPS satellites to the ground user.

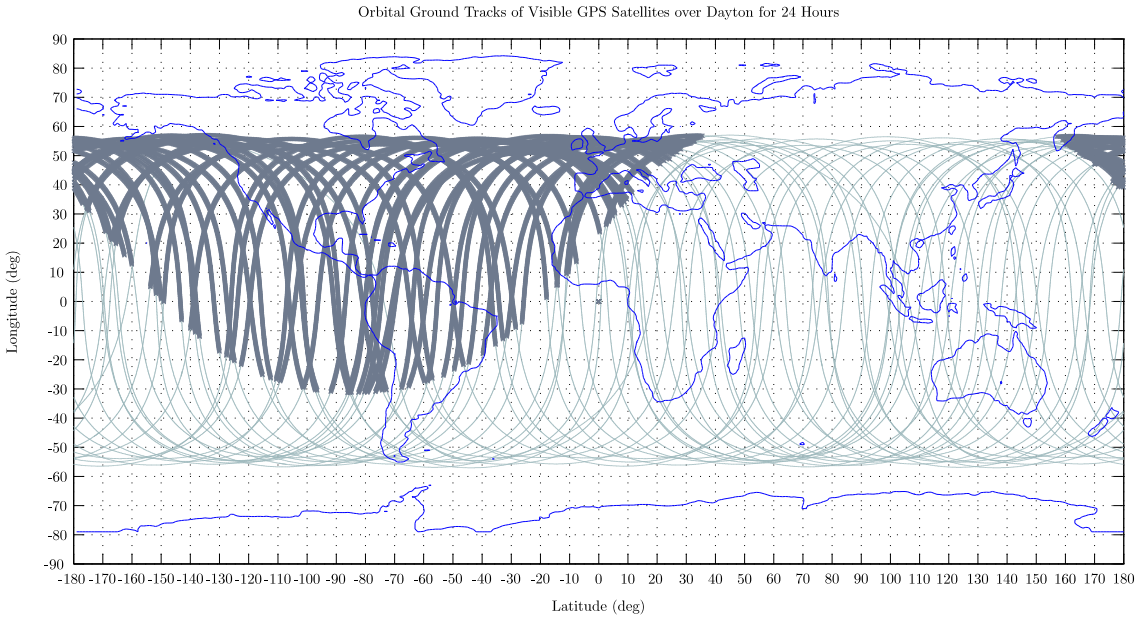

Figure 4.4: Visible Satellite's Orbital Ground Tracks over Dayton for 24 hours.

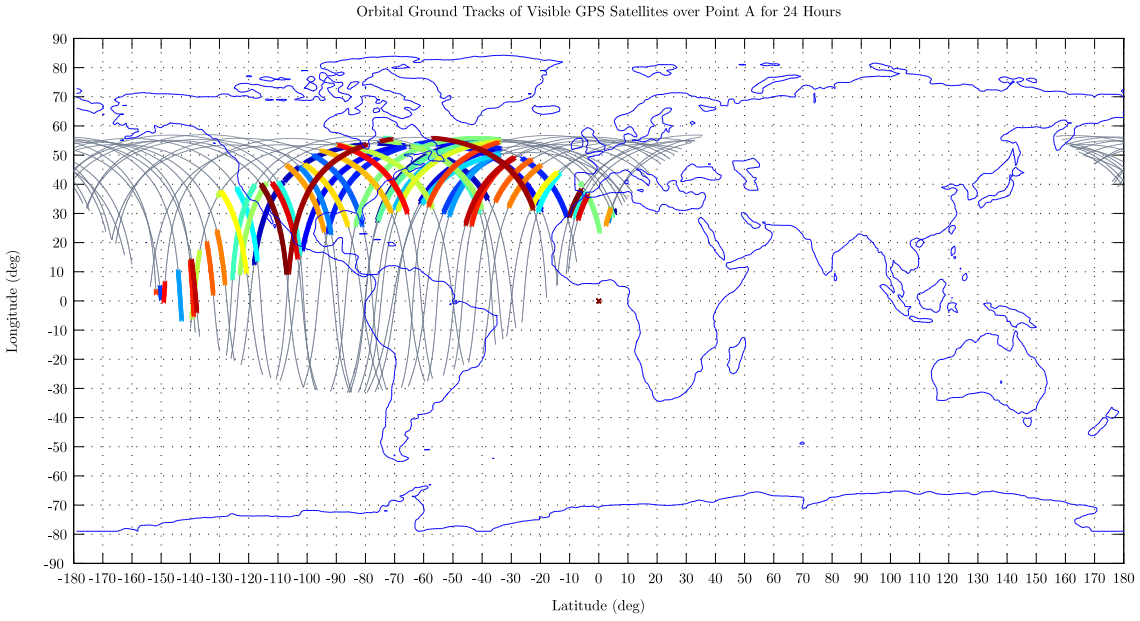

Figure 4.5: Visible Satellite's Orbital Ground Tracks over Point A for 24 hours in UTZ type II.

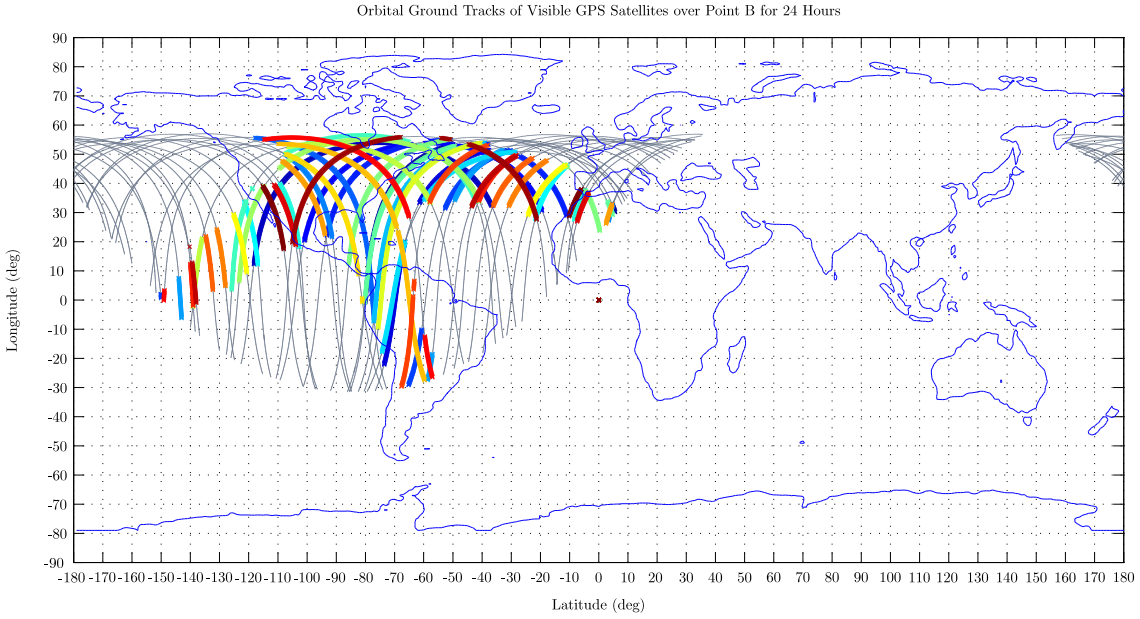

Figure 4.6: Visible Satellite's Orbital Ground Tracks over Point B for 24 hours in UTZ type II.

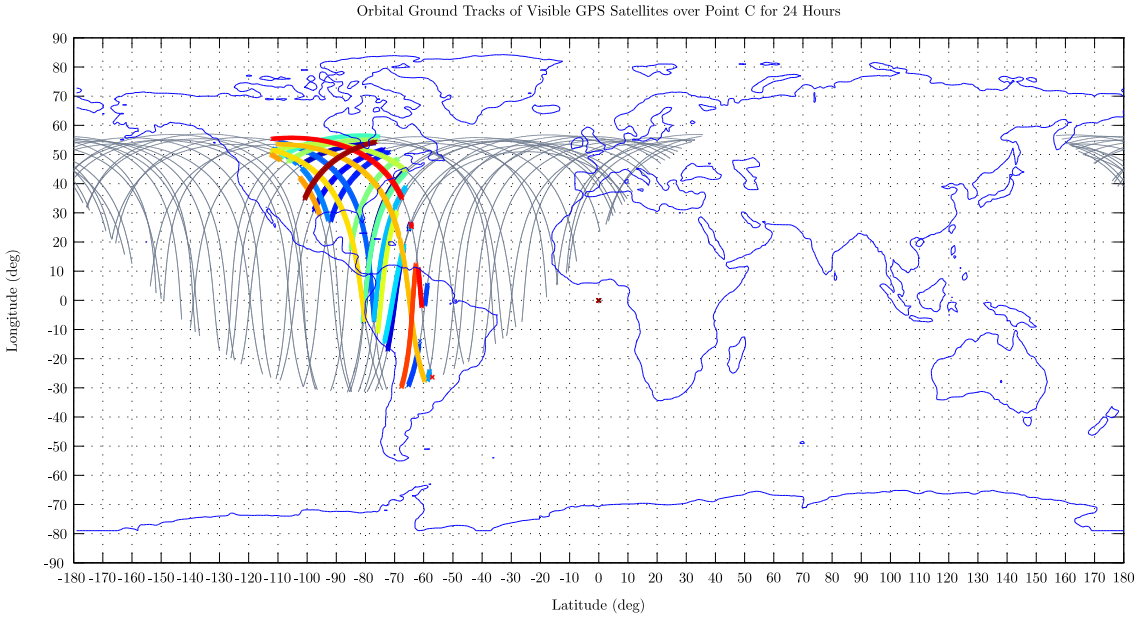

Figure 4.7: Visible Satellite's Orbital Ground Tracks over Point C for 24 hours in UTZ type II.

It is stated in Section 3.7, that accuracy and availability of a navigation system increases as the number of visible satellites increases. Point B has a better view towards the satellites, since it is located at the intersection of the streets. Thus, it is advantageous for availability compared to other two points. On the other hand, Point C has the worst line of sight amongst the three points. GPS satellite constellation consists 6 orbital planes with inclination of 55° (±3°) relative to the equatorial plane. This means that the highest latitude any GPS satellite passes directly over is 55° (±3°). Because Dayton, OH is at 39.7647 North latitude and 84.1807 West longitude, the ground user in the simulation practically cannot see much amount of satellites in its North. Therefore, point C is the most disadvantageous point to obtain signals from GPS satellites. If the assumed ground user location in the simulation had been on the equatorial plane, the user standing on point C could have seen more satellites in south-north direction.

In order to present a different perspective about the effects of building's geometric dimensions on satellite's visibility, the analysis is repeated using the same worldwide grid, but this time the ground user is standing on point B in UTZ type VI (detached houses). As a reminder, each building in UTZ type VI is 6 m high, and has a 100 square-m footprint area which represented by product of 12.5 m length by 8 m width. The streets are 15 m wide. Figure 4.8 demonstrates a side view of the UTZ type VI.

As shown in Figure 4.9, by lowering the dimensions of the buildings and increasing separation between them, more satellites are visible; hence, a higher availability can be obtained.

4.3 GPS-only Results

GPS is fully operational and primary navigation system for United States (US) authorized military and selected government agency users. It has become a powerful navigation and positioning tool in recent years. On the other hand, there are still

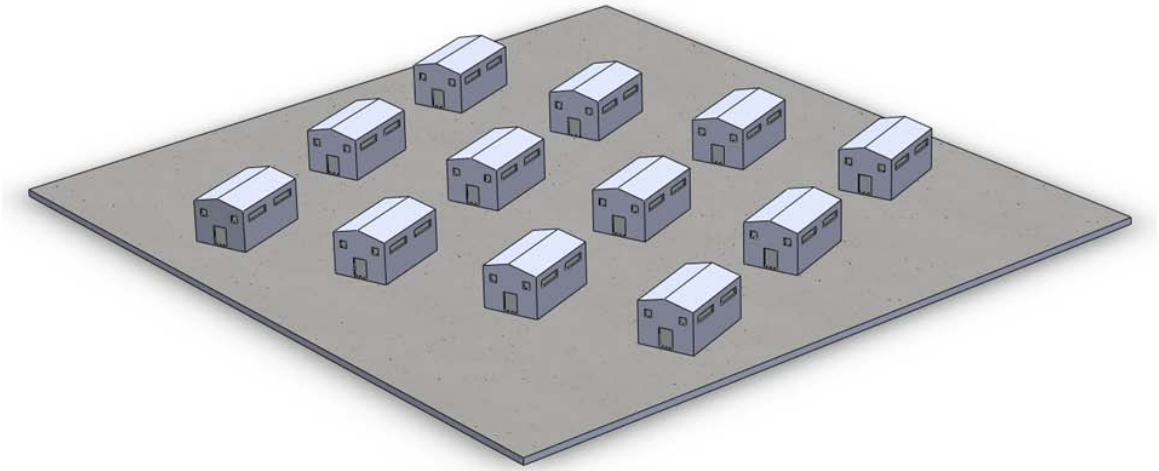

Figure 4.8: Side view of the UTZ type VI.

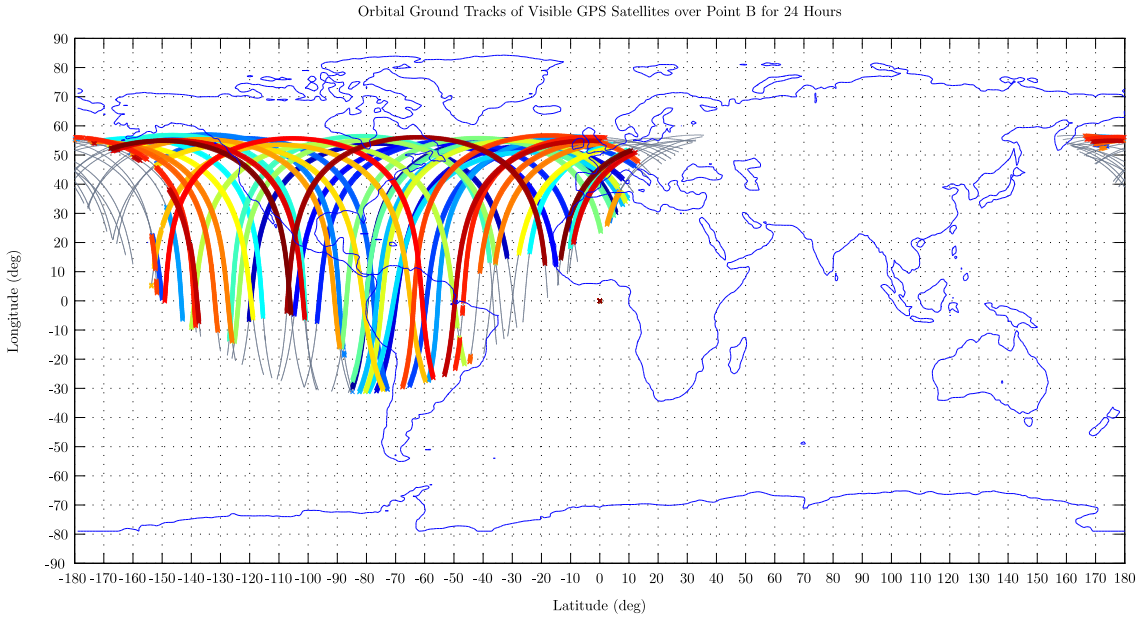

Figure 4.9: Visible Satellite's Orbital Ground Tracks over Point B for 24 hours in UTZ type VI.

some drawbacks to the operations of GPS such as the obstruction of the sky view that cause the degradation of precision in position solution.

Figures 4.10, 4.11 and 4.12 depict GPS only Position dilution of precision (PDOP) values for point A, B and C in UTZ type II. Additionally, the number of satellites in view at a specific time is also demonstrated at the bottom of the PDOP graphs with the same time axis. Gaps in the lines of bottom graphs would indicate that the pseudo-random noise (PRN) code, which belongs to a spesific GPS satellite, is not in view for this particular time. Similarly, blank areas on the PDOP graphs mean that there are less than 4 GPS satellites visible, thus dilution of precision (DOP) matrix could not be calculated. In order to indicate the time periods of acceptable navigation service, a threshold value of 6 is set on the PDOP graph. Those areas where PDOP value is below the threshold are accepted as available for GPS navigation.

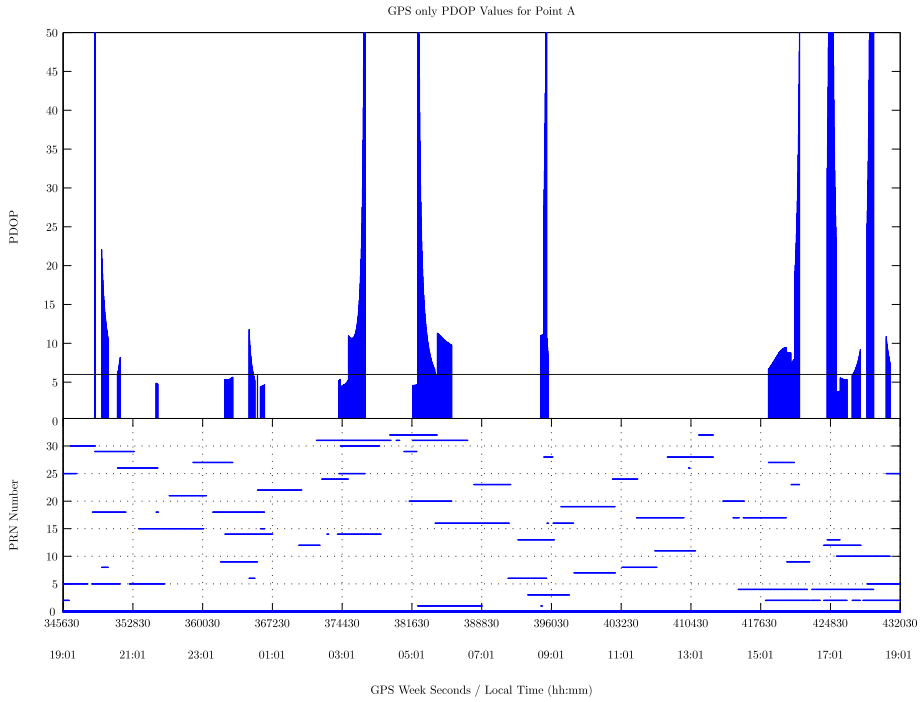

Figure 4.10: GPS only PDOP values over Point A for 24 hours in UTZ type II.

It is clear from the figures that, the number and geometry of visible satellites are not sufficient to reliably carry out the GPS operation in UTZ type II. In the

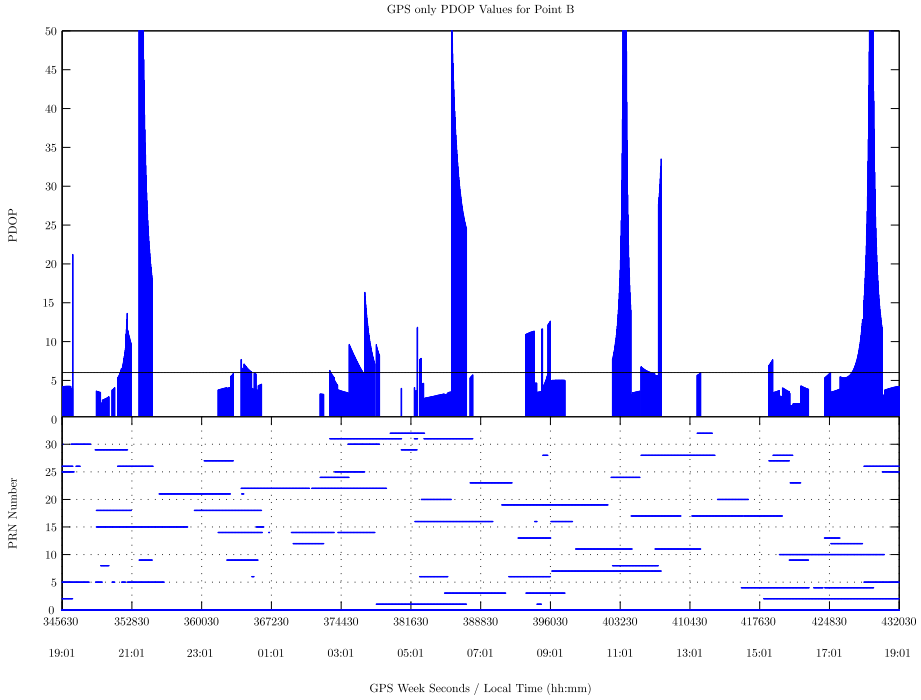

Figure 4.11: GPS only PDOP values over Point B for 24 hours in UTZ type II.

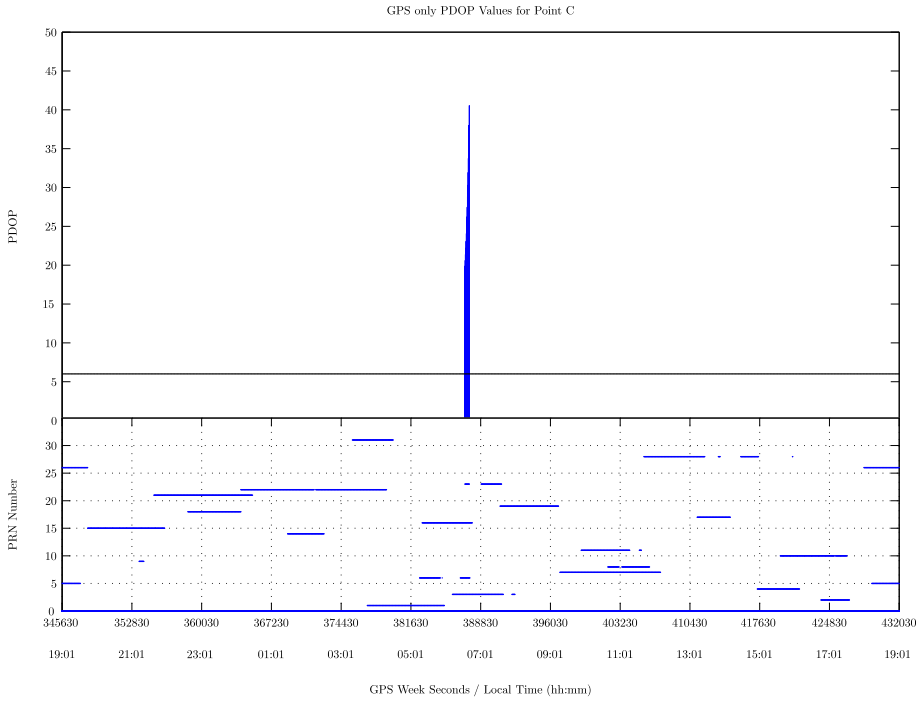

Figure 4.12: GPS only PDOP values over Point C for 24 hours in UTZ type II.

worst situation, at point C, the satellite signals were almost completely lost. This problem, emerging from space-borne satellite positioning system, can be addressed by additional ranging signals transmitted from an airborne pseudolite. This augmentation can not only provide an additional signal but also strengthen the geometry of positioning solutions and thus the availability can be improved.

Appendix A includes graphs of the visible satellite's orbital ground tracks and GPS only PDOP values for ground user located on point B in different types of UTZ's. According to the results, approximately 96 percent of the urban terrains, near city cores, suburbs and city edges, are suitable for GPS operation most of the time without augmentation. However, the geographically small (4 percent) but strategically important city cores are the most challenging environments for GPS operation even with the various augmentation systems. As stated earlier in Chapter 3, these UTZ's valuable structures and great limited line of sight (LOS) characteristics make them significantly attractive to the opponent actions.

4.4 Combined GPS/Pseudolite Results

Pseudolites can be used to tackle problems of GPS operation that arise with harsh observing conditions. In GPS positioning, low elevation satellites generally are not tracked in order to avoid signal degradation caused by the atmosphere. Hence, the horizontal coordinates are generally more accurate than the vertical component. However, this problem can be addressed by combining additional signals transmitted from pseudolites. They can improve the geometric strength of positioning solutions especially for the vertical component due to the enhanced signal transmitter geometry by including low elevation pseudolites. In order to analyze this enhancement, one airborne pseudolite is added to the system and same simulation has been carried out. Initially this pseudolite is navigating with PPS type receiver. Later, the effects of changing the type of receiver associated with the pseudolite will be considered.

Figure 4.13 depicts the sky view of visible satellite tracks and the possible pseudolite locations over user with a clear line of sight in all directions for 24 hours. More than 40,000 possible pseudolite locations are defined over ground user at 1000 ft above ground level (AGL). Although possible pseudolite locations are defined with certain latitude and longitude separations (lower than 0.0005°), they do not appear to be evenly distributed since the ground user observes them close to each other as the elevation angles decrease. Each red dot indicates a possible pseudolite location and each blue line belongs to a GPS satellite track from the perspective of looking at the sky directly overhead from user. The user is located at the center of circles. The outer circle represents the observer's horizon and the center represents the zenith. The two inner circles correspond to different elevation angles such as 30° and 60°. The azimuth is 0° at North and increases in the clockwise direction. Figure 4.14 shows the same graph over point B in UTZ II. It is clear from these two figures that the dimensions and the geometry of the buildings significantly limits the LOS characteristics of the ground user.

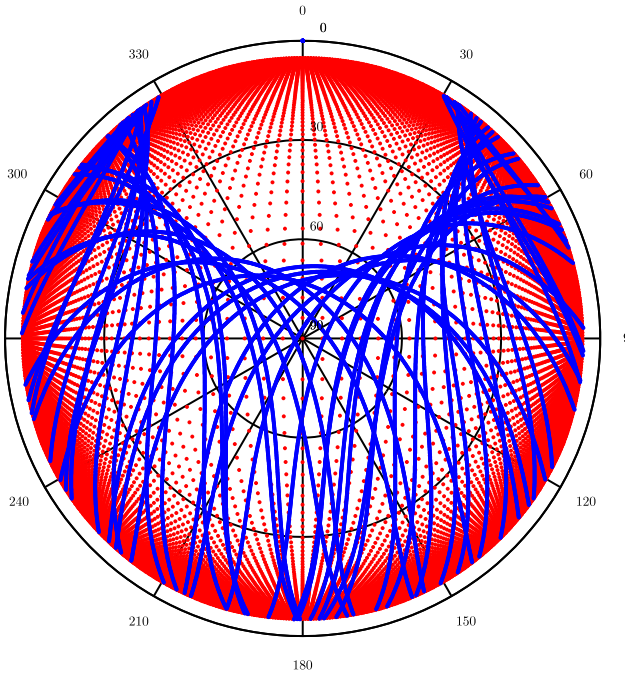

Figure 4.13: Unobstructed skyview over user for 24 hours.

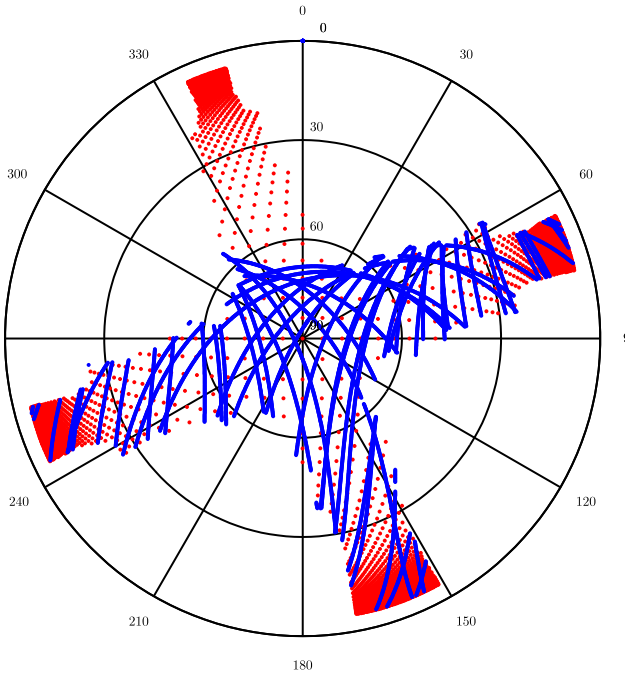

Figure 4.14: Skyview over Point B for 24 hours in UTZ type II.

Figures 4.15, 4.16 and 4.17 show the difference between GPS only and combined GPS/Pseudolite PDOP values for point A, B and C in UTZ type II. The solid red line at the bottom of the graphs indicates that pseudolite is assigned to PRN code 33 and visible to the ground user for the entire simulation. PDOP values are calculated with respect to the geometry of all visible satellites and one selected pseudolite location amongst all possible locations that gives minimum PDOP result. It can be seen from the figures that a combination of GPS/Pseudolite system has lower PDOP values compared to GPS only system. In Figure 4.15 for point A in UTZ type II, GPS only PDOP values are larger than designated threshold most of the time and availability is 5.2%, while airborne pseudolite augmented system availability is 12.6%. For point B in UTZ type II, a combination of GPS/Pseudolite system provided PDOP values are still acceptable most of the time and availability is 71.7% compared to 28.6% GPS only system provided availability.

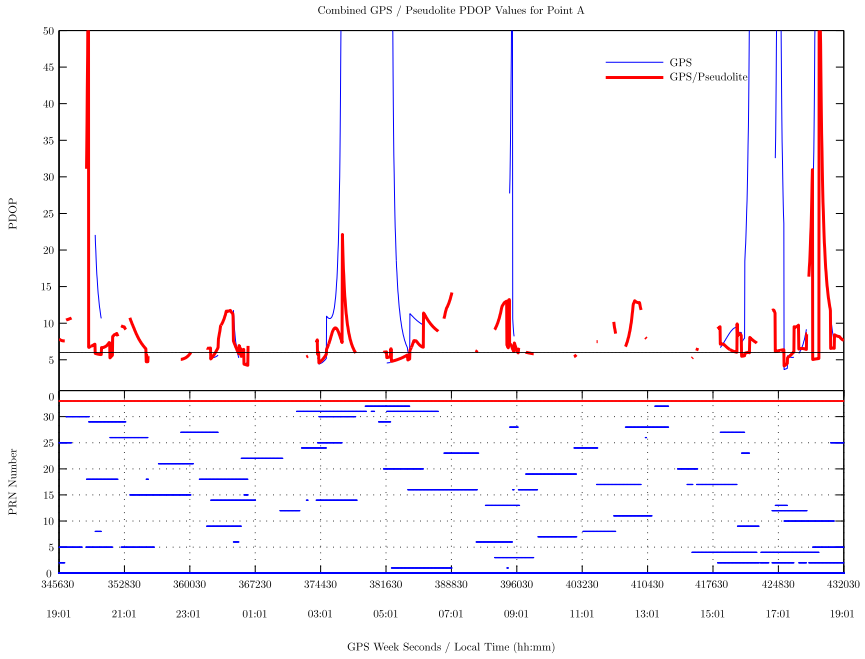

Figure 4.15: Combined GPS/Pseudolite PDOP values over Point A for 24 hours in UTZ type II.

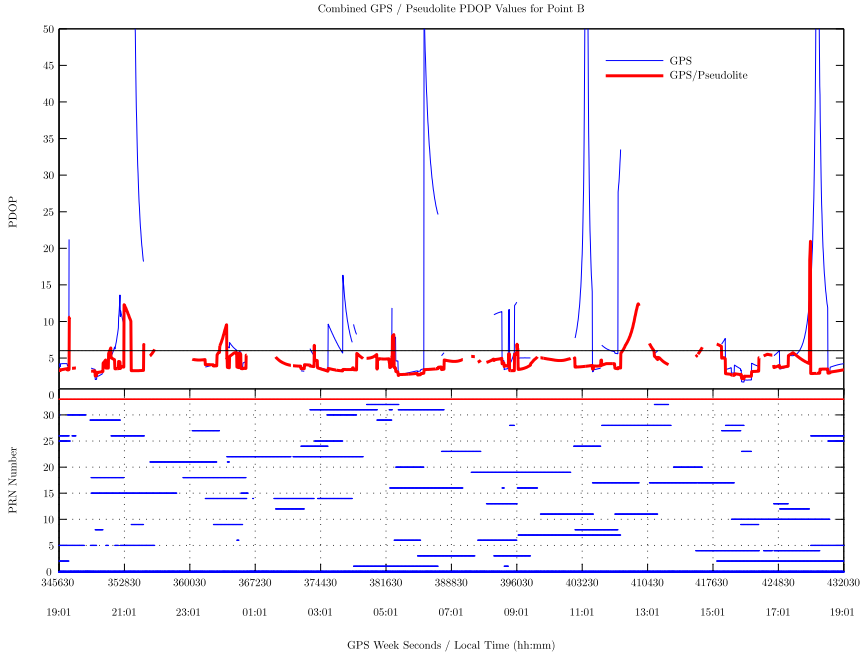

Figure 4.16: Combined GPS/Pseudolite PDOP values over Point B for 24 hours in UTZ type II.

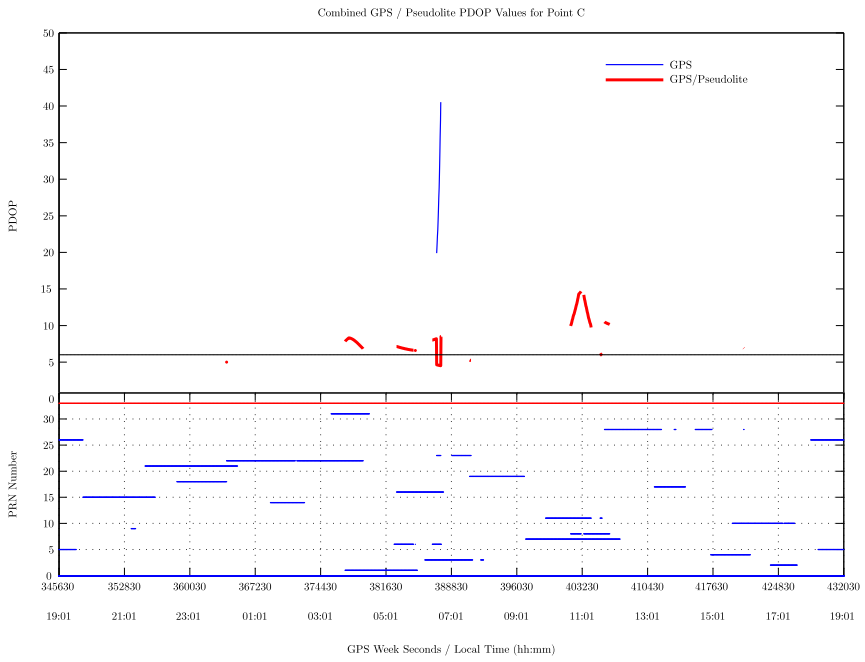

Figure 4.17: Combined GPS/Pseudolite PDOP values over Point C for 24 hours in UTZ type II.

As shown in Figure 4.17, PDOP values calculated both with and without the pseudolite are either above the threshold or cannot be calculated due to insufficient amount of transmitters most of the time. An airborne pseudolite augmented GPS system is provide 0.9% availability, while the GPS only system cannot provide any availability. In other words, even combined GPS/Pseudolite systems augmenting by only one pseudolite does not useful for precise positioning at point C in UTZ type II. Therefore, addition of second airborne pseudolite to the system for point C will be investigated in following Section 4.7.

4.5 Geometric Analysis of Pseudolite Locations

The geometry of the GPS satellite constellation with respect to the user can be improved by strategically placing airborne pseudolite as an additional transmitter. Therefore, optimization of the pseudolite location is critical and necessary. In order to avoid from significant atmospheric and multipath errors, the measurement from

GPS satellites with low elevation angles are usually rejected. On the other hand, high quality pseudolite measurements can provide high precision even at very low elevation angles. Figure 4.18 shows the possible pseudolite locations that provide minimum PDOP values over point B for 24 hours in UTZ type II. It is clear from the figure that minimum PDOP values were achieved from the airborne pseudolites with elevation angles lower than 30° most of the time. On the flip side of the coin, it is meaningful to note that the airborne platform altitude has an important impact on the final results. To provide low elevation angles with the high altitude airborne platforms, slant range to the user would be much bigger. Problems, such as loosing control of the airborne platform due to flying out of the effective operating area or magnifying the atmospheric and multipath errors, can arise from this issue.

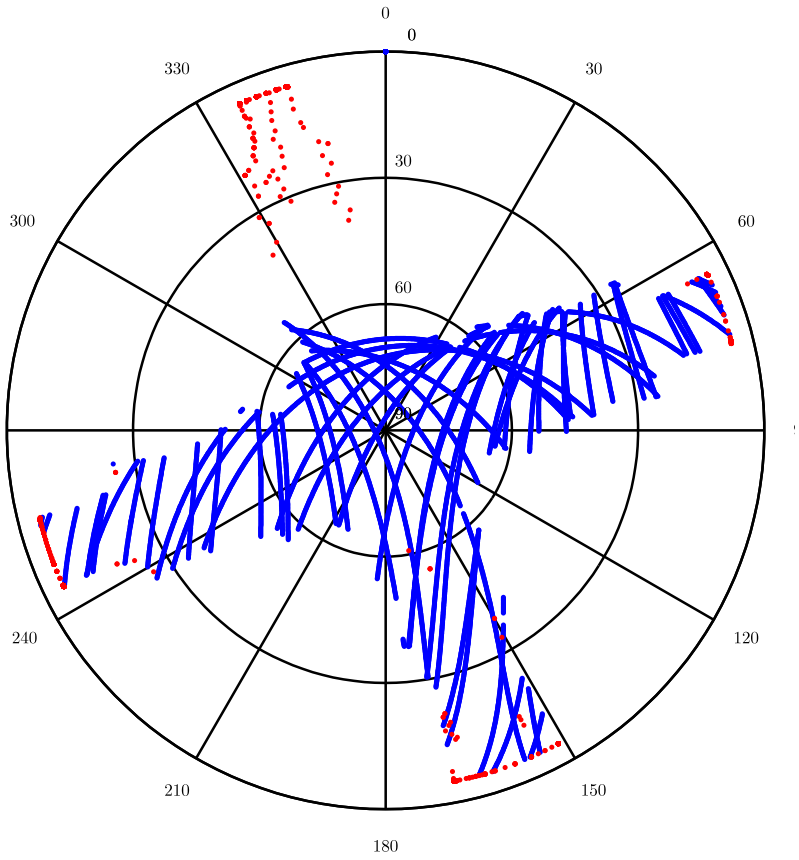

Figure 4.18: Possible Pseudolite locations that provide minimum PDOP values over Point B for 24 hours in UTZ type II.

It is understandable to expect that a GPS/Pseudolite combined system should provide better availability with lower PDOP values than GPS only results. However, this statement is not always true and can be change with respect to pseudolite location. In order to analyze this, geometric analysis of pseudolite location is investigated. One PPS-GPS receiver driven airborne pseudolite is placed directly at zenith angle of the ground user at 1000 ft AGL and the same simulation has been carried out. Figure 4.19, depicts the difference between GPS only and zenith placed combined GPS/Pseudolite PDOP values for point B in UTZ type II.

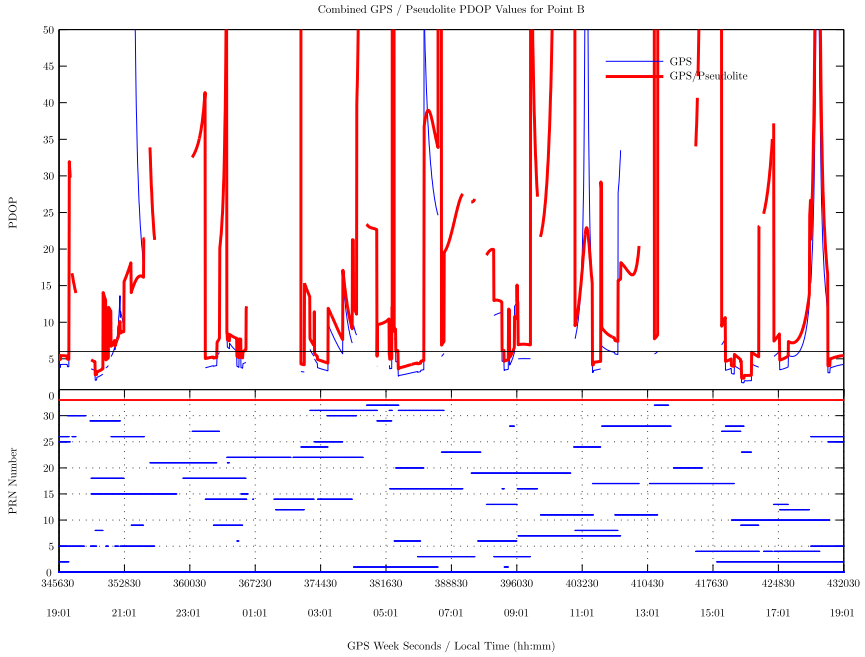

Figure 4.19: Zenith Placed Combined GPS/Pseudolite PDOP values over Point B for 24 hours in UTZ type II.

According to the Figure 4.19, combined GPS/Pseudolite PDOP values are larger than GPS only results most of the time. It means that several visible satellites have very high elevation angles as the zenith placed pseudolite and make the geometry matrix ill-conditioned. In order to reveal more detailed examples, instant contour graphs of computed PDOP values that associated with possible pseudolite locations are examined. Each graph shows calculated PDOP values of each possible pseudolite location with respect to visible satellites over point B in UTZ type II for a particular

time. The user is located at the center of circles and visible satellites are represented by black triangles. Magenta triangle indicates the optimum pseudolite location that gives the minimum PDOP value at this moment. PDOP values are classified with respect to their magnitudes and represented by different color codes. Blue color is symbolizing the magnitude of PDOP values lower than 6, while red is symbolizing between 30 and 40. Blank areas on the contour graph means that the PDOP value for this area is bigger than 40 and cannot be symbolized by any color code.

In Figure 4.20, there are three visible satellites at 04:41:00 (hh:mm:ss) local time (380430 GPS week seconds). Addition of one pseudolite as a new ranging signal source has made possible to calculate DOP matrix where the number of the visible satellites is insufficient. It can be seen from the figure that zenith placed pseudolite is represented by yellow color for its PDOP value of 22.7. However, placing the pseudolite at low elevation angles such as the location illustrated by magenta triangle will not only provide more favorable geometry, but also reduce PDOP significantly to value of 5.3.

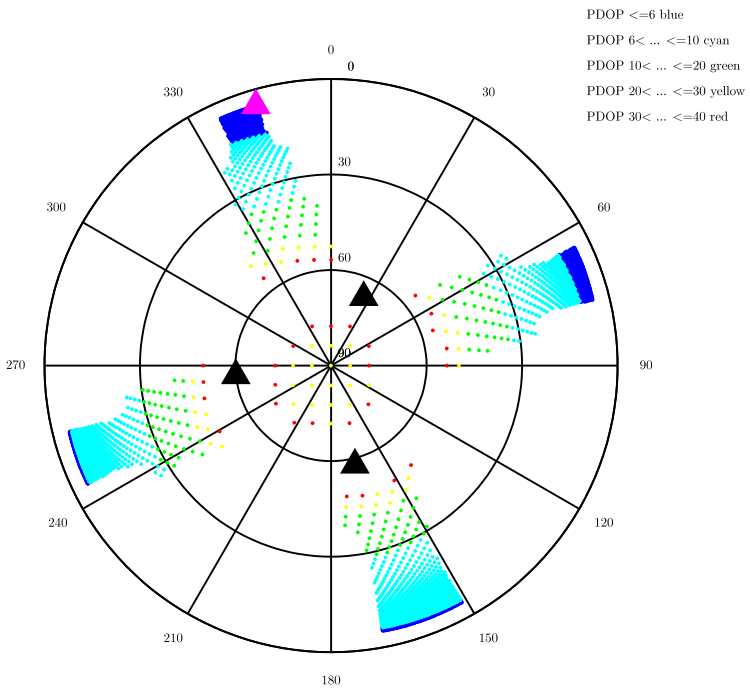

Figure 4.20: Skyview over Point B at 04:41:00 (hh:mm:ss) local time in UTZ type II.

The contour map of possible pseudolite locations' PDOP values at 21:25:30 (hh:mm:ss) local time (354300 GPS week seconds) is shown in Figure 4.21. With four visible satellites, PDOP is 31.4 at here. Even though the addition of zenith placed pseudolite is reduced PDOP to 16 that color coded with green, it is still very large and above the desired availability threshold. On the other hand, very good PDOP (less than 6) value can be achieved if the pseudolite was located in the azimuth band 300 to 360, or from 230 to 270 degrees with lower than 45 degrees elevation angles.

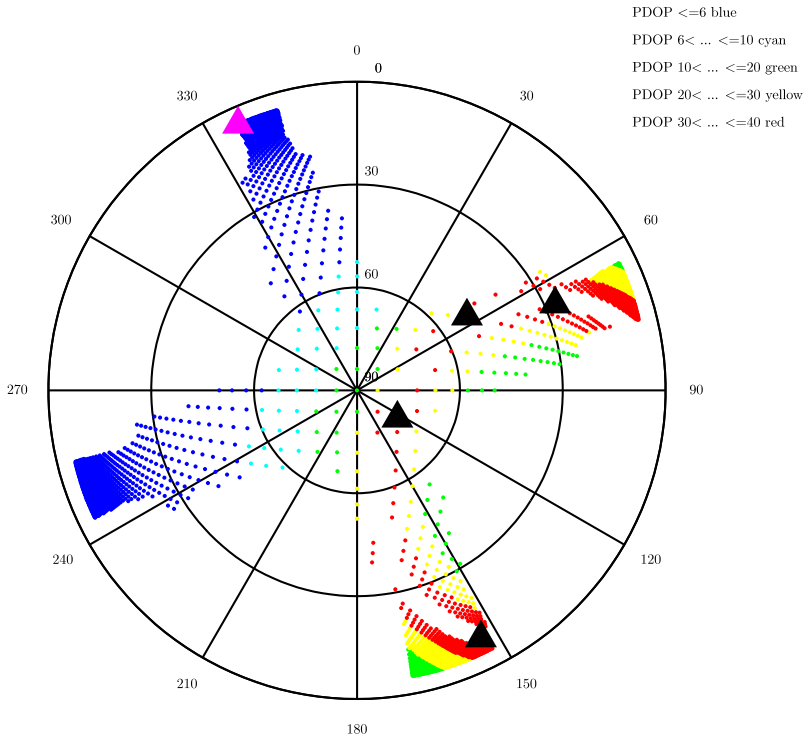

Figure 4.21: Skyview over Point B at 21:25:30 (hh:mm:ss) local time in UTZ type II.

Figure 4.22 shows the same graph for the specific time of 16:55:30 (hh:mm:ss) local time (424500 GPS week seconds) as the last case. GPS only PDOP value is obtained from 4 visible satellites as 5.4. Adding a zenith placed pseudolite to these well distributed satellites disrupts the elevation angle diversity that caused the worse PDOP (larger than 6) value than GPS only result here. Similar to the previous cases, very good PDOP values as low as 3.7 can be achieved via placing the pseudolite to the lower elevation angles such as the position of magenta triangle.

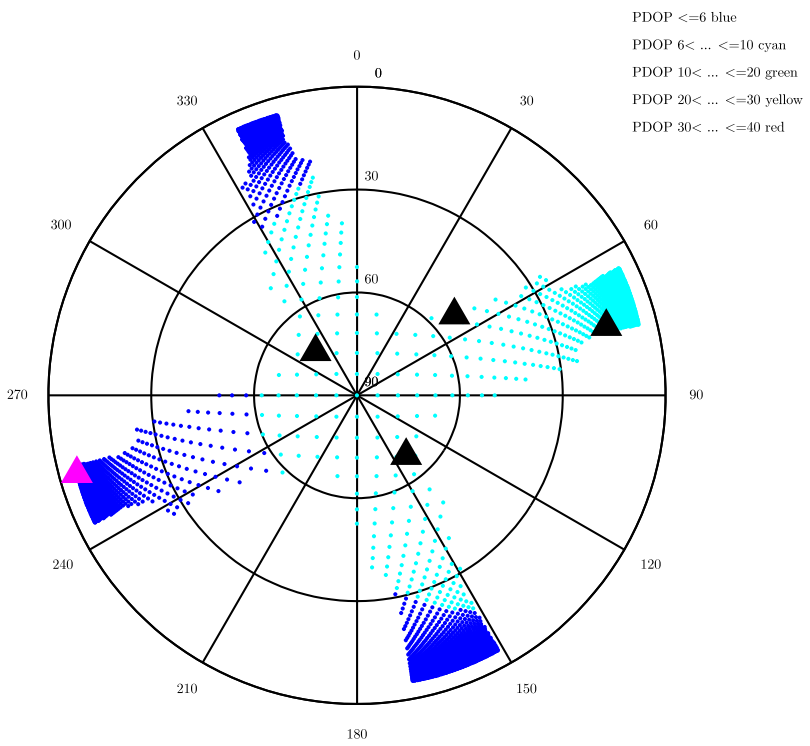

Figure 4.22: Skyview over Point B at 16:55:30 (hh:mm:ss) local time in UTZ type II.

Due to fact that GPS satellites are fielded in nearly circular orbits with a radius of 26,560 km, they have a speed of 3.873 km per second. This means that GPS satellites are not very fast with respect to the user who stands on the surface of the earth. Nevertheless, Figure 4.18 shows that pseudolite locations which provides minimum PDOP values, were mostly located at the same azimuth band with low elevation angle and jumped only when satellites rise or set. Taking into account this issue and considering the maneuvering capabilities of unmanned air vehicles, possible pseudolite locations are restricted to the elevation angles between 5° and 10° and the azimuth band 340° to 350° where GPS satellites are not visible due to the user takes place geographically in north. These restricted possible pseudolite locations are portrayed in Figure 4.23.

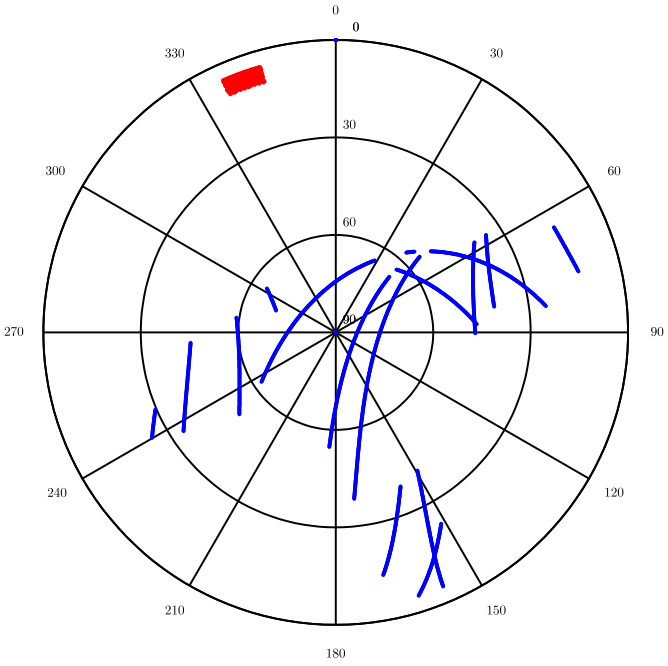

Figure 4.23: Skyview over Point B for 4 hours in UTZ type II.

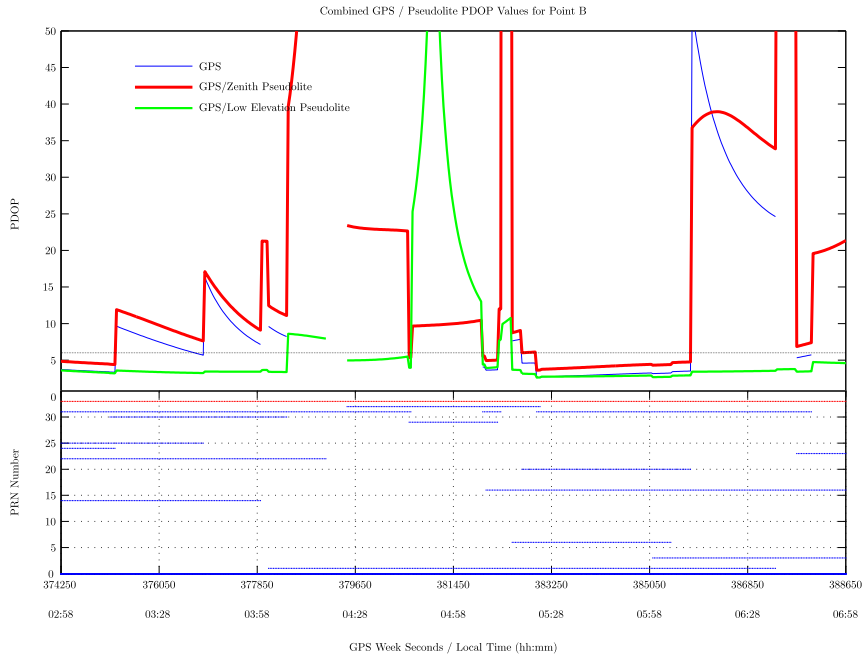

Figure 4.24: Combined GPS/Pseudolite PDOP values over Point B for 4 hours in UTZ type II.

Figure 4.24 shows the calculated PDOP values of GPS, zenith placed pseudolite augmented GPS, and constrained low elevation angle located pseudolite augmented GPS for 4 hours. After adding the zenith placed pseudolite to GPS satellites, the PDOP values began to degrade. They are larger than GPS only results unless the visible satellites are not evenly distributed. However, PDOP values of low elevation angle pseudolite enhanced GPS are lower than both cases most of the time.

As shown in the previous examples, different pseudolite locations change the geometry significantly. In order to guarantee the visibility of the pseudolite, placing it directly above the user does not always provide better availability than GPS-only systems. In many different situations, adding a pseudolite to PDOP calculations degrades PDOP values because of poor distribution of transmitters. As a rule of thumb, pseudolites should be placed in low altitude azimuth sectors where GPS satellite signals are blocked.

It is stated earlier in Chapter II that Japan Aerospace Exploration Agency has been investigating a new navigation and positioning service using pseudolites installed on the stratospheric platforms. After preceding discussion about geometric analysis of airborne pseudolite location, it is worthwhile to take a look at their concept again. In their concept, a stratospheric airship constellation, which consist nine platforms at an altitude of about 20 km, has been assumed above Tokyo metropolitan area. The average distances between the platforms are about 55 km and the slant range between the pseudolites and the user is from 20 km to 100 km. This means that the elevation angles of the pseudolites vary from 11° to 90° with respect to the user standing at the center of the constellation. Due to fact that their concept includes not only a single zenith angle placed stratospheric platform, but also well distributed eight other stratospheric platforms, user can receive GPS-like ranging signals from low elevation pseudolites most of the time and desired augmentations that would improve accuracy and availability can be achieved.

4.6 Impacts of Pseudolite's GPS Receiver Type

Based on the assumption that airborne pseudolite is navigating itself using GPS, the accuracy of its final position solution would be a limiting factor for such an augmentation system. Furthermore, broadcast ephemeris error in pseudolite case is more serious than GPS with respect to lower height of the airborne pseudolite than GPS satellites. Even though this ephemeris error does not affect ground-based pseudolite augmentation systems, it dominates the system's total error budget in the airborne case since the airborne pseudolite is always moving. Therefore, the quality of the onboard GPS receiver that used for airborne platform and applied service type is crucially important. In order to analyze these impacts on the final positioning accuracy of the user, the same simulation has been carried out for 4 hours with various GPS service types, standard positioning service (SPS), PPS, local area differential GPS (LADGPS) and carrier phase differential GPS (CPDGPS). Restricted possible pseudolite locations as illustrated in Figure 4.23 are again used in the simulation.

Figure 4.25 and 4.26, depict the difference between GPS only and various combined GPS/Pseudolite systems' PDOP values for point B in UTZ type II. As can be understood from the figures that SPS type GPS receiver applied airborne pseudolite cannot provide lower PDOP values than GPS only system, as long as the visible satellites are evenly distributed. Combined GPS/SPS equipped airborne pseudolites PDOP values are larger than GPS only results most of the time.

A snapshot of 11:08:00 (hh:mm:ss) local time (403680 GPS week seconds) can be shown as an exception to this statement. It can be seen from the Figure 4.27 that geometry of visible satellites to the user is not favorable in this case. Elevation angle of all four visible satellites are bigger than 35°. Even though there are four visible satellites, GPS only PDOP value is 398 at this time. However, combined GPS/SPS driven airborne pseudolite provided PDOP value is between 10 and 20 that color coded with green.

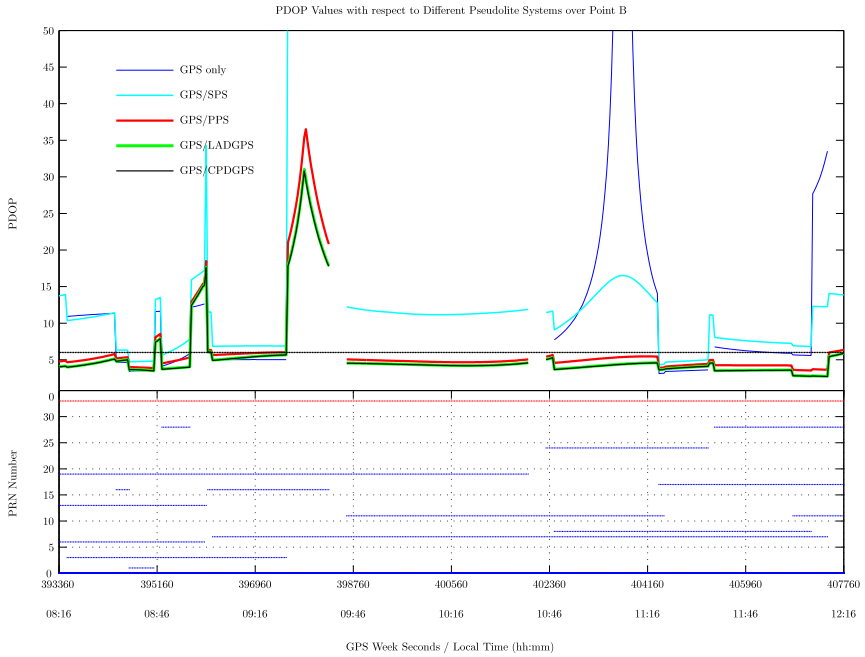

Figure 4.25: PDOP values for Different Pseudolite Systems over Point B for 4 hours in UTZ type II.

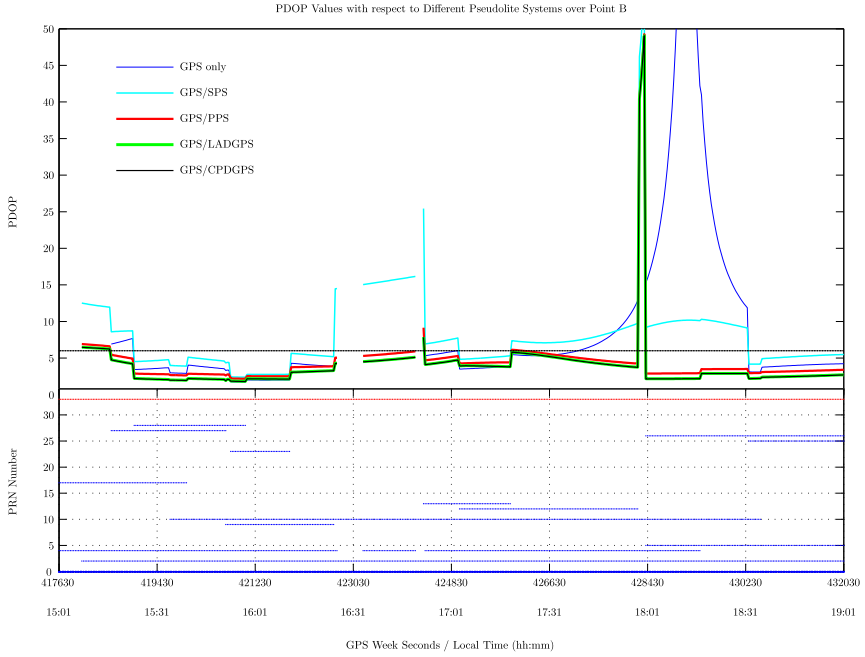

Figure 4.26: PDOP values for Different Pseudolite Systems over Point B for 4 hours in UTZ type II.

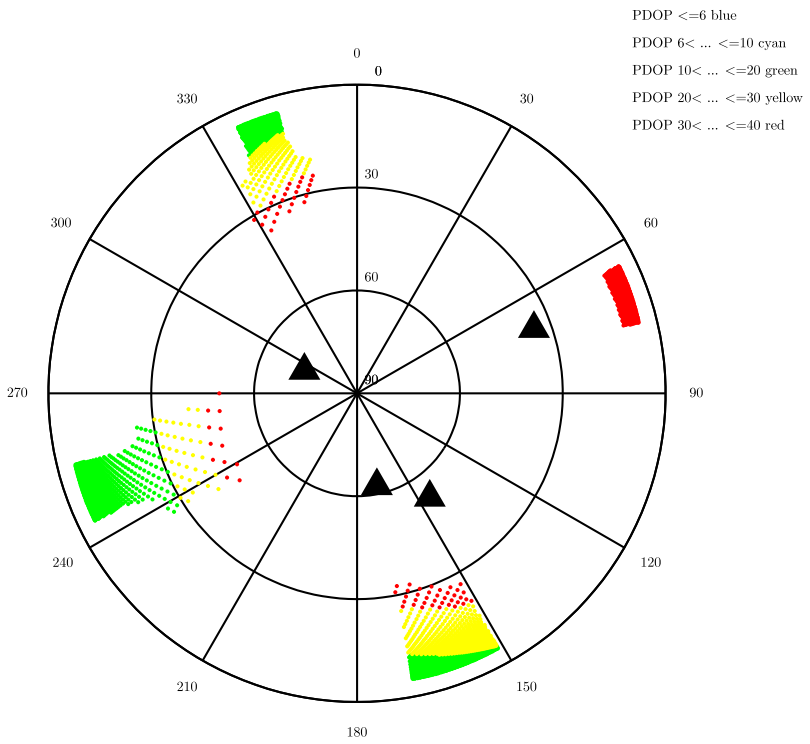

Figure 4.27: Skyview over Point B at 11:08:00 (hh:mm:ss) local time in UTZ type II.

Various DGPS methods can be used to improve the positioning performance of GPS. These methods require at least one reference station equipped with one or more GPS receiver at a surveyed location. The reference station computes the coordinate differences between the surveyed location and the position estimate provided by GPS and transmits the corrections to the user via a data link. As shown in Figures 4.25 and 4.26 combined GPS/LADGPS pseudolite and GPS/CPDGPS pseudolite systems provide equal or very close results to each other and the best availability compared to others. On the other hand, they are not offering a drastic improvement over combined GPS/PPS pseudolite system which also yields availability most of the time. Moreover, DGPS method's dependency to the reference stations and data links, make them logistically difficult to implement. This fact means that PPS driven airborne pseudolites not only offer more feasible approach to the problem, but also yield desired availability most of the time with only a negligible decrease in accuracy.

4.7 Addition of Second Pseudolite

It is presented earlier in Section 4.2 that point C in UTZ type II (widely spaced high rise office buildings) is the most challenging case since the ground user in the simulation practically can not see much amount of satellites in its North. Either making the surrounding buildings height shorter or changing the user location closer to the equator can change this condition positively. Figure 4.28 depicts GPS only and combined GPS/Pseudolite PDOP values for point C in UTZ type VI (detached houses), while Figure 4.29 portrays the same graph for the same user in UTZ type II.

One understands from the Figure 4.28 that if the surrounding buildings are shorter or street widths are wider, the desired availability can be provided by only GPS satellites for all of the time. However, Figure 4.29 shows that PDOP values are either above the threshold or cannot be calculated due to insufficient amount of transmitters most of the time in UTZ II. If such applications are inevitable in that kind of situation, then the addition of second airborne pseudolite as an another ranging signal source to the system should be considerable.

It is clear from the discussion about geometric analysis of pseudolite location in Section 4.5 that first pseudolite should be placed in the North azimuth sector with low elevation angle where GPS satellite signals are not available. In order to provide a more favorable geometry and better availability, location of the second pseudolite is investigated.

In the first case, the second pseudolite is symmetrically placed in South azimuth sector with low elevation angle. In Figure 4.30, possible pseudolite locations for both sectors and visible satellites tracks are demonstrated with red and blue dots respectively. Figure 4.31 shows GPS only and combined GPS/Pseudolite PDOP values for two pseudolites augmented system. The two solid red lines at the bottom of the graph indicate that two different pseudolites are visible to the ground user for the entire simulation and assigned to PRN codes 33 and 34. According to the Fig-

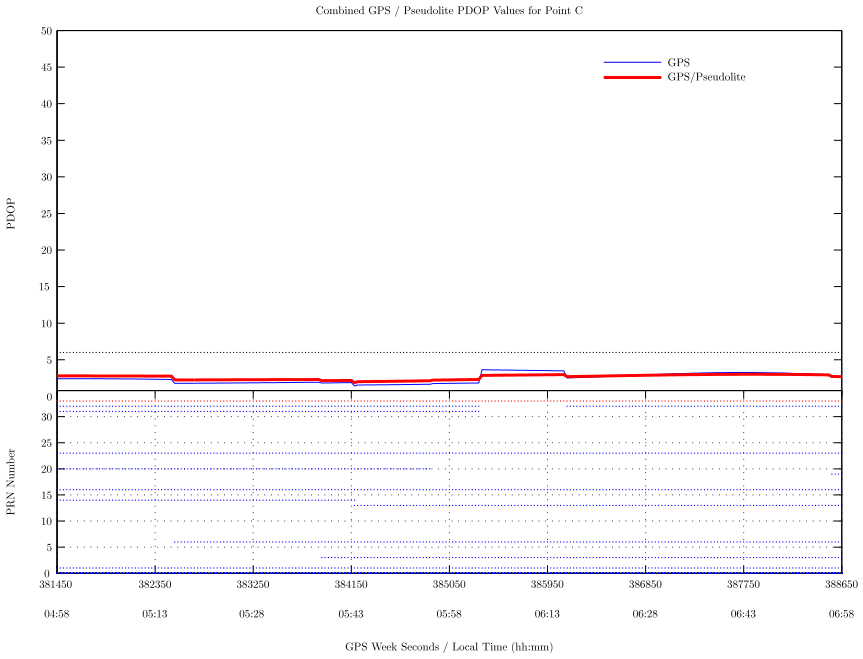

Figure 4.28: Combined GPS/Pseudolite PDOP values over Point C for 2 hours in UTZ type VI.

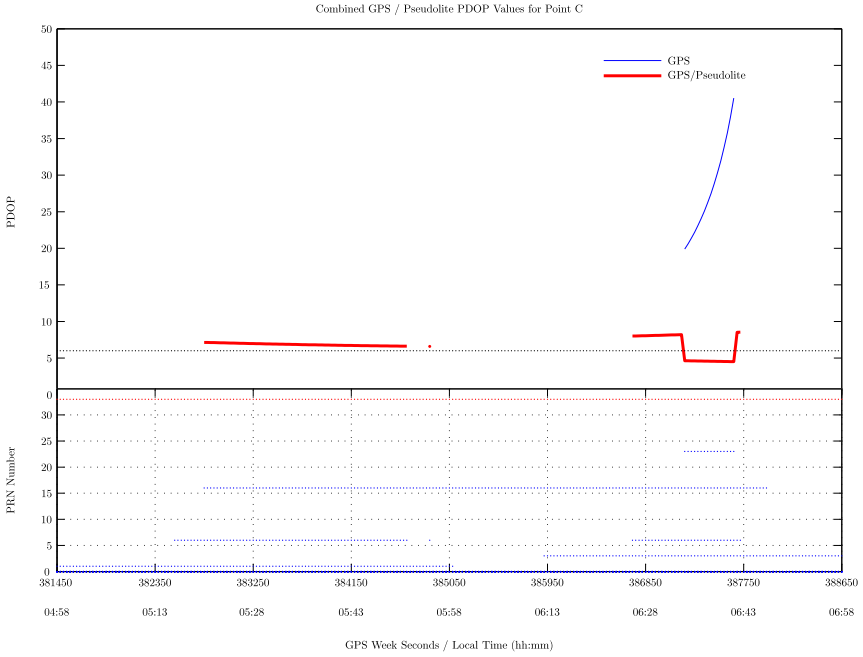

Figure 4.29: Combined GPS/Pseudolite PDOP values over Point C for 2 hours in UTZ type II.

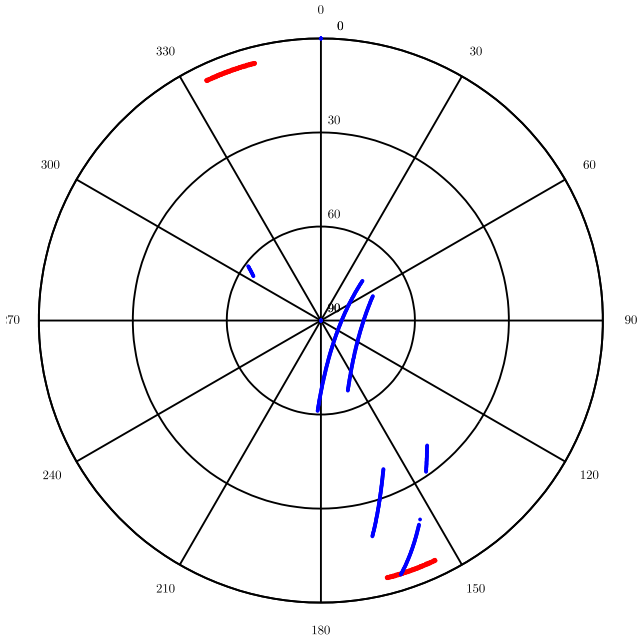

Figure 4.30: Skyview over Point C for 2 hours in UTZ type II.

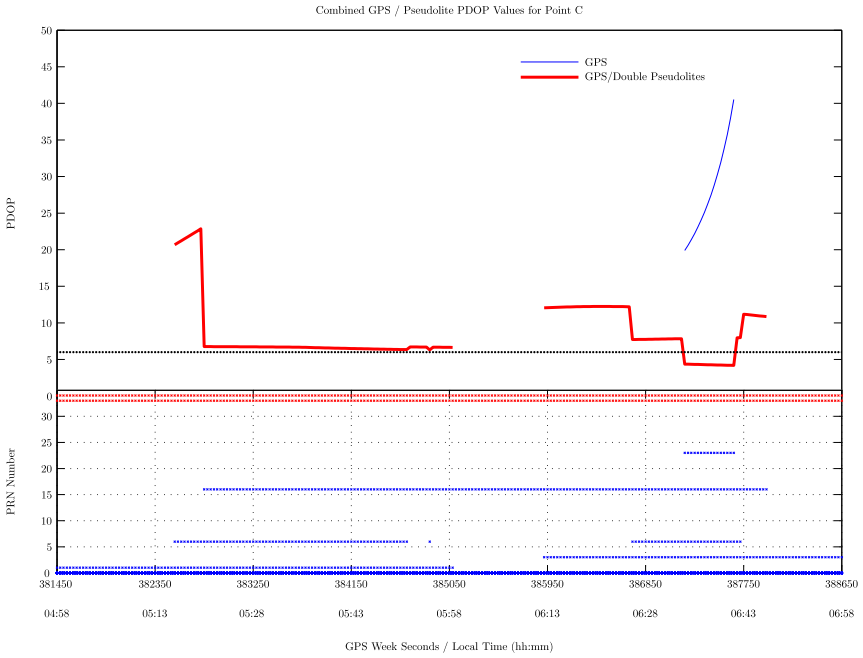

Figure 4.31: Combined GPS/Pseudolite PDOP values over Point C for 2 hours in UTZ type II.

ure 4.31, pseudolite augmented PDOP values are below the designated threshold for approximately 7 minutes.

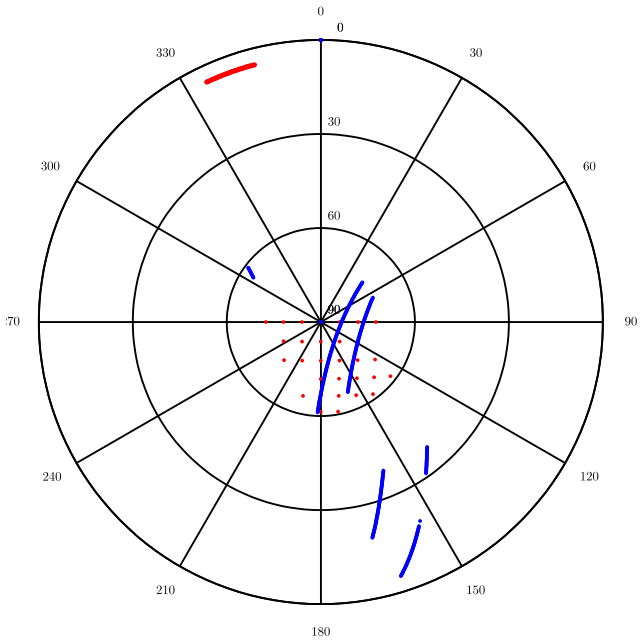

Figure 4.32: Skyview over Point C for 2 hours in UTZ type II.

In the second case, it is again placed in South azimuth sector but this time with high elevation angle. In Figure 4.32, possible pseudolite locations for both sectors and visible satellites tracks are demonstrated with red and blue dots respectively. Figure 4.33 shows GPS only and combined GPS/Pseudolite PDOP values for two pseudolites augmented system. It is obvious from the Figure 4.33 that desired augmentation and availability can be obtained by using well distributed two airborne pseudolites for approximately 48 minutes even at point C in UTZ II.

Consider a scenario in which armed forces are planning an attack operation using GPS-aided smart weapon systems in the middle of a block on a straight street bordered on both sides by tall buildings, such as point C in UTZ type II. Almost for the whole day, the number of visible satellites is not sufficient in order to provide reliable precise position and navigation information to the troops. However, these results proved that appropriate usage of two airborne pseudolites can increase GPS

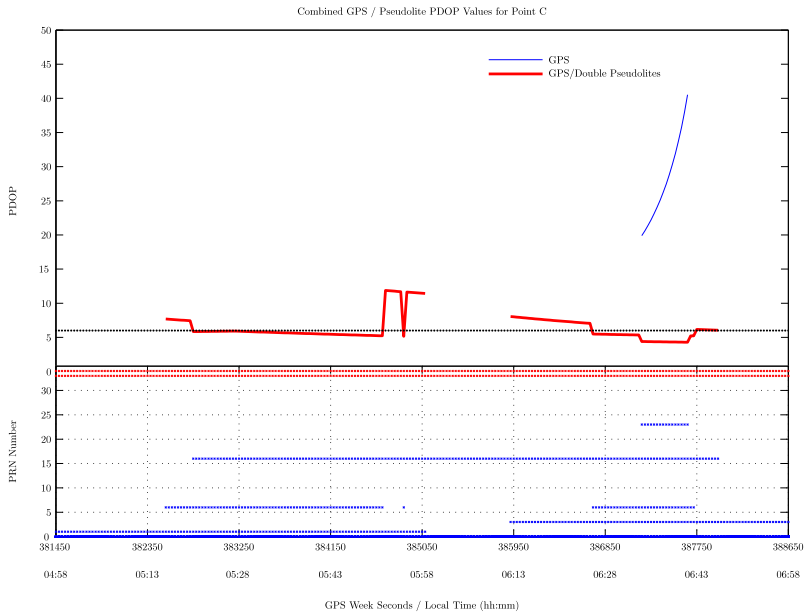

Figure 4.33: Combined GPS/Pseudolite PDOP values over Point C for 2 hours in UTZ type II.

availability and provide required accuracy for limited periods of time which can be determined in advance. The simulation tool presented in this research can be helpful to determine the vulnerability period of time with respect to expected availability over the target zone in planning phase of the mission.

4.8 Summary

This chapter first described the scenario and showed the impacts of satellite outages in GPS availability for various urban terrain zones. This background was helpful to portray augmentation needs in such applications. Next, the ability of the airborne pseudolite to improve both availability and accuracy was investigated. The geometric analysis of the airborne pseudolite location and application of differential GPS services to the airborne pseudolite system were discussed. As the last case in this chapter, the improvement effects of the addition of the second pseudolite to the most challenging urban environments were analyzed. In Chapter V, the conclusions and the recommendations for future work will be given.

V. Conclusions and Recommendations

5.1 Overview

One of the most challenging problems of navigation systems based on Global Positioning System (GPS) is degradation of their performance when some or all satellite signals are obstructed by taller and numerous buildings in urban environments. Line of sight (LOS) visibility is critical for GPS operation. When a vehicle is navigating in an urban environment, LOS to the satellites are often blocked and this blockage severely impacts the availability of GPS. Therefore, it is highly desired to augment the performance of GPS in these environments. Pseudolites, which transmit GPS-like ranging signals, can be deployed in order to provide additional ranging signals and strengthen the geometry between transmitters and receivers.

The previous research, which mostly used several pseudolites and various layouts of several ground stations, has indicated that pseudolites can be used successfully to enhance GPS availability. This research concentrated on the conceptual design of the airborne pseudolite augmentation system in order to provide precise positioning in an urban environment. The impact of the restricted satellite availability due to obstructions was examined for several urban terrain zones. Then the ability of the pseudolite to improve both availability and accuracy was investigated. A comparison between the performances of a GPS only system and an airborne pseudolite augmented system was presented for various positioning scenarios. Moreover, the improvements gain by the addition of second pseudolite to the most challenging urban environments was examined.

Due to the fact that the airborne pseudolite is not fixed at a pre-surveyed location, the accuracy of its position solution, determined by using GPS in this scenario, is a limiting factor for such an augmentation system. Although the ephemeris algorithms for satellite vehicles are accurate for several hours, both intended maneuvers and unintended motion due to air turbulence make airborne platforms highly dynamic. Accurately transmitting the pseudolite position to the user promptly is the

most challenging issue [29]. Hence, the impact of applying differential corrections to the airborne pseudolite are investigated.

5.2 Conclusions

Based on the results presented in this research, the geometry and dimensions of the buildings significantly limits the visibility of the GPS satellites to the ground user. As shown in the results, approximately 96 percent of the urban terrains, near city cores, suburbs and city edges, provide desired GPS availability most of the time without augmentation. On the other hand, the geographically small (4 percent) but strategically important city cores are the most challenging environments for GPS operation even with the various augmentation techniques.

Simulations showed that augmenting GPS with a single low-altitude airborne pseudolite can significantly improve availability for GPS operations in challenging urban environments, such as areas mostly composed of high-rise office buildings. Placing the pseudolite directly to the zenith of user is shown to not always guarantee better availability and, in some conditions, it causes a degradation of accuracy. For the scenario simulated, better performance is often achieved with pseudolites in low altitude azimuth sectors.

Even though differential GPS services can more precisely pinpoint the location of airborne pseudolites, their dependency on reference stations and data links make them logistically difficult to implement, especially during combat operations. Airborne pseudolites navigating with Precise Positioning Service (PPS) receivers not only offer a more feasible approach to the problem, but, according to the results, also yield desired availability most of the time with only a negligible decrease in accuracy.

These results clearly indicate that airborne pseudolite performance is complementary with satellite operation and high quality pseudorange measurements can be obtained from them.

This research provides a simulation tool for showing impacts of airborne pseudolites on a military GPS receiver's positioning accuracy in challenging GPS environments. Possible uses range from urban areas to canyons or harsh geographical conditions for tactical purposes of armed forces. It extends the research efforts into expanding the GPS "operating envelope" for military.

5.3 Recommendations

While this research is primarily concentrated on augmentation of GPS availability with airborne pseudolites in urban environment, there is still much work to do before application of these results to the real theater. The following recommendations are listed for further research related to this topic.

- The environments used during this research are 3D models representing different urban terrain zones, which were developed by the Dr. Ellefsen's urban terrain zone classification system. For the further studies, simulation can be performed for a more detailed model of a real city environment.
- In this research simulations have been carried out for a stationary user in different locations in urban canyon. New simulations should be developed for mobile receivers.
- In order to predict the motion of the airborne pseudolite more accurately, an unmanned air vehicle (UAV), possibly one currently being used by the Army, can be chosen and simulations can then be performed with regard to real performance characteristics of this UAV.
- Short-term signal outages due to LOS obstructions during maneuvers of UAV can be taken into consideration.
- In contrast to the assumption of all 32 GPS satellites are operational and active, simulations should be carried out with the current GPS constellation.

- With respect to the buildings construction types, wall materials and size of the windows, the effects of taking reflected signals into account should be studied in greater detail in the error budget.
- A lower dilution of precision (DOP) value does not automatically guarantee a lower position error. The position error depends upon the both measurement geometry and pseudorange measurement errors [19]. Thus obtained results from this research that lower position dilution of precision (PDOP) values of pseudolite augmented systems than GPS only cases, do not guarantee lower position errors. To achieve higher fidelity, actual receiver positions can be calculated for both the pseudolite and the ground receiver. A monte carlo simulation can be conducted to determine error characteristics.

Appendix A. GPS PDOP Plots

This appendix includes graphs of the visible satellite's orbital ground tracks and GPS only PDOP values for ground user located on point B in different types of UTZ's.

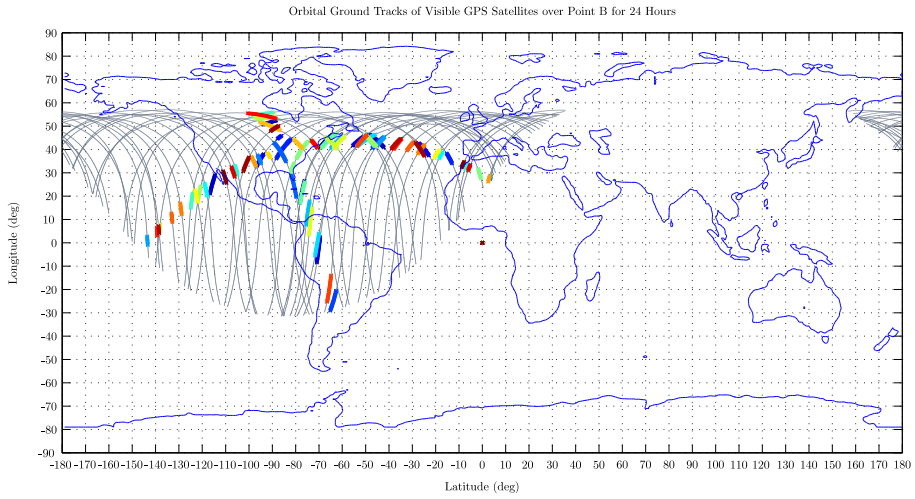

(a)

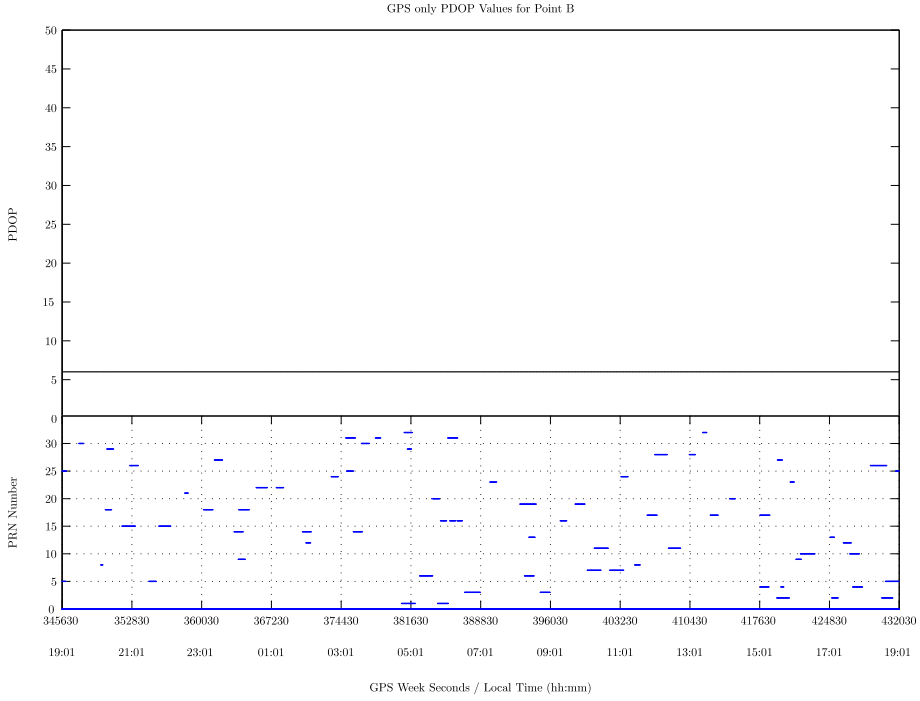

(b)

Figure A.1: Visible Satellite's Orbital Ground Tracks and GPS PDOP Values over Point B for 24 hours in UTZ type I

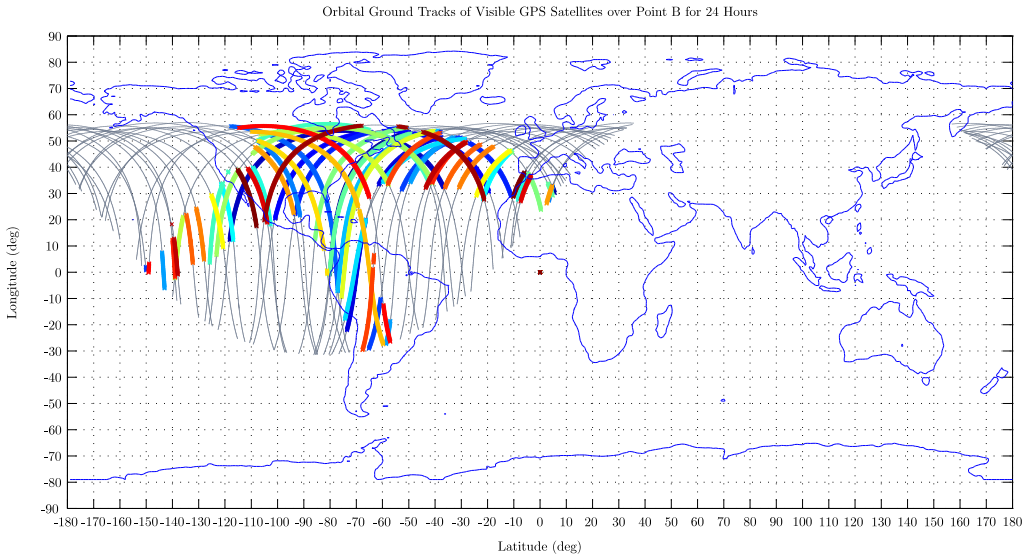

(a)

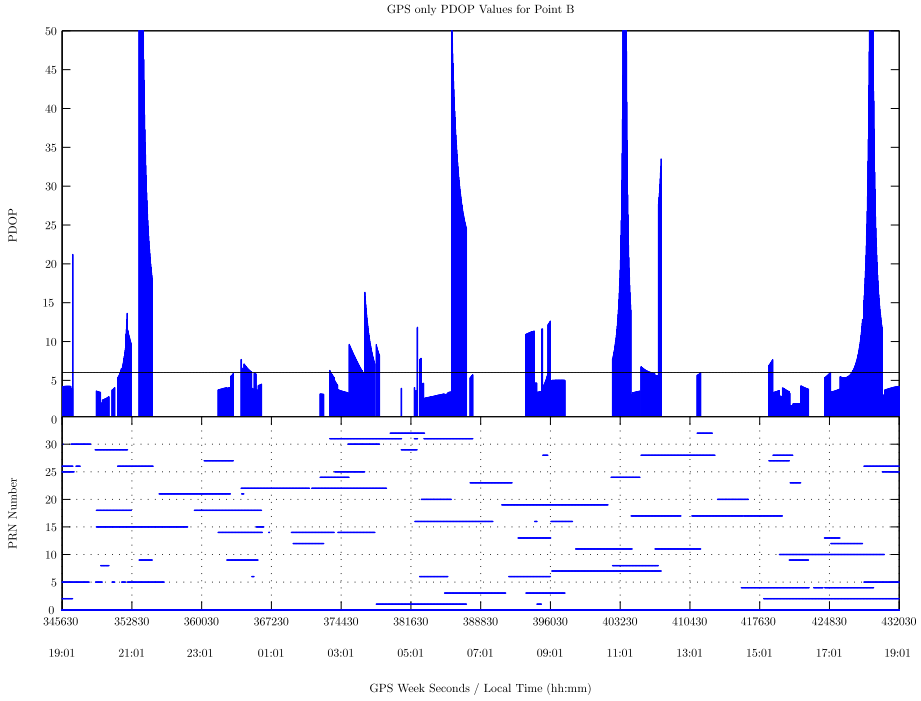

(b)

Figure A.2: Visible Satellite's Orbital Ground Tracks and GPS PDOP Values over Point B for 24 hours in UTZ type II

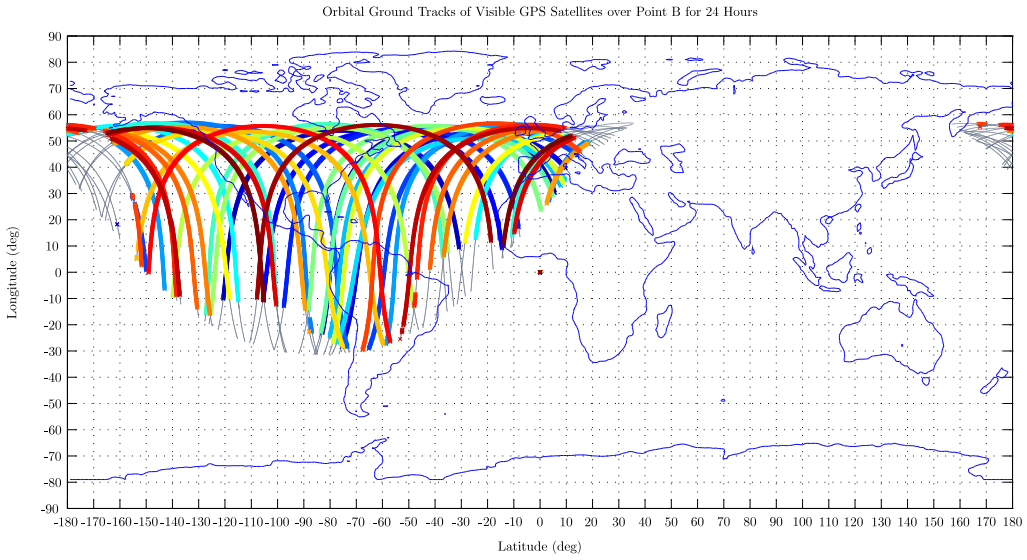

(a)

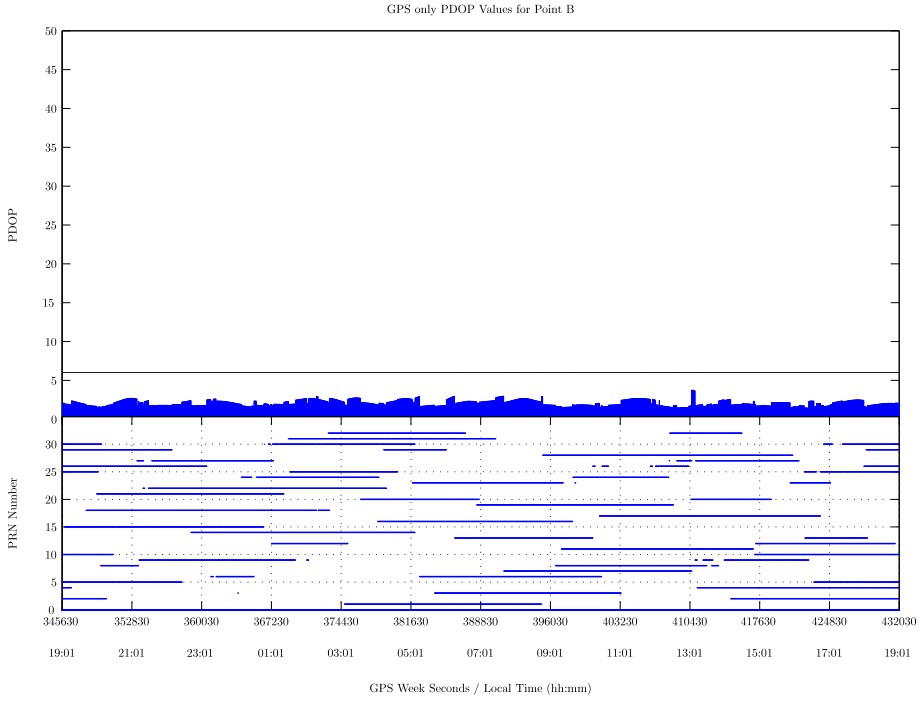

(b)

Figure A.3: Visible Satellite's Orbital Ground Tracks and GPS PDOP Values over Point B for 24 hours in UTZ type III

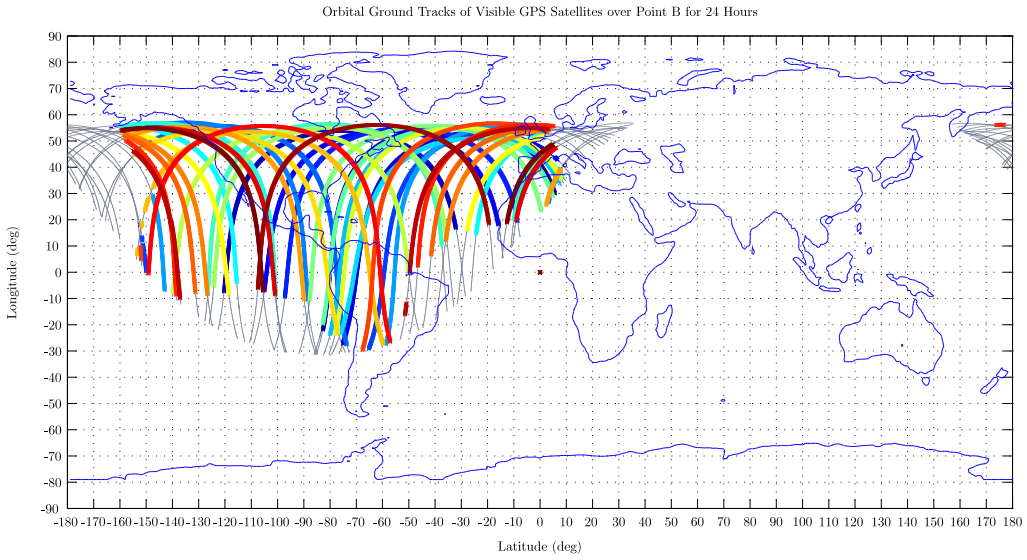

(a)

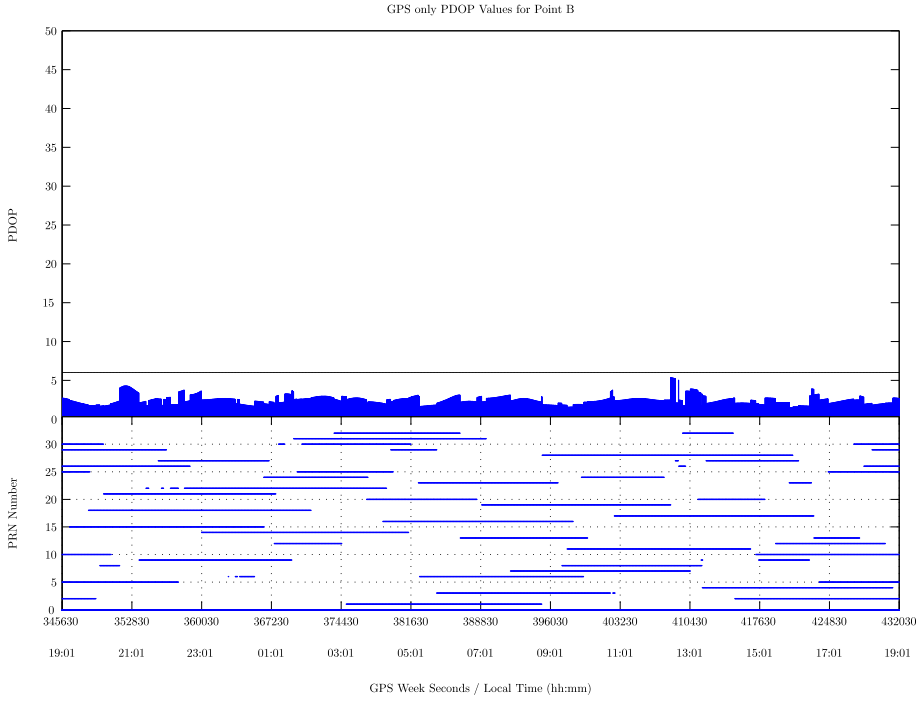

(b)

Figure A.4: Visible Satellite's Orbital Ground Tracks and GPS PDOP Values over Point B for 24 hours in UTZ type IV

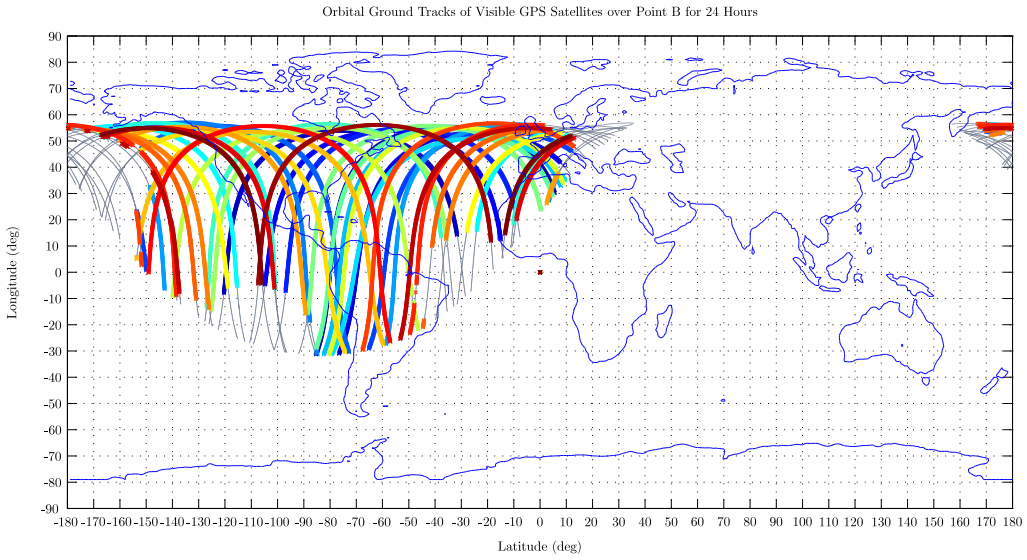

(a)

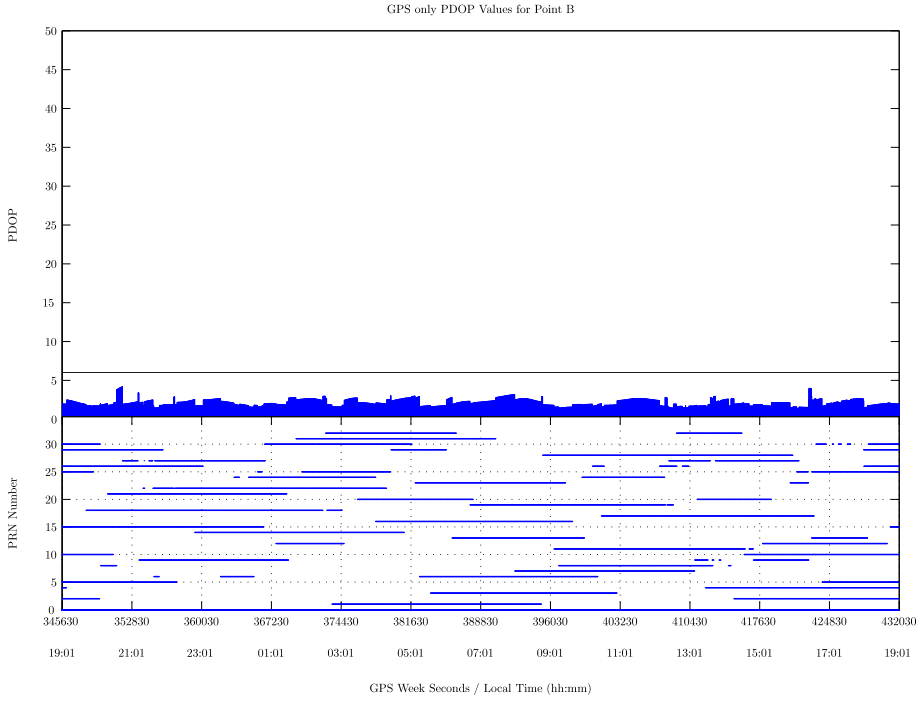

(b)

Figure A.5: Visible Satellite's Orbital Ground Tracks and GPS PDOP Values over Point B for 24 hours in UTZ type V

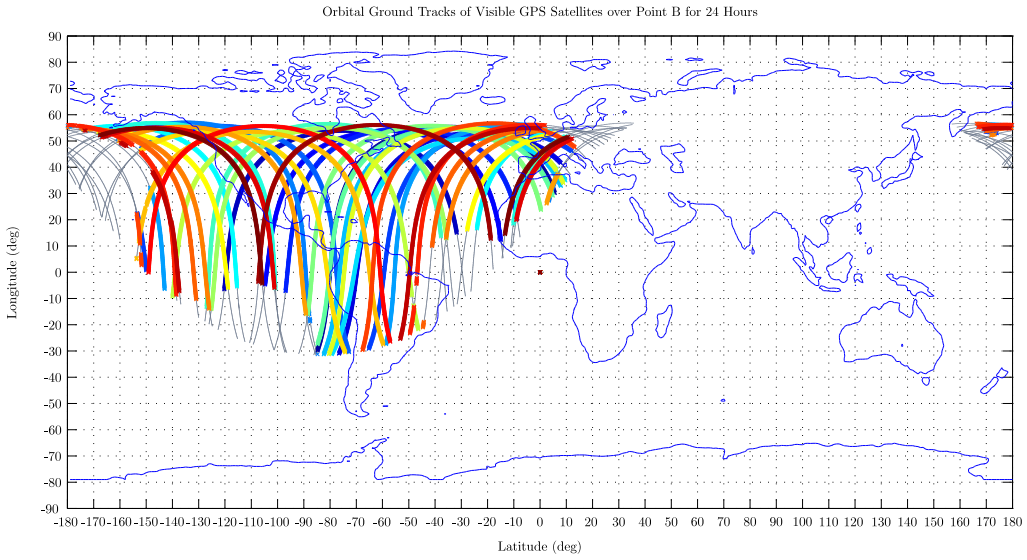

(a)

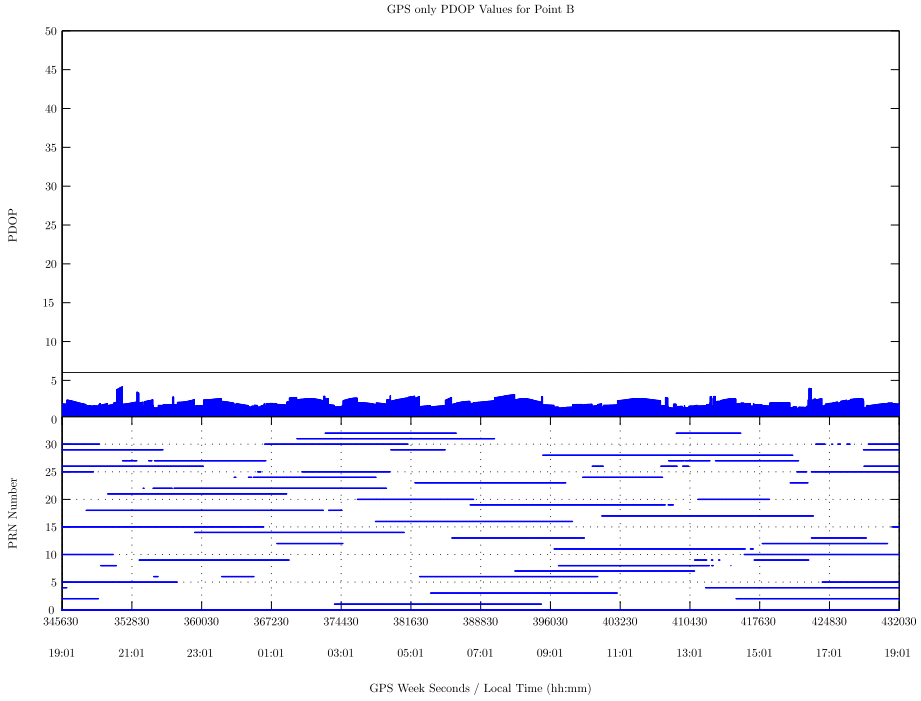

(b)

Figure A.6: Visible Satellite's Orbital Ground Tracks and GPS PDOP Values over Point B for 24 hours in UTZ type VI

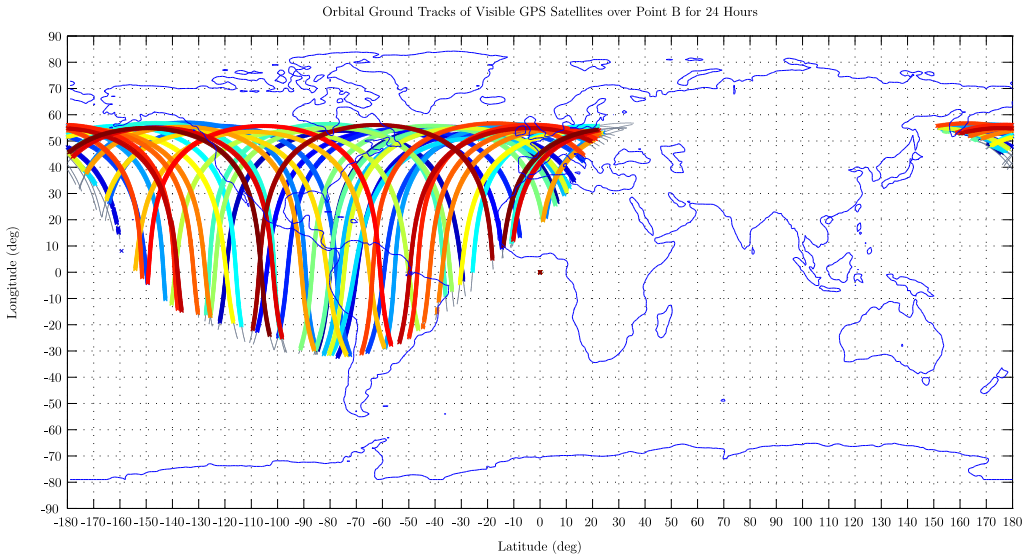

(a)

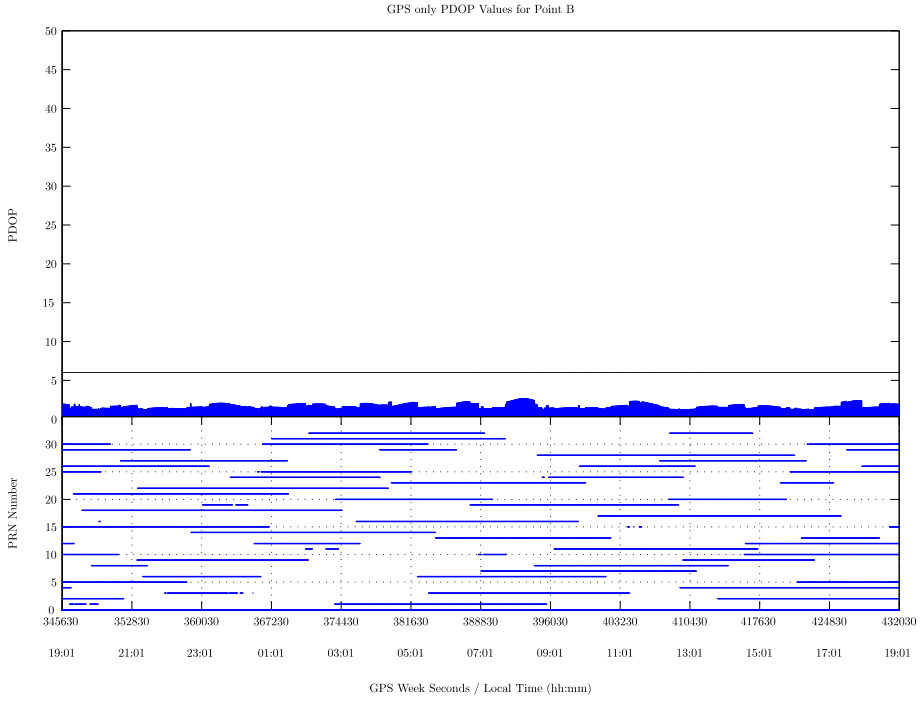

(b)

Figure A.7: Visible Satellite's Orbital Ground Tracks and GPS PDOP Values over Point B for 24 hours in UTZ type VII

Vita

First Lieutenant Halit OKTAY was born in Izmir, Turkey. He graduated from the Turkish Air Force Academy, Istanbul and earned the degree of Bachelor of Science in Aeronautical Engineering in August 2002. In the same year, he began his flight training at the 2nd Main Jet Base, Izmir. Following graduation from F-16 Basic Training Program, he was assigned to the 9th Main Jet Base, 191st Squadron, Balikesir as a wingman in 2005. After serving 4 years, he attended the Graduate School of Engineering and Management, Air Force Institute of Technology in August 2009.

Bibliography

1. "GPS Primer, A Student Guide to the Global Positioning System", 2003.
2. "Mayday 23: World Population Becomes More Urban Than Rural", May 2007.
3. Amt, John Harold Robert. *Methods for Aiding Height Determination in Pseudolite-Based Reference Systems Using Batch Least-Squares Estimation*. Master's thesis, Graduate School of Engineering, Air Force Institute of Technology (AETC), Wright-Patterson AFB OH, March 2006. AFIT/GE/ENG/06-03.
4. Berefelt, F., B. Boberg, J. Nygrds, P. Strmbck, and S.-L. Wirkander. "Collaborative GPS/INS Navigation in Urban Environment". *Proceedings of the ION 2004 National Technical Meeting*, 1114–1125. Swedish Defence Research Agency (FOI), January 2004.
5. Bouska, Terry J. *Development And Simulation Of A Pseudolite-Based Flight Reference System*. Master's thesis, Graduate School of Engineering, Air Force Institute of Technology (AETC), Wright-Patterson AFB OH, March 2003. AFIT/GE/ENG/03-03.
6. Chandu, Burri, Rajkumar S. Pant, and K. Moudgalya. "Modeling and Simulation of a Precision Navigation System using Pseudolites Mounted on Airships". *Proceedings of the 7th AIAA Aviation, Technology, Integration, and Operations Conference (ATIO)*. Indian Institute of Technology Bombay, Mumbai Maharashtra, 400076, India, 2007.
7. Ciampa, Michael A. *Failure Detection Of A Pseudolite-Based Reference System Using Residual Monitoring*. Master's thesis, Graduate School of Engineering, Air Force Institute of Technology (AETC), Wright-Patterson AFB OH, March 2009. AFIT/GE/ENG/09-08.
8. Cobb, H. Stewart. *GPS Pseudolites: Theory, Design, and Applications*. Ph.D. thesis, Stanford University, September 1997.
9. Crawford, Matthew Perri. *Optimal geometric deployment of a ground based Pseudolite navigation system to track a landing aircraft*. Master's thesis, Graduate School of Engineering, Air Force Institute of Technology (AETC), Wright-Patterson AFB OH, June 2006. AFIT/GAE/ENY/06-02.
10. D., Klein and Parkinson B.W. "The Use of Pseudo-Satellites for Improved GPS Performance". *Journal of the Institute of Navigation*, 31:303–15, 1985.
11. Dai, Liwen, Jun Zhang, Chris Rizos, Shaowei Han, and Jingling Wang. "GPS and Pseudolite Integration for Deformation Monitoring Applications". *Proceedings of the ION GPS 2000 Meeting*. School of Geomatic Engineering University of New South Wales, Sydney, NSW 2052, Australia, September 2000.

12. Jovanevic, Aleksandar, Nikhil Bhaita, Joseph Noronha, Brijesh Sirpatil, Michael Kirchner, and Deepak Saxena. "Piercing the Veil". *GPS World*, 30–37, March 2007.

13. Kanli, Mustafa Ozgur. "Limitations of Pseudolite Systems Using Off-The-Shelf GPS Receivers". *Journal of Global Positioning Systems*, 3:154–166, November 2004.

14. Kaplan, Elliot D. and Christopher J. Hegarty. *Understanding GPS Principles And Applications*. Artech House, 2 edition, 2006.

15. Langley, Richard B. "Dilution of Precision". *GPS World*, 52–59, May 1999.

16. LeMaster, Edward A. and Stephen M. Rock. "A Local-Area GPS Pseudolite-Based Navigation System for Mars Rovers". *Journal of Autonomous Robots*, 14:209–224, 2003.

17. McKay, Jason B. and Meir Pachter. "Geometry Optimization for GPS Navigation". *Proceedings of the 36th Conference on Decision and Control*, 4695–4699. Institute of Electrical and Electronics Engineers (IEEE), Department of Electrical and Computer Engineering, Air Force Institute of Technology, Wright-Patterson AFB, OH, August 1997.

18. McKay, Jason Bryce. *Optimization of a GPS-Based Navigation Reference System*. Master's thesis, Graduate School of Engineering, Air Force Institute of Technology (AETC), Wright-Patterson AFB OH, December 1996. AFIT/GE/ENG/96D-12.

19. Misra, Pratap and Per Enge. *Global Positioning System Signals, Measurements, And Performance*. Ganga-Jamuna Press, 2 edition, 2006.

20. Monda, Eric. *Global Positioning System Pseudolite-Based Relative Navigation*. Technical report, Sandia National Laboratories, March 2004.

21. Person, Jon. "Writing Your Own GPS Applications: Part 2", 2008.

22. Raquet, John F., G.Lachapelle, W.Qiu, C.Pelletier, T.Nash, F.B.Snodgrass, P.Fenton, and T.Holden. "Development and Testing of a Mobile Pseudolite Concept for Precise Positioning". *Journal of The Institute of Navigation*, 43:149–165, 1996.

23. Rizos, Chris. "Pseudolite Augmentation of GPS", 2008.

24. Samama, Nel. *Global Positioning Technologies And Performance*. Wiley Interscience, 2008.

25. Shockley, Jeremiah A. *Estimation and Mitigation of Unmodeled Errors for a Pseudolite Based Reference System*. Master's thesis, Graduate School of Engineering, Air Force Institute of Technology (AETC), Wright-Patterson AFB OH, March 2006. AFIT/GE/ENG/06-51.

26. Sklar, Jay R. "Interference Mitigation Approaches for the Global Positioning System". *Lincoln Laboratory Journal*, 14:167–180, 2003.

27. Tsujii, Toshiaki, Masatoshi Harigae, and Kazuki Okano. "A New Positioning/-Navigation System Based on Pseudolites Installed on High Altitude Platforms Systems (HAPS)". *24th International Congress of the Aeronautical Sciences*. Japan Aerospace Exploration agency and GNSS Technologies Inc, 2004.

28. Tsujii, Toshiaki, Chris Rizos, Jinling Wang, Liwen Dai, Craig Roberts, and Masatoshi Harigae. "A Navigation/Positioning Service Based on Pseudolites Installed on Stratospheric Airships". *Journal of the 5th International Symposium on Satellite Navigation Technology and Applications*, 2001.

29. Tuohino, Jeffrey L., Michael G. Farley, and Robert R. James. "Military Pseudolite Flight Test Results". *Proceedings of the ION GPS 2000 Meeting*, 2079–2088. Rockwell Collins and SSC San Diego, September 2000.

30. United States Department of Defense. *Global Positioning System Standard Positioning Service Performance Standard*, September 2008.

31. Vanschoenbeek, Inge, Bernard Bonhoure, Marco Boschetti, and Jerome Legenne. "GNSS Time Offset Effects on GPS-Galileo Interoperability Performance". *Inside GNSS*, 60–70, September–October 2007.

32. Vick, Alan, John Stillion, David R. Frelinger, Joel Kvitky, Benjamin S. Lambeth, Jefferson P. Marquis, and Matthew C. Waxman. *Aerospace Operations in Urban Environments Exploring New Concepts*. RAND, 2000.

33. Wang, Jianguo Jack and Jinling Wang. "Tropospheric Delay Estimation for Pseudolite Positioning". *Journal of Global Positioning Systems*, 4:106–112, July 2005.

34. Wang, Jinling. "Pseudolite Applications in Positioning and Navigation: Progress and Problems". *Journal of Global Positioning Systems*, 1:48–56, July 2002.

35. Wang, Jinling and Hung-Kyu Lee. "Impact of Pseudolite Location Errors in Positioning". *Geomatics Research Australasia*, 81–94, November 2002.

36. Wang, Zheng, Yuqing He, and Jianda Han. "Simultaneous Locating and Calibrating Pseudolite Navigation System for Autonomous Mobile Robots". *Proceedings of the IEEE International Workshop on Intelligent Data Acquisition and Advanced Computing Systems: Technology and Applications*, 519–524. Institute of Electrical and Electronics Engineers (IEEE), September 2009.

REPORT DOCUMENTATION PAGE

Form Approved
OMB No. 074-0188

1. REPORT DATE *(DD-MM-YYYY)*	**2. REPORT TYPE**	**3. DATES COVERED** *(From – To)*
24-03-2011	Master's Thesis	Sep 2009---Mar 2011

4. TITLE AND SUBTITLE

Airborne Pseudolites in a Global Positioning System (GPS) Degraded Environment

5a. CONTRACT NUMBER

5b. GRANT NUMBER

5c. PROGRAM ELEMENT NUMBER

6. AUTHOR(S)

Halit OKTAY, AFIT, 1 Lt, TURAF

5d. PROJECT NUMBER

5e. TASK NUMBER

5f. WORK UNIT NUMBER

7. PERFORMING ORGANIZATION NAMES(S) AND ADDRESS(S)

Air Force Institute of Technology
Graduate School of Engineering and Management (AFIT/EN)
2950 Hobson Way
WPAFB OH 45433-7765 DSN: 785-3636

8. PERFORMING ORGANIZATION REPORT NUMBER

AFIT/GSS/ENY/11-M03

9. SPONSORING/MONITORING AGENCY NAME(S) AND ADDRESS(ES)

Hava Kuvvetleri Komutanligi
06100 Bakanliklar / Ankara - Turkey
Telephone number: (+90-312)–417-2150; e-mail: basin@hvkk.tsk.tr

10. SPONSOR/MONITOR'S ACRONYM(S)
TURAF

11. SPONSOR/MONITOR'S REPORT NUMBER(S)

12. DISTRIBUTION/AVAILABILITY STATEMENT
Approved For Public Release; Distribution Unlimited

13. SUPPLEMENTARY NOTES
This material is declared a work of the U.S. Government and is not subject to copyright protection in the United States.

14. ABSTRACT

The high accuracy of the Global Positioning System allows for precision navigation in support of current and future military operations. However, generating a three-dimensional position using GPS requires a clear line-of-sight between the user and at least four GPS satellites, and so the GPS service can be denied in scenarios such as a street surrounded by tall buildings. Therefore, there is a need for augmentation in these environments. Pseudolites, which transmit GPS-like ranging signals, can be deployed in order to improve the geometry and provide additional ranging signals. Users can then receive and process both GPS and pseudolite signals simultaneously with slight software modifications.

In this thesis, in order to provide precise positioning in an urban environment, a conceptual design of the airborne pseudolite augmentation system is introduced. The impact of the restricted satellite availability due to obstructions is examined for various urban terrain zones. Then the ability of the pseudolite to improve both availability and accuracy is investigated. A comparison between the performances of a GPS only system and an airborne pseudolite augmented system is presented for various positioning scenarios. Simulations show that required accuracy and availability can be obtained by using an appropriately equipped airborne pseudolite. Finally, the improvement gained by the addition of second pseudolite to the most challenging urban environments is examined.

15. SUBJECT TERMS
GPS, Pseudolite

16. SECURITY CLASSIFICATION OF:			**17. LIMITATION OF ABSTRACT**	**18. NUMBER OF PAGES**	**19a. NAME OF RESPONSIBLE PERSON**
REPORT	**ABSTRACT**	**c. THIS PAGE**			Lt Col M. Stepaniak
U	**U**	**U**	**UU**	113	**19b. TELEPHONE NUMBER** *(Include area code)* (937) 255-3636; email: Michael.Stepaniak@afit.edu

Standard Form 298 (Rev: 8-98)
Prescribed by ANSI Std. Z39-18